A COMPUTER INTERFACED RAPID SCAN STOPPED-FLOW SYSTEM FOR THE STUDY OF TRANSIENTS IN ENZYME REACTIONS

Dissertation for the Degree of Ph. D. MICHIGAN STATE UNIVERSITY RICHARD B. COOLEN 1974



This is to certify that the

thesis entitled A COMPUTER INTERFACED RAPID SCAN STOPPED-FLOW SYSTEM FOR THE STUDY OF TRANSIENTS IN ENZYME REACTIONS

presented by

Richard B. Coolen

has been accepted towards fulfillment of the requirements for

Ph.D. degree in Chemistry

Date June 20, 1974

O-7639



ABSTRACT

A COMPUTER INTERFACED RAPID SCAN STOPPED-FLOW SYSTEM FOR THE STUDY OF TRANSIENTS IN ENZYME REACTIONS

Ву

Richard B. Coolen

A rapid scan stopped-flow apparatus was interfaced to a remote PDP8I computer. The data transmission system permits high frequency (less than 10MHz) parallel digital data transfer over several thousand feet. A frequency multiplication system allows sampling to occur at a constant maximum rate which is independent of scan speed and limited essentially by the computer. The data acquisition software establishes a sampling bandpass which varies with time to produce significant real time S/N enhancement in two dimensions while simultaneously reducing absolute storage requirements. A versatile display system facilitiates the analysis of data.

An existing rapid scan stopped-flow apparatus was modified to permit the study of changes in the spectrum of substrates, transient intermediates, and products of enzyme catalyzed reactions. Significant improvements in the present stopped-flow system include: (1) variable temperature capability; (2) increased reliability and resolution; (3) a multiple push capability for improved reproducibility; (4) a special flag system which permits

easy calculation of the flow velocity and the location of time zero for the reaction; and finally (5) an improved all quartz double mixer with dual pathlength capability. The overall performance of the instrument was evaluated by using a variety of standard reactions. Mixing is complete within the dead time of the instrument. By studying absorbance changes at 600 nm which accompany the formation of peroxychromic acid, at 600 nm, dead times for the short (1.99 mm) and long (1.85 cm) path lengths were found to be 2.5 and 5.5 ms respectively.

Three enzyme systems were examined in order to test the feasibility of doing rapid scanning enzyme kinetics studies with this system, and to illustrate the utility of the technique.

Rapid scanning of the absorption spectrum during reaction allowed direct observation of the spectra of the $T_{l_{\downarrow}}$ and $R_{l_{\downarrow}}$ complexes which are formed by the interaction of glyceraldehyde-3-phosphate dehydrogenase (GAPDH) and NAD⁺. The $T_{l_{\downarrow}}$ complex formed rapidly followed by a first-order growth of the $R_{l_{\downarrow}}$ complex. The rate constant for the $T_{l_{\downarrow}} \rightarrow R_{l_{\downarrow}}$ isomerization was 1.37 sec⁻¹ which is nearly a factor of four larger than previously reported. No effect on either the $T_{l_{\downarrow}}$ or $R_{l_{\downarrow}}$ absorption bands or the rate of $R_{l_{\downarrow}}$ formation was observed when less than saturating levels of NAD⁺ were used. The rate constant for the formation of the $R_{l_{\downarrow}}$ complex is independent of wavelength.

The enzyme L-threonine dehydrase (TDH) is known to exhibit a peak at 415 nm due to Schiff base formation between pyridoxal phosphate and a lysine residue of the The shift of the absorption to give a new band protein. at 460 nm (composite at 430 nm) upon the addition of Lthreonine and AMP has been previously observed and presumably reflects the formation of a Schiff base between the enzyme-bound pyridoxal phosphate and aminocrotonate, a dehydrated intermediate derived from Lthreonine. Toward the end of reaction when product formation is nearly complete, the transient absorption of the enzyme-bound complex decays back to that of the enzyme alone. This system was studied with the rapid scan system in an effort to detect other possible intermediate species which have been postulated for the overall mechanism. Other than the 430 nm band, no additional absorptions were detected on the short time scale (less than 10 sec.). Product growth is first order, and in the presence of 25 mM L-threonine the steady-state concentration of the enzyme-substrate complex was achieved in less than 100 ms. An isosbestic point occurs at about 405 nm.

A third test system involved the enzyme equine liver alcohol dehydrogenase (LADH) and its catalysis of the reduction of the substrate analog p-nitroso-N, N-dimethylaniline (NDMA) by reduced nicotinamide adenine dinucleotide (NADH). The disappearance of the NDMA band at 440 nm

followed Michaelis-Menten kinetics. By following the entire decay scheme and fitting the data with a general non-linear curve-fitting program, values of K (effective) and V_{max} could be obtained from single decay curves. During the decay of the NDMA absorption, the absorption band at 340 nm shifted to 335 nm with a slight increase at the maximum. The 335 nm band then decayed by a first order process with a rate constant of 0.70 + 0.04 sec-1. Coincident with the decay of the NDMA band is the growth of an absorption at 540 nm with an isosbestic at about 510 nm. The decay of the 540 nm band is first order with a rate constant of 0.1447 + 0.01 sec-1. Since the 540 nm decay is slower than that at 335 nm, the two absorptions do not represent the same species. The rapid scanning stoppedflow technique is clearly a powerful tool for the study of transients in enzyme catalyzed reactions.

A COMPUTER INTERFACED RAPID SCAN STOPPED-FLOW SYSTEM FOR THE STUDY OF TRANSIENTS IN ENZYME REACTIONS

Ву

Richard B. Coolen

A DISSERTATION

Submitted to
Michigan State University
in partial fulfillment of the requirements
for the degree of

DOCTOR OF PHILOSPHY

Department of Chemistry

To Barbara

ACKNOWLEDGEMENTS

The author wishes to express his appreciation to Professor James L. Dye whose guidance and encouragement greatly contributed to the completion of this work.

He also wishes to give special thanks to Professor Clarence Suelter for his invaluable assistance in the enzyme studies, and to Dr. Nicholas Papadakis for his help and patience during the development of the interface and stopped-flow systems.

The author is indebted to Ann Aust for her suggestions during the preparation of the enzyme solutions, and to Messrs. James Avery and Richard Teets for their contributions to the computer interface project.

Finally, financial support from the National Science Foundation is gratefully acknowledged.

TABLE OF CONTENTS

	Page
I. INTRODUCTION	. 1
1.1Computerization of the Scanning Stopped-Flow Experiment	. 3
1.4Scanning Enzyme Kinetics Results	
II. HISTORICAL	. 6
2.1Instrumental and Experimental Method for the Study of Enzyme Kinetics 2.1.1Manual Mixing Method 2.1.2Flow Methods 2.1.3Relaxation Methods 2.2The Stopped-Flow Method 2.3The Scanning Stopped-Flow System 2.4Data Analysis Techniques for the	. 7 . 7 . 9 . 10 . 13
study of Enzyme Kinetics	. 20
Assumptions	22222324
III. EXPERIMENTAL	. 28
3.1Glassware	303132
IV. THE COMPUTER SYSTEM: DESIGN CONSIDERATIONS AND CONSTRAINTS	• 37 • 40 • 46 • 49

TABLE OF CONTENTS -- Continued

4.8System Software	55
4.9System Performance	- 60
4.10-Results	61
V. THE STOPPED-FLOW SYSTEM: DESIGN, CONSTRUCTION	
AND TESTING	69
	- ,
5.1Flow System Design	71
5.2Flow and Reference Cells	
	71.
5.3Pushing and Stopping System	74
5.3.1Syringe and Plunger Design	
5.3.2Mechanical and Framework	79
5.3.3Thermostat System	80
5.3.4Solution Mixers	82
5.3.5Stopping Syringe System	82
5.3.5.1Start and stop flags	, 84
5.4 Solution Handling and Delivery System.	
5.5Optical System Design	
5.5.1Light Sources and Detectors	
5.6Performance Results	92
5.6.1Optical Calibration Data	
	, 72
5.6.2Flow Calibration	93
5.6.3Flow Cell Performance, Fixed	~~
Wavelength	95
5.6.3.1Mixing Efficiency	95
5.6.3.2Dead Time	96
5.6.4Quantitative Measurements	97
VI. TRANSIENT STATE ENZYME RESULTS	, 98
6.1Glyceraldehyde-3-phosphate dehydrog-	
enase	, 98
6.1.6Complex Formation Between	. •
NAD and GAPDH	. 99
6.1.2Reaction with Substrate	
6.2The Threonine Dehydrase System	
	_
6.3Alcohol Dehydrogenase (Horse liver)	
6.3.1LADH Rate Measurements	, 117
6.3.2Kinetics of NDMA Disappearance	
(440 nm)	119
6.3.3Kinetics at 335 nm and 540 nm.	, 122
6.3.4Rate Law for 440 and 540 nm	. 129
VII. SUGGESTIONS FOR FUTURE WORK	. 136
REFERENCES	138

LIST OF TABLES

TABLE		Page
I.	Sampling Parameters for the GAPDH, TDH and LADH Runs	33
II.	Scanning Monochromator and Phase - Locked Loop Parameters	39
III.	The effect of NAD ⁺ concentration, wavelength and functional form on the first order rate constant(s) for the growth of the R ₁ complex of GAPDH, and a comparison with Kirschner's results	106
IV.	Comparison between steady-state and full-time-course integration kinetic parameters for substrate disappearance in the LADH system	121
v.	First order decay constants for the transient intermediates of the LADH system	127
VI.	Rate constants for the Michaelis-Menten growth and first order disappearance of the 540 nm intermediate (from equation 4)	132

LIST OF FIGURES

FIGUR	E	Page
1.	Example of the averaging scheme for a fixed wavelength case	42
2.	Timing diagram for a scanning experiment	48
3.	Block diagram of the computer interfaced stopped-flow system	50
4.	Phase-locked-loop and divide by N circuit principle	54
5.	Flow-chart for the data acquisition routines	57
6.	Holmium oxide spectrum, collected while scanning at 75 spectra per second	62
7.	Time-cuts for the formation of peroxychromic acid showing the slow decomposition process	64
8.	Spectra collected during the reaction for the formation of peroxychromic acid. "A" is from group 1, while "B" is from group 4	65
9•	Time-cuts for the formation of the FeSCN complex showing the capabilities of the display routines	66
10.	Overall spectral changes in the LADH catalyzed reduction of NDMA by NADH	68
11.	Schematic diagram of the mixing and observation cell. A-Fisher-Porter 2 mm quartz joints, B-~0.5 cm, C-cross-section of a mixer	
12.	Syringe and adjustable plunger design	76
13.	Schematic diagram of the thermostated stopped- flow apparatus. A - Joints for rinsing solutions, B - Joints for reactants, C - ther- mostated burettes, D - reactant reservoirs, E - mixing and observation cell, F - reference cell, G - pushing syringes, H - pneumatic pis- tons, I - stopping syringe, J - quartz light fibers, K - thermostat bath, L - to vacuum, M - to vacuum and "waste", 1, 2, 3, 4, 5-flow valves.	86

LIST OF FIGURES -- Continued

FIGURE		Page
nt.	The absorbance of solutions of p-nitropheno- late (360 nm) which were measured on a Cary 15 plotted against the absorbance measured using the long path length on the stopped-flow apparatus	94
15.	Selected difference spectra obtained during	
-/•	the T _{li} R _{li} isomerization reaction of the NAD-GAPDH complex at 39.9°C	101
16.	Time-cut at 366 nm from Figure 15	102
17.	Single exponential fit of the growth of the R ₄ complex of GAPDH (366 nm)	103
18.	Double exponential fit of the growth of the R _{\(\psi\)} complex of GAPDH (366 nm)	105
19.	Spectrum at various times during the reaction of GAPDH with NAD+ and GAP. (solvent back-ground has been subtracted)	109
20.	Spectrum at various times during the reaction of GAPDH with NAD+ and GAP (data of Figure 19 with NAD+ subtracted)	110
21.	Time-cuts of the data from which Figure 20 was taken	111
22.	Selected spectra from Groups 1,2,3for the deamination of L-threonine by TDH (no baseline subtracted)	113
23.	TDH time-cuts at 330 nm and 440 nm, (growth at 440 (100 ms) not shown)	114
24.	Appearance of an isosbestic during product growth (at left), and decay of the transient (at right), in the TDH system	1 15
25.	Calculated and observed decay of substrate (440 nm) in the LADH catalyzed reduction of NDMA	120
26.	Time-cuts at various wavelengths for the LADH system. The residual absorbance at 325 nm is due to excess NADH	123

LIST OF FIGURES -- Continued

FIGURE		Page
27.	First-order decay of the 325 nm transient in the LADH system	1 25
28.	First-order decay of the 540 nm transient in the LADH system	126
29.	Growth and decay of the 540 nm transient intermediate in the LADH system	131
30.	Substrate (440 nm) and transient (540 nm) absorptions in the LADH system showing the isosbestic at 510 nm during substrate decay. Spectrum 4 is the residual absorption	133
31.	Overall spectral changes in the LADH catallyzed reduction of NDMA by NADH	135

I. INTRODUCTION

Although stopped-flow techniques which utilize absorption spectroscopy have found wide use in the study of enzyme catalyzed reactions, the variation in transmittance has usually been examined at only one or two wavelengths after a given push. Recent developments in the study of enzyme reactions and continued improvements in overall instrumental sensitivity have lead to an increased interest in enzymic processes which involve transient or intermediate forms. However, progress in this area has been hampered by the necessity to work at fixed wavelength and by the restrictions imposed by conventional methods of data treatment. Traditionally one of the major obstacles encountered in the study of complex enzymic reactions has been the problem of solving complex mathematical expressions. This has resulted in the use of a large number of simplifying assumptions.

In the present work an existing rapid scanning stoppedflow apparatus was modified to permit the study of changes in the spectrum of substrates, transient intermediates, and products of enzyme catalyzed reactions. One of the primary goals of this modification was to permit the study of processes which involve short-lived intermediates whose spectral properties differ from those of the reactants and products. Rapid, repetitive scans of the appropriate spectral region during an enzymic reaction can provide information on the number and types of species present as well as the kinetics of formation and decay of intermediates. Such data can provide explicit information which could only be inferred from measurements made at a single wavelength. However, the nature of these intermediates is such that highly sensitive and accurate instrumentation is required. The large volume and inherent complexity of the data from a scanning stopped-flow experiment are such that rapid, efficient data processing schemes are a necessity.

The second major objective of this work, therefore, was to develop suitable data handling methods for systems having complex spectral and time developments during reaction. If there are wavelength shifts, bandshape changes, or intermediate absorbances present during reaction, interpretation and analysis become more difficult. Systems with overlapping absorbances which have different time dependent components, or systems involving intermediate species with unknown molar absorptivities can be particularly troublesome. Systems which show wavelength-dependent time developments generally lead to complex rate expressions. Thus, sophisticated data analysis techniques are required to overcome the inherent complexity of the scanning experiment and to resolve whatever mechanistic information is contained in the data.

To achieve the overall objectives of this research, the work was separated into four relatively independent projects. In addition to their roles in the overall system, each of the individual projects incorporated a number of more specialized objectives. These projects will be presented in the thesis somewhat independently and roughly in the chronological order in which they were done. A brief description of each area is presented below.

1.1--Computerization of the Scanning Stopped-Flow Experiment

To overcome some of the problems inherent in the scanning stopped-flow experiment and to enhance resolution in both time and wavelength, the instrument was interfaced to a remote PDP 8-I computer. A previous system was noise limited by FM tape, and data analysis was too slow to permit decision-making during a run (51). Therefore signal enhancement, rapid data reduction, and an interactive capability were important aspects of the computerization project.

1.2--Design and Construction of the Stopped-Flow Apparatus

The emphasis here was to develop a stopped-flow instrument suitable for use with both enzyme and air-sensitive systems. Two additional considerations were: (1) to overcome some of the problems of the previous flow

system; (2) to make the new system computer compatible.

Significant improvements in the present system include:

(1) variable temperature capability; (2) increased reliability and resolution; (3) a multiple push capability for better reproducibility; (4) a special flag system which permits easy calculation of the flow velocity and the location of time zero for the reaction; and finally,

(5) an improved all quartz double mixer with dual pathlength capability. Introduction of these improvements required a number of design changes from the previous system and, in fact, an entirely new flow system was constructed.

1.3--System Testing and Performance

The third project involved testing the overall system and the determining the instrument parameters. Resolution and reproducibility tests were carried out for both the interface and stopped-flow systems, and flow system parameters such as mixing efficiency, dead time, and the path lengths were measured.

1.4--Scanning Enzyme Kinetics Results

Suitable enzyme systems were to be examined in order to test the feasibility of doing scanning enzyme kinetics with this system, and to illustrate the utility of the technique. Results for the three test enzyme systems which were studied not only provide new information on

these systems, but also clearly demonstrate the potential of a rapid scanning stopped-flow system coupled with appropriate data handling capabilities.

The design, construction and testing of the computer interfaced stopped-flow system required several man-years of the combined efforts of Dr. N. Papadakis and the author. For additional information about the system and an example of its application to the study of an air-sensitive reaction, the reader is referred to the Ph.D. thesis of Papadakis (32).

In the final chapter of this thesis some suggestions for future work are presented.

II. HISTORICAL

Virtually all intracellular processes are mediated by enzymes. Thus it is necessary to study the rate behavior or kinetics of enzyme catalyzed reactions. Indeed, kinetics studies have probably contributed more to our knowledge of the mechanisms of enzyme catalyzed reactions than any other method of approach (1-4). Our ability to understand individual enzyme reactions is determined to a large extent by the available methodologies. Although development in the area has been continuous, one is always limited experimentally by at least three factors: (1) sensitivity of the apparatus to the physical parameter being measured, (2) response time of the detection system, and (3) the limited availability of high purity enzymes in quantity. The instrumental techniques described in this section represent various trade-offs among these three factors.

In contrast to the actual experimental measurement, the analysis of rate data is far less constrained. It is true that even the simplest of enzyme mechanisms can lead to complex rate expressions; however, the availability of sophisticated computer programs should go a long way

experimental conditions are imposed in order to simplify mathematical treatment of the data. As a result of these restrictions and the imposition of simplifying assumptions, only a limited fraction of the available information can be extracted from the data.

In this section the experimental and analytical techniques which have found wide application in the study of enzymic processes are reviewed. The limitations of these methodologies, especially in the areas of complex rate phenomena and transient intermediate processes, provide the rationale for the extension of the existing scanning stopped-flow system and curve-fitting techniques (KINFIT) to the study of these systems.

2.1--Instrumental and Experimental Methods for the Study of Enzyme Kinetics

2.1.1 -- Manual Mixing Method

A number of references are available that discuss in detail the instrumental and experimental methodologies commonly used in the study of enzyme kinetics (1-4). Perhaps the most widely used method is one in which substrates are manually mixed in a cuvette with very small quantities of enzyme to produce linear rate curves. Progress of the reaction is generally followed spectrophotometrically at a single wavelength, or if conditions permit, a scanning system such as a Cary 15 Spectophoto-

meter can be used (5). The technique is useful provided the reaction rate remains small (t<10 sec) and constant. Using a variety of substrate, modifier and enzyme levels in conjunction with the initial slope method of analysis one can learn a great deal about the mechanisms of enzyme reactions. The method has the advantage that secondary additions of substrates or quenching agents are simple, and in fact, the entire process is easy to use and relatively inexpensive. Because of the manual mixing process however, the high levels of enzyme generally required for the formation of detectable levels of transients or intermediates cannot be used.

A number of variations of the manual method involving non-spectrophotometric detectors have been utilized.

They are presented here to illustrate the wide range of
physical parameters which have been used to follow the progress of enzyme systems, not only by the manual technique,
but by other methods as well.

Enzyme reactions in which gases are produced or consumed can be followed by manometric techniques (6, 7). Polarimetry has been used to study sugar enzymes by monitoring optical activity (8). Amperometric (9), coulometric (10), potentiometric (11), polarographic (12), and specific ion electrode techniques (13) have been used to study a wide variety of enzyme systems. Enzyme electrodes (transducers with immobilized enzyme) similar to those

described for glucose by Hicks (14) can even permit simple, direct and continuous in vivo analysis of important body constituents.

Steady-state or assay type analysis can be readily automated (15). Computerized parallel fast analyzers (16) (using multiple cuvettes and centrifugal mixing) are capable of performing multiple simultaneous assays. Some commercial models also provide for appropriate calculations, including linear regression analysis and quality control.

2.1.2--Flow Methods

Flow methods were developed in order to permit the study of faster reactions. Initially they were used primarily to extend the range of the manual mixing technique. As sensitivity and time response improved, more rapid processes were studied. More importantly however, is the fact that comensurate with instrumental improvements came the discovery of many new phenomena. Frequently, the appearance of transient intermediates or induction phases can be observed only with the most sensitive equipment and only when the reaction system is perturbed far from equilibrium. The development of flow techniques and their application to the study of enzyme reactions will be considered in more detail in a later section.

2.1.3--Relaxation Methods

Although flow methods have permitted measurements on a millisecond time scale, a large number of important reactions still cannot be approached directly. The classic work of Eigen and his collaborators (17) has provided values for the rate constants of many ionic reactions which are important in the study of biological phenomena. These investigators used the so-called relaxation technique. With this technique, a system at equilibrium is perturbed by changing some intensive property very rapidly (typically in a few microseconds). Relaxation of the system to a new equilibrium position occurs by first order processes provided the perturbation is small. Most of these fundamental data obtained by Eigen utilized the temperature-jump method, electric field jump technique or sound abosrption measurements. Bimolecular reactions with rate constants as high as 10¹¹ M sec have been measured by these methods.

The temperature jump apparatus designed by de Maeyer (18) which used joule heating has become the most widely used device for the perturbation of equilibria of biological interest. Although there are descriptions of other temperature jump devices in the literature (19, 20) and in commercial production, all of the improvements of the method which have been successful and practical came from the work of Eigen and de Maeyer (21). Accurate resolution of very small changes in light transmission and the measure-

ment of fluorescence changes on the microsecond time scale during chemical relaxation processes has permited the observation of multiple relaxation processes. Although the so-called relaxation spectrum of an enzyme system contains a great deal of information, its interpretation can be very difficult.

The great advantage of the relaxation method arises because neither mixing nor transport of the reaction system are required to initiate observation of the changes. Thus the time-limiting features of the flow methods are avoided. A number of important applications of relaxation techniques to the study of enzyme-catalyzed reactions have been made, most notably by Hammes (22, 23). Individual mechanistic processes such as protein conformational changes, the presence of multiple equilibria and the determination of binding steps have all been elucidated with this technique. Gutfreund (21) and Gibson (24) have reviewed some of the recent successes of both relaxation and flow methods, and give several examples of their application to the study of transient processes. An excellent example of the complimentary use of flow and relaxation methods is the work by Kirschner et al on yeast glyceraldehyde-3-phosphate dehydrogenase (25, 26).

The combined flow-perturbation method (27) can be used in either the continuous or stopped-flow mode. If the turnover is very rapid and steady states can be maintained only for very short periods, the continuous-flow

mode is preferable. However, the heated solution
(T-jump) remains in the observation chamber for a
very short period so that only very fast relaxations
can be measured. The stopped-flow mode overcomes difficulties of this kind, but if the utilization of substrate
is not slow compared with the relaxation, large changes in
the steady state concentration of intermediates can make
the smaller changes due to relaxation uninterpretable.

Despite these difficulties, the stopped-flow temperature
jump technique has yielded new information about several
systems. The mechanism of ribonuclease is an example
(28). Theoretical and practical discussions on the combined techniques are reviewed by Erman and Hammes (27).

Relaxation techniques are generally useful but are somewhat limited in their applicability to the studies of enzyme reactions. Many enzyme-catalyzed processes have very small or very large equilibrium constants, and it is often not possible to produce significant perturbations. In T-jump experiments, processes must be faster than a few hundred milliseconds because of cooling effects.

Since the time scale of most relaxation processes is microseconds, only spectrophotometric detection at a single wavelength is feasible. If perturbations are large enough, complex relaxation spectra can result which are difficult to interpret. Indeed, if the phenomenon is wavelength dependent the situation might become hopeless without additional information.

2.2--The Stopped-Flow Method

In the last ten years several comprehensive surveys of rapid reaction techniques have been published (29-31). Both for historical reasons and because of its wide application to the study of enzyme reactions, the stopped-flow spectrophotometer has received special attention. For a detailed discussion of the development of the stopped-flow method itself the reader is referred to the comprehensive review in the Ph.D. thesis of Papadakis (32). Although many minor improvements on the simple design of Gibson (33) have been introduced (30, 34), no significant improvement in overall performance has been achieved in recent years.

Berger et al. (35) have described a stopped-flow device which provides a time resolution of about 250 µs. However, this instrument has so far provided very limited data. The only flow method which has been used successfully for the study of reactions with half-times of less than 1 ms is the continuous flow device of Chance et al. (36).

The range of physical parameters and the sensitivity of their detection provide the widest scope for the improvement of flow methods. Split-beam and dual wavelength systems similar to the one designed by Hess (37) for the measurement of the spectral characteristics of transients in the stopped-flow mode have been described. Systems capable of rapidly scanning the absorption spectrum during

reaction have been reported (38); however, none of these systems have been applied to the study of enzymic processes. Computers and transient recorders have proven useful for improving the overall reproducibility, sample throughput, and data analysis. More importantly, they permit automatic collection and processing of data obtained during the observation of transients.

The resolution of second-order processes involved in enzyme-substrate and other ligand-macromolecule interactions which characteristically approach 10⁸ M⁻¹ sec⁻¹ depends on the detection of the reaction in very dilute solutions. Fluorescence changes have proved especially valuable for this purpose. A number of designs similar to those of Gibson (39) and Fernley and Bisaz (40) have been used with only minimal modification of the transmission optics of the stopped-flow apparatus. Second-order rate constants approaching 10⁹ M⁻¹ sec⁻¹ have been measured on the millisecond time scale (39). There is no doubt that a stopped-flow spectrofluorimeter built for the analysis of fluorescence spectra of transients will provide more information than merely increased resolution of concentration changes.

Many other physical sensing devices have been used for following rapid reactions and characterizing transient intermediates. However, each has only been applied to one or two systems (39). The use of thermocouples for recording reactions in the stopped-flow mode has been

reported (41); however, it has not been applied to biochemical systems.

Rapid quenching techniques have been developed (42); however, the necessity for analyzing a large number of samples individually has limited its application. The use of automated analysis may make this method feasable for the study and isolation of stable transients.

Sirs (43) and Prince (44) used stopped-flow measurements of electrical conductance and pH respectively for the study of relatively slow enzymic processes; and Chance (45) and Clark (46) used platinum microelectrodes for following changes in oxygen concentration in a stopped-flow apparatus.

Although flow systems have been developed for use with an ESR apparatus (47) no design has as yet appeared for carrying out stopped-flow work with aqueous solutions.

The relatively long response times and dead volumes of most thermal and electrochemical detection devices has limited their application to very rapid processes; consequently, spectrophotometry remains the most versatile and most popular detection system for stopped-flow studies.

2.3--The Scanning Stopped-Flow System

The rapid scan stopped-flow system developed in this laboratory has been applied successfully to the study of reactions of the solvated electron and of aromatic radical ions in non-aqueous media (48-50). A detailed discussion of the development of this system was recently reviewed (32), therefore only a general description will be presented here along with some of the major shortcomings. Additional information may be found in a later chapter of this thesis which is devoted exclusively to the modification of the previous apparatus.

The system has undergone more or less continuous development to accomodate a variety of problems associated with either the acquisition, storage, and processing of scanning data, or to the sensitivity of reactive compounds to air and moisture (51). The reactive nature of solvated electrons and aromatic ions towards air, moisture, and stopcock lubricants necessitated the development (51) of a vacuum-tight, greaseless stopped-flow system in which the solution comes into contact with only glass, quartz, and Teflon. Construction of the mixing chamber and observation cell was based upon the extensive developments in this field by Chance (52), Gibson (53, 54), and others (30). Vacuum-line techniques of solution preparation were required so that dilutions could be made in a closed system. After

experimenting with Plexiglass mixing cells, a method was devised for the construction of an all-quartz precision-bore mixing and observation chamber. To completely exclude air from the system, the syringes used for pushing and stopping were specially constructed to permit back-pumping between two 0-rings.

A Perkin-Elmer Model 108 Scanning Monochromator is used to scan the spectrum during reaction. This permits one to scan the complete spectrum (limited only by the light source and the detector) at a rate of up to 150 spectra per second. Of course, the signal-to-noise ratio (S/N) is less favorable under scanning conditions because of the increased signal bandpass which is required and because of vibrations of the monochromator system. However, the ability to determine changes in the shape of the absorption spectrum during reaction has proved most valuable. Once the general features of the spectrum have been studied, it is possible to increase the S/N by studying the absorbance at a fixed wavelength. Reactions with half-lives less than about 15 msec should also be studied at fixed wavelength.

The introduction of a scanning capability has not been without its problems. One of these is the wide dynamic range of the output voltage from the photomultipliers during a scan. The variations of both the lamp output and the photomultiplier sensitivity with wavelength

make it not uncommon for the signal to change by a factor of 100 or more during a scan. To overcome this problem and also to provide a more convenient display, double-beam techniques together with a logarithmic operational amplifier have been used, so that intensity is converted to absorbance.

Because of the rapidity with which data are collected, it is necessary to store data during a run. The previous scanning stopped-flow system used an Ampex SP-300 FM tape recorder to initially store the data. The analog signal stored on tape was then converted to digital form for computer analysis by using an off-line Varian computer of averaged transients (CAT) coupled to a card-punch.

The instrument response as a function of wavelength was calibrated during each run with didymium or holmium oxide glass filters as well as neutral-density filters.

The entire system was calibrated from time-to-time by using standard solutions and standard reactions. Path lengths of 1.0 and 2.0 mm have been used and the absorbance follows Beer's law up to an absorbance of at least two (87). Computer programs have been written to correct the raw data for variations of the instrument response as a function of both absorbance and wavelength.

Although the FM tape recorder was far more versatile and convenient than the earlier oscilloscope - camera combination, there remained several disadvantages. Chief

among these was the noise which was introduced by the tape recorder. This made it difficult to obtain good data, especially near the end of the reaction. Another major disadvantage of the previous system was the inability to rapidly analyze data during a run. With a scanning system it would be an advantage to be able to test for the presence of intermediates or side reactions and to alter conditions to make use of this information. Finally, the information collected during a run of one or two days' duration required several weeks to edit and transfer to punched cards. For all of these reasons, the data collection system was modified to permit use of a PDP 8-I digital computer for data collection and handling.

The stopped-flow method has proven to be an effective tool for the study of a variety of enzymic reactions. At present, only spectrophotometric detection is capable of covering the broad range of reaction rates and signal levels that are encountered in kinetics studies. The ability to either scan the spectrum during reaction or to study absorbance changes at fixed wavelength has proved extremely valuable and should be equally valuable in the study of enzymic reactions.

2.4--Data Analysis Techniques for the Study of Enzyme Kinetics

2.4.1 -- Initial Rate Method

Even the simplest enzyme catalyzed reaction mechanism gives rise to complex rate expressions which are coupled non-linear differential equations that have not yet been solved in analytical form. Most studies in enzyme kinetics avoid this problem by using only "initial rate" data together with three simplifying assumptions; (1) steady-state is maintained for all enzyme-substrate complexes during the initial rate period, (2) inhibition due to product formation is insignificant at early times, and (3) only a small fraction of the substrate reacts so that the substrate concentration may be assumed equal to its initial concentration (S₀). With these assumptions it is possible to derive initial velocity expressions that are functions of only kinetic constants $(K_m, V_{max}, etc.)$ and initial concentrations (S_0, E_0) . These functions of kinetic constants become more complicated as the reaction mechanisms become more complex; however, the equations relating the initial velocity (Va) to initial substrate concentration still have a simple form. Values for the kinetic constants $(K_m, V_{max}, etc.)$ are most often obtained graphically (55) by using simple plots of 1/v_i versus 1/S_o. Although the initial rate method is simple, it has several disadvantages: (1) many runs are needed to construct a single $1/v_1$ versus 1/S plot; (2) "initial rate" analysis provides no information about progress curves for the enzyme-substrate complex. (3) the steady-state assumption may be invalid, and the size of this type of error is often not evaluated (56, 57) (4) in order to differentiate between mechanisms both forward and reverse reactions must be analyzed (58, 59). In general, for a given reaction the "initial rate" method cannot determine as many rate constants as the method of full-time-course integration (56). Indeed, whenever E_0/S_0 is not small, or the enzyme mechanism involves regulatory processes, the "initial rate" method cannot be applied.

Approximate solutions to enzyme kinetic equations have been obtained for some mechanisms (60, 61) using primarily the three techniques which are briefly outlined below.

2.4.2--Approximate Solutions

2.4.2.1 -- Algebraic Solutions After Simplifying Assumptions

It is possible to obtain explicit algebraic solutions by assuming (1) steady-state on all intermediates, (2) rapid equilibrium preceding further steps, and (3) the pseudo-first-order approximation. These assumptions linearize the differential equations and render them solvable. However, such assumptions are not always justifiable, and the errors which they introduce are often not specified.

2.4.2.2 -- Pertubation Schemes

Explicit algebraic solutions can also be obtained by using Self Consistent Well-Ordered Perturbation Schemes. In this technique a perturbation parameter is defined, which, as it approaches zero, linearizes the equations and makes them solvable (for an example see Heineken (56)). The concentration variables are expressed as Taylor's series. The series are then substituted into the differential equations and the series coefficients are determined. As long as the series converges, an exact solution is possible and errors can be estimated. Accuracy can be improved by including higher order coefficients. The perturbation scheme can be used to determine the fulltime-course of the reaction for all species. Although the technique is quite general in scope, it has not found widespread application in enzyme kinetics, probably because of the complexity of the equations obtained.

2.4.2.3--Numerical Solutions - (by Newton, Runge Kutta, Monte-Carlo or analog methods)

By far the most general method for solving complex differential equations is by numerical integration with the aid of a computer. This method will always work and it is simple to use no matter how non-linear the differential equations are. Although it yields no explicit algebraic solution, and computing costs can be considerable

for some cases, the numerical integration technique provides all of the information available from full-time-course integration, without confining the solution to any set of artificial experimental or mathematical assumptions.

2.4.2.4 -- Present Study

Since it is not the goal of the present work to develop analytical solutions to differential equations, all experimental data are fitted over their entire time course by using appropriate analytical functions or by numerical integration of selected differential equations. Data analysis is accomplished with the help of a general non-linear weighted least squares computer program KINFIT (62). Appropriate statistical information permits estimation of the errors, and "goodness of fit."

Other data treatment schemes are available to calculate absolute absorbance, time, variance etc. and are described elsewhere (63). No general procedures are available to accommodate the presence of several time-dependent phenomena at a single wavelength. It is not difficult to discern the presence of wavelength dependent rate phenomena; that is, check for the presence or absence of "clean" stoichiometry (64). It is another matter however to resolve complexity when data which do not show "clean" stoichiometry are fitted to selected rate expressions.

2.5--Computer Systems

The fundamental advantages of computer interactive instrumentation are manifold and well established. Frazer has presented a review on the general use of small computers in the laboratory (65). Others have presented discussions of terminology and practice in the design and use of digital systems (66-68). In fact, the digital computer has become a common instrument in many laboratories and it is no longer necessary to describe its operating characteristics or the fundamental interfacing procedures in detail. It is not generally true however, that existing on-line systems are currently being used to fully exploit the capabilities of computerized instrumentation.

In the present work, a computer interactive system for acquiring and processing data from the rapid scan stopped-flow apparatus is described. A number of interactive on-line stopped-flow systems have been reported (69-71) which were designed primarily for analytical applications at a fixed wavelength. Pardue (72) and a commercial concern (73) have described computerized rapid scanning systems which utilize silicon-vidicon detectors. The performance of these systems, however, has not been tested on enzyme systems which demonstrate spectral intermediates in the ultraviolet region of the spectrum.

The previous data processing system for the scanning stopped-flow apparatus has already been described (87).

25

and some of its major disadvantages were discussed earlier. Since the computer-interfaced system is presented independently in a later chapter, the reader is referred to that section for more details on its operating characteristics.

Although the computer system was designed and constructed specifically for this project, it utilizes typical hardware components and general interfacing and software techniques wherever possible. The hardware and software systems are described in detail in two laboratory manuals (63, 74).

2.6--Transient-State Enzyme Studies

Three enzyme systems were chosen in order to test the rapid-scan stopped-flow system. Although it was necessary to work at wavelengths above 300 nm, this restriction will soon be removed. The systems chosen and the reasons for their choice are as follows:

1. Complex formation between the co-enzyme nicotin-amide-adenine dinucleotide (NAD⁺) and the enzyme yeast glyceraldehyde 3-phosphate dehydrogenase (GAPDH) has been extensively studied by Kirschner (25, 26) who showed that a conformational change occurs upon binding accompanied by the growth of an absorption band at 350 nm. We chose to study this system because of its well-known spectral changes in an easily ascessible region. The system provides a good test of sensitivity since a maximum absorbance

change of only about 0.08 absorbance units occurs on a rather large background. Also, the necessity to work at 40 °C provided a good test of the thermostat system.

- 2. A large number of enzymes show complex absorption spectra in the visible region because of Schiff-base formation between the enzyme and a co-enzyme. The enzyme L-threonine dehydrase (TDH) of E. coli has an absorption band at 415 nm because of Schiff-base formation between pyridoxal phosphate and lysine residue of the enzyme (5.75). The addition of L-threonine in the presence of AMP causes a transient shift of the absorbance to a new band at 450 nm during the formation of product. Because of the very low turnover number even at high enzyme concentrations, it is difficult to follow both the rapid formation of the complex and the growth of product. However, the averaging scheme available with our system is ideally suited for this purpose. This cooperative study with W. A. Wood of the Biochemistry Department also gave us the opportunity to find out how much information could be obtained with a small amount (6 ml) of solution and less than 10 mg of enzyme. The wealth of information available from a single scanning push in this preliminary study indicates the power of this new instrument for transient-state studies.
- 3. A third test system for the scanning stopped-flow instrument which proved to be most interesting involved the enzyme equine liver alcohol dehyrogenase (LADH) and

its catalysis of the reduction of the substrate analog p-nitroso-N,N dimethylaniline (NDMA) by reduced nico-tinamide adenine dinucleotide (NADH). This system was selected for several reasons:

- a) At least one transient species is formed which has an absorption spectrum distinct from those of reactants and products and which appears to form in excess of the active site concentration. The similarity of its spectrum to that of NADH has led to its assignment as a complex between NADH and the substrate analog (109).
- b) The time course of disappearance of the substrate analog and the intermediate are different which affords an opportunity to use the scanning stopped-flow system to study the kinetics at a number of wavelengths for a single push. The absorption bands occur in a convenient wavelength region.
- c) The enzyme LADH is well characterized and commercially available in satisfactory purity.

Additional background information for these systems will be discussed in the Results section.

III. EXPERIMENTAL

The following experimental details refer only to the runs with enzyme. Experimental details for the other systems which were used for performance tests are given elsewhere (32).

3.1--Glassware

All glassware, including the flow system, was soaked overnight with 2N HCl, and subsequently extensively rinsed with quartz distilled conductance water. The glassware was then rinsed with the appropriate buffer solution in preparation for the run.

Stock solutions were made up in Pyrex bottles which were equipped with Teflon valves (Kontes Co., Vineland, N. J.) and the appropriate joints (Fisher Porter 5 mm Solv-Seal) for connecting the bottles to the input ports of the flow system. Stock solutions were degassed under vacuum and subsequently re-pressurized with purified helium. This process helps to reduce foaming which can lead to denaturation of the enzyme solutions.

3.2--Glyceraldehyde-3-phosphate dehydrogenase

Crystalline yeast glyceraldehyde-3-phosphate dehydrogenase (GAPDH) was prepared essentially as described by Kirschner and Voigt (76) with only a few minor modifications. These were associated with the application of the charcoal treatment after the first fractionation with ammonium sulphate and before the protamine sulphate step (as suggested by Kirschner (25)) to remove bound nucleotides. The preparation attained a value of $E_{280}/E_{260} = 2.05 \pm .07$ compared to Kirschner's value of $2.15 \pm .05$. The enzyme was assayed in the direction of formation of 3-phosphoglycerate using essentially the assay technique of Stancel (77). An average specific activity of 133 Units/mg was obtained which is substantially larger than the value of 80 Units/mg reported by Stancel.

The concentration of GAPDH for kinetics studies was determined spectrophotometrically using both $E_{280}^{12} = 0.894$ ml mg⁻¹ cm⁻¹ for the pure enzyme and the Biuret method for total protein. The enzyme was electrophoretically homogeneous; however, the kinetics results indicate that the fraction which was used contained components with different kinetic properties. GAPDH from the DEAE Sephadex column was dialyzed against the buffer just prior to use. The buffer (pH 8.5) for all solutions was 0.05M sodium pyrophosphate, 5 mM EDTA, 5 mM sodium arsenate, and

0.2mM dithiothreitol.

Nicotinamide adenine dinucleotide (\$\beta\$- NAD⁺, grade
III, Sigma Co.) was used for the kinetics studies.

D,L-3-phosphoglyceraldehyde (GAP) was prepared from the barium salt of the diethylacetate (Sigma - Dowex preparation), and assayed using NADH production at 340nm to determine the concentration of the D enantiomer for kinetics experiments. Concentrations of GAP refer to the D enantiomer only. In general, concentrations refer to the concentration of the species upon reaction (i.e. after mixing). Solutions for the GAPDH runs were equilibrated to 39.9 \(\frac{1}{2}\). 1°C in the bath prior to reaction.

Additional information is given in TABLE I.

3.3--Threonine Dehydrase

Threonine dehydrase (TDH) from E. coli was a gift from Professor Wood (78). TDH concentrations were determined spectrophotometrically using $E_{lcm, 466}^{1\%} = 1.75$ (5). A specific activity of 395 Units/mg was determined from the production of α -ketobutyrate at 310nm, $\epsilon = 20.4 \, \text{M}^{-1} \text{cm}^{-1}$ (5) in an assay solution containing 1 ml of 50mM L-threonine in buffer, pH 8.0, 28 °C.

Stock enzyme solutions were made up in 0.1M sodium phosphate buffer pH 8.0 containing lmM adenosine monophosphate and lmM dithiothreitol. In a typical push, solutions of TDH (0.74 mg/ml final) and L-threonine (25mM) equilibrated

to 24.5 °C were rapidly mixed in the stopped-flow. Sampling parameters for the TDH run are shown in TABLE I.

3.4--Liver alcohol dehydrogenase

The commercially available compounds acetonitrile (Baker Chemical Co., reagent grade), p-nitroso-N,N-dimethyl-aniline (NDMA, Aldrich Chemical Co.), and nicotinamide adenine dinucleotide (NADH, Sigma Co., grade V) were used without further purification. The concentrations of NDMA, NADH and LADH stock solutions were determined spectrophotometrically using extinction coefficients of $\epsilon_{\mu\mu0} = 3.5\mu$ X 10⁻⁶ M⁻¹ cm⁻¹, $\epsilon_{3\mu0} = 6.22$ X 10³ M⁻¹ cm⁻¹, and $\epsilon_{280} = 0.455$ ml mg⁻¹ cm⁻¹ respectively. Solutions were made up in 0.05M sodium pyrophosphate buffer, pH 8.75. NDMA stock solution was prepared by dilution with buffer of an aliquot of 1 mM stock solution of NDMA in acetonitrile.

Equine liver alcohol dehydrogenase (LADH, Sigma Co.) was further purified by overnight dialysis of a concentrated LADH solution against several liters of buffer. A specific activity of 22.9 Units/mg was determined at 440 nm using an assay mixture of 3.18 x 10⁻⁵N NDMA, 8.18 x 10⁻⁵M NADH, and 4.9 x 10⁻³ mg/ml LADH in buffer.

Rapid mixing experiments were carried out at $23 \pm .1$ °C. Appropriately buffered solutions of NADH (4.09 X 10^{-5} N after mixing) and NDMA (1.59 X 10^{-5} N) were premixed (just prior to reaction) and subsequently reacted with LADH (3.62 X 10^{-6} N). Refer to TABLE I for the

sampling parameters.

3.5--Sampling Parameters

The RCA 6903 photmultiplier tubes were used for all three enzyme runs. Glass filters and copper sulphate solutions were used to eliminate unwanted UV and IR radiation. A path length of 1.85 cm and a scan speed of 75 spectra per second were used for all three enzyme runs. The monochromator gives both a forward and a reversed spectrum for each scan. Since only foward scans were collected, the actual scan rate was 37.5 spectra per second (ie. the duration of each spectrum was 13.33 ms and the time between spectra was 13.33ms). A slit of 0.5mm was used for the GAPDH run, and 0.6mm was used for the TDH and LADH runs. The remaining sampling parameters for each of the enzyme systems are given in TABLE I.

3.6--Data Analysis

Results from the enzyme runs, stored digitally on magnetic tape, were first examined extensively with the display scope. Subsequently, the time development at several selected wavelengths was output for each push to punched cards. The raw data were submitted to the CDC 6500 along with program ABSTIM (63) for additional processing. The ABSTIM routine converts the raw data to absolute absorbance using the values for the

TABLE I

Sampling parameters for the GAPDH, TDH and LADH Runs.

Sampling frequency=20.4KHz

Sampling Parameter	GAPDH-NAD ⁺ Complex Formation	GAPDH Reaction with Substrate	TDH	LADH
Number of Groups	6	5	7	6
Samples/Point	4	4	6	5
Spectra/Group	8	10	12	12
Points/Spectrum	64	64	40	48
Grouping Factor	2	2	3	2

calibrated neutral-density filters in the same way as program PUNDAT (79). Each push has associated with it all the sampling parameters (SAVPAGE). Thus, the time for each point can be determined, and appropriate adjustments for flow and stopping times can be made. Variances are computed from estimates of the standard deviation, taking into account the degree of averaging within each group of points. Finally, data are repunched in a format suitable for direct submission with the KINFIT program.

IV. THE COMPUTER SYSTEM: DESIGN CONSIDERATIONS AND CONSTRAINTS

The following chapter is essentially in the form of a manuscript which will be submitted for publication.

The stopped-flow technique involves the rapid mixing of solutions from two syringes in a specially designed mixing and observation cell followed by rapid stopping of the mixed reactions by a third syringe located downstream. In our case the extent of reaction is monitored spectrophotometrically either at a single wavelength or by rapidly scanning the absorption spectrum.

Rapid scanning stopped-flow kinetics presents special problems to the experimenter which are not encountered in fixed wavelength work. Since the duration of the experiment ranges from a few seconds to several minutes and the monochromator can scan at speeds up to 150 complete spectra per second, an enormous amount of three dimensional data must be rapidly processed and stored.

Actual stopped-flow runs require only a small fraction of the total experimental time, so that a dedicated computer is not necessary. Therefore, although the stopped-flow apparatus was located in the basement, it was interfaced to an existing computer system located on the fourth floor.

Thus, needless duplication of expensive equipment, particularly the peripheral Input/Output devices was avoided. A remote parallel digital data transmission system of this type should be generally useful where the availability of small computers is limited and high frequency data transmission over relatively long distances is required.

4.1--Signal Enhancement in Real Time

In typical rate studies, the signal varies rapidly at first and then progressively more slowly as the reaction approaches completion (or equilibrium). It is therefore desirable to use a wide bandpass at the beginning of a reaction but this necessity decreases as time increases. Most systems are designed for a fixed bandpass; that is, filters are selected prior to the experiment and then not changed during the experiment. Even in these cases, one must be careful in selection of the filters since analog filtering can distort the signal shape. In contrast to this, digital filtering (appropriate averaging or smoothing) can provide a bandpass which varies with time as needed.

Narrow slitwidths resulting in decreased light intensities, coupled with the mechanical vibrations of the monochromator are the primary causes for the inherently poorer S/N associated with scanning experiments. This is particularly troublesome in the case of enzyme reactions where absorbance changes are generally small and spectral perturbations are often subtle.

Optimum on-line use of the mini-computer is achieved by sampling the data signal at a maximum constant rate which is limited by the computer software and not by the experiment (80). Data storage requirements are reduced and simultaneous real time S/N enhancement in both the wavelength and time domains is achieved by establishing a variable bandpass with the system software.

4.2--Determination of the Maximum Sampling Rate

In the rapid scanning stopped-flow experiment full scale signal deflections occur on the millisecond time scale as a result of changing wavelength and extent of reaction. With traditional fixed wavelength systems some kind of clock oscillator provides a convenient sampling frequency which remains constant during the entire reaction. More sophisticated instruments have utilized programmable clocks to decrease the sampling rate as the reaction proceeds, thus reducing the quantity of stored data. These approaches were rejected for several reasons: (1) asynchronous sampling would preclude the ultimate effectiveness of spectral averaging, (2) the wavelength variable continues to change on the millisecond time scale even at equilibrium; hence, reduced sampling rates would lead to poorly defined spectra, and (3) decreased sampling rates near the end of reaction ignore some of the most vital data for fitting the kinetic record to complex rate expressions.

present work the guiding principle was to use the maximum sampling frequency and to perform appropriate digital averaging. This results in real time S/N enhancement and simultaneously reduces absolute storage requirements. It was estimated that approximately 40 µs would be required by the computer to complete the data acquisition, averaging and storage cycle. Thus the maximum sampling frequency was approximately 25 KHz. This sampling frequency is well within the capabilities of a moderately priced medium speed A/D converter.

We also wanted to synchronize sampling with the nutating mirror of the monochromator. Wavelength is scanned by the change in angle (relative to the light beam) of this mirror as it rotates. The gear attached to the mirror shaft has 136 teeth which interrupt a light beam and produce a signal (GT) whose frequency varies with the scan speed up to a maximum of 10.2 KHz at 150 spectra per second (see TABLE II). Once during each revolution the light beam is reflected from a polished tooth to produce the beginning of scan (BS) pulse. The GT signal is input to a frequency multiplication system which ultimately generates the trigger used for sampling. In this way, a sampling frequency of 20.4 KHz is readily obtainable at any scan speed and is compatible with the time requirements of both the computer and the ADC.

Scanning Monochromator and Phase-Locked Loop Parameters. Output Sampling Frequency = 20.4 KHz. TABLE II

Spectrum											
# of Samples per Spec	136	170	272	340	680	1360	2720	3400	5440	6800	
Hz Mult. Factor (÷N)	4	S	ω	10	20	40	80	100	160	200	
GT HZ Flip Flop	5100	4080	2550	2040	1020	510	255	204	127.5	102	
GT Freq. Hz	10200	8160	5100	4080	2040	1020	510	408	255	204	
msec/spectrum	6.67	8,33	13,33	16.67	33,33	66.67	133,3	166.7	266.7	333.3	
Rev/sec	75	09	37.5	30	15	7.5	3,75	3.0	1,875	1.5	
Scans/sec	150	120	75	09	30	15	7.5	0.9	3.75	3.0	

4.3--Averaging Scheme

Stopped-flow data must be stored initially in computer core because of the time scale of the experiment and the relative slowness of peripheral computer storage (magnetic tape). For a given push, data storage is limited to whatever space remains after resident system software has been loaded. This fact was of primary importance in the development of data acquisition software for the scanning system. At a sampling frequency of 20.4 KHz one would rapidly exhaust the storage capacity of the 8K computer. While a bandpass which simply increases with time in a pre-determined way would be satisfactory for fixed-wavelength data. it is not applicable to scanning data since the signal changes with time in a way which is determined by the spectrum and the scan rate and not merely by the rate of reaction. We have devised a scheme which operates equally well in either mode. For simplicity its operation with fixedwavelength data will be considered first.

Consider an absorbance peak which decays as a function of time (see Figure 1 for example). Initially the signal is changing very rapidly with time and excessive averaging would distort the decay curve. At long times, when the signal is slowly changing with time we would like to average a number of adjacent samples (not simply

decrease the sampling rate) in order to increase the S/N in the very important "tail" of the reaction. Thus, what is needed is a variable frequency bandpass as the reaction proceeds. The averaging process chosen is best represented by an example.

Consider a reaction in which the absorbance decays in a second order fashion with a half-life of 50 ms. Suppose we have an absorbance with an initial S/N of 100 (based upon four samples per point). As the reaction proceeds through six half-lives, the absorbance decreases to 1.56 per cent of its initial value with a concomitant decrease in S/N expected if the number of samples per point were not changed. In the averaging scheme selected for this example, the total time is arbitrarily divided into 10 groups of 16 data points each (see Figure 1). In an actual experiment the number of groups and the number of points would be pre-set. These parameters are chosen according to the rate of reaction and the number of half-lives to be measured. A grouping factor is selected which determines the modulus by which the averaging bandpass is increased as the reaction proceeds. Each of the stored points in Group 1 is actually the average of four 49 \(\mu \) samples (20.4 KHz) and the first group extends in time to 3.14 ms of reaction. The second group also contains 16 points, each of which is the average of eight 49 us samples. Group 2 extends in time to 9.4 ms. In this

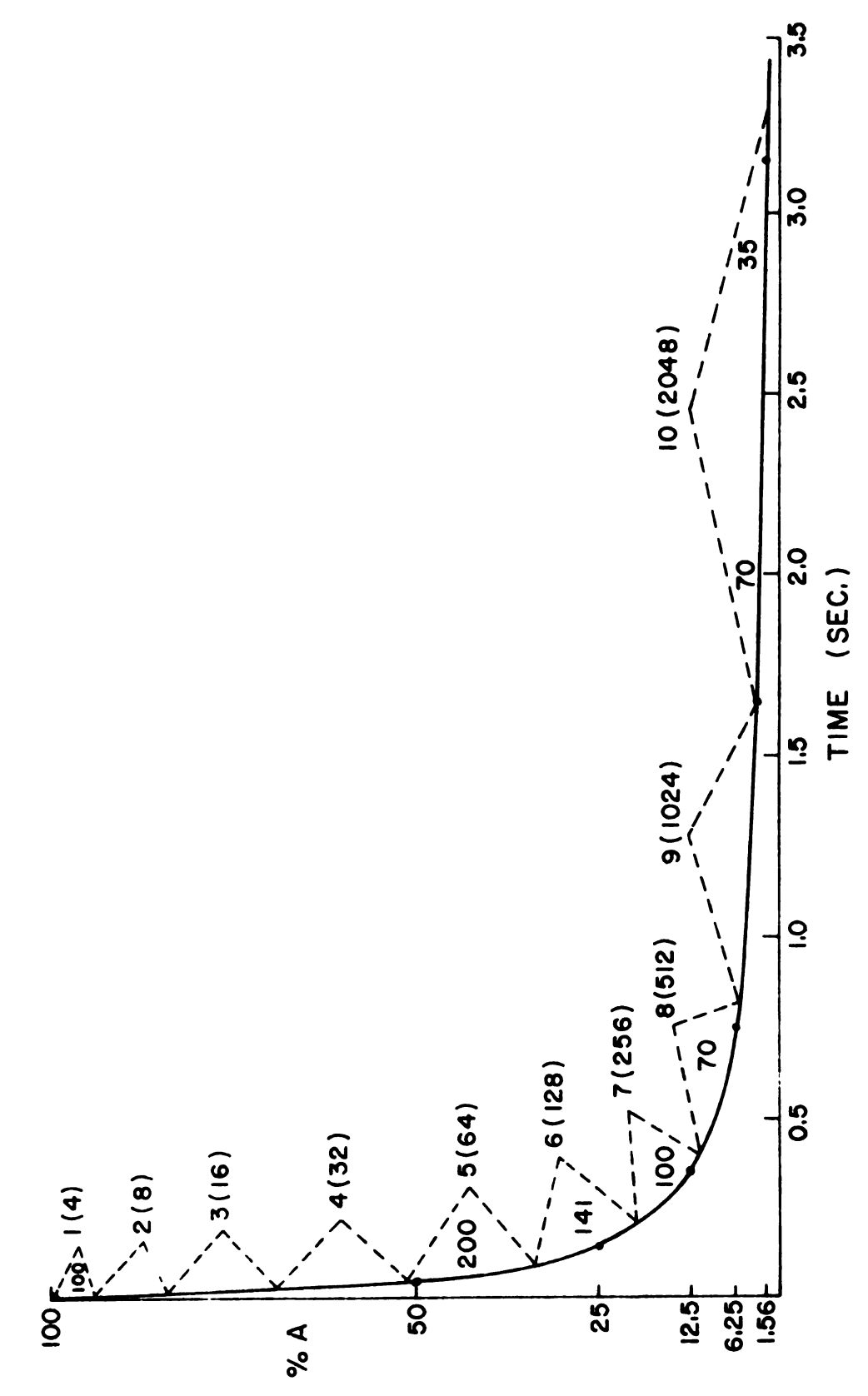


Figure 1. Example of the averaging scheme for a fixed wavelength case.

way each group contains twice as many samples per point as the preceding group and the total elapsed time doubles. For an arbitrary grouping factor, g, group number, n, elapsed time at the end of the group, t_n , and samples per point s_n we have

$$s_n = g^{n-1} s_1 \tag{1a}$$

$$t_n = (g^n - 1)t_1 \tag{1b}$$

After six half-lives only 160 points are stored; however, 65,472 samples are actually measured. One ebvious advantage of the technique is that the total number of stored locations is reduced without ignoring useful information. Secondly, we can expect significant S/N enhancement. For a random, constant noise level we have for the signal in group n (Sn)

$$(S/N)_n = g^{\frac{n-1}{2}} \cdot (S/N)_1 \cdot \frac{Sn}{S_1}$$
 (2)

For example, at the ends of the first (Group 5) and sixth (Group 10) half-lives we can expect S/N values of 200 and 35 respectively. Because of this S/N enhancement, small changes in the signal at long times can still be detected. Obviously, for very fast processes little can be done to improve the S/N in real time since

6

b a.

ma pr

fi. br

308

the res

Spe.

ing ing

iete

1991

io ti

An p

10

excessive averaging would lead to signal distortion.

The ability to scan wavelength during reaction adds another dimension to the averaging problem. In this case the number of points per spectrum (P/S) is selected by averaging an appropriate number of adjacent samples as the spectrum is scanned. Once this selection is done the averaging bandpass for the wavelength variable remains fixed (for that reaction) while averaging in time proceeds according to the scheme outlined above for fixed wavelength. For moderately fast reactions involving broad featureless spectra, the S/N is enhanced by averaging more adjacent samples. As wider wavelength regions are scanned or as the complexity of the spectrum increases, the number of points per spectrum required for adequate resolution also increases. As the number of points per spectrum increases however, the total number of spectra which can be stored for a given push decreases. The averaging bandpass for the wavelength variable is, therefore, determined by the reaction conditions, wavelength resolution desired and the amount of storage available.

Averaging in time is accomplished by averaging appropriate numbers of consecutive spectra. Analogous to the fixed wavelength case, once the number of samples per point and points per spectrum are determined, the time course of the reaction is divided into groups.

Each group contains the same pre-determined number of spectra. Each of the "stored" spectra within a particular group actually represents the average of c consecutive spectra where c is determined by the group number n and grouping factor g according to (3)

$$c_n = g^{n-1} \tag{3}$$

The total number of samples averaged into each point of the stored spectrum is given, as before, by equation la. The grouping factor has a marked effect upon the total time span. For example, choosing a grouping factor of 2 with 10 spectra per group and 5 groups yields a total of only 50 stored spectra out of 310 measured spectra. For a grouping factor of 3, the 50 stored spectra would result from 2430 collected spectra. Obviously when the time development at a particular wavelength is extracted from the scanning record, times appropriate to the averaging scheme must be used.

A software-generated variable bandpass averaging scheme is extremely versatile, limited essentially by the experimental conditions and/or data storage capacity.

There is a trade-off between resolution and S/N enhancement on the one hand and storage limitations on the other. The relationship among the sampling parameters for the available storage in our system is given by

$$(P/S) (S/G) (NG) \le 3456_{10}$$
 (4)

for P/S points per spectrum, S/G spectra per group and NG groups.

One of the primary advantages of the variable bandpass technique is that both rapid and slow processes can be recorded in the same experiment. Early groups contain the rapidly changing information while later groups continue to follow slow processes. Even reactions with induction periods can be effectively studied since any number of spectra or samples can be skipped before data collection begins.

4.4--System Control and Timing

On line experiments require certain instrument generated triggers or timing pulses in order to synchronize sample acquisition and storage with the various components of the system. In our scanning stopped-flow system, trigger signals are provided which mark the flow start and stop, the beginning of each spectral scan and the wavelength. These signals are necessary because the three main components of the system (monochromator, stopped-flow apparatus and computer) operate asynchronously.

A common problem in stopped-flow measurements is the determination of the exact zero of time for the reaction. This problem had been particularly troublesome in our scanning experiments when fast reactions were studied

because the time at which flow stops had no relation to the wavelength of the spectral scan. One must have an accurate knowledge of the zero of time in order to establish initial absorbance values at all wavelengths and to avoid using data collected during the period of deceleration. In order to directly compare replicate pushes in the scanning mode therefore one must determine precisely when flow stopped with respect to any particular wavelength. This is accomplished by using trigger signals from the stopped-flow apparatus. Two metal flags attached to the stopping plunger break light beams and cause light sensitive transistors to give the start and stop pulses shown in Figure 2. The start pulse is used to start both the Time Shift Clock and the Flow Velocity Clock (Heathkit Co., Universal Digital Instrument). The Time Shift Clock utilizes the computer real time clock (81) to measure the time between the start flag and the next beginning of scan (BS) trigger.

When the stopping plunger is at a measured small distance from the stopping plate, the stop pulse occurs and stops the Flow Velocity Clock. Since the separation of the two phototransistors is known, the flow velocity can be calculated from the start-to-stop time interval. Measurement of the flow velocity profile showed that the velocity is constant between the start and stop pulses. From Figure 2 it can be seen that knowledge of the flow

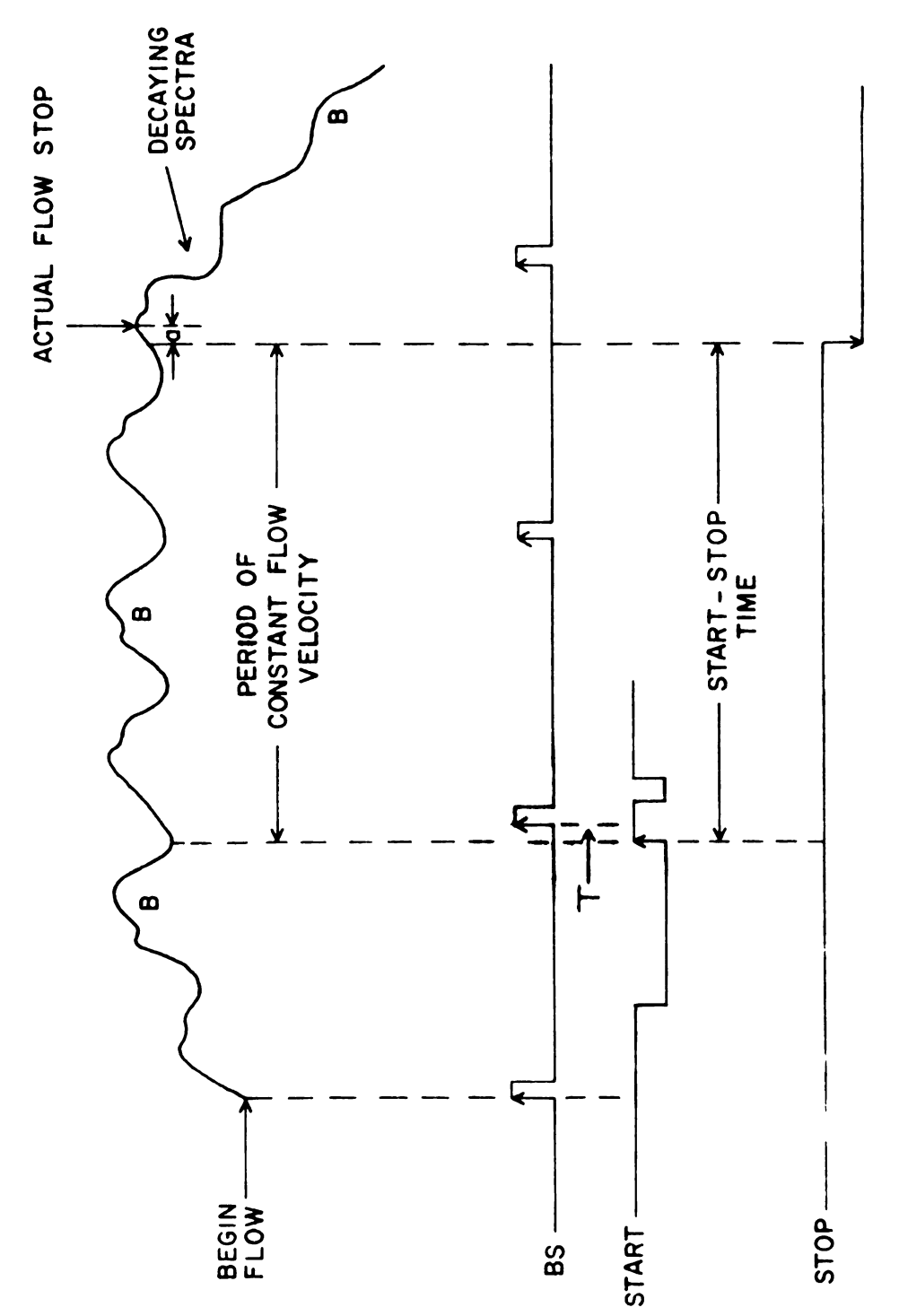


Figure 2. Timing diagram for a scanning experiment

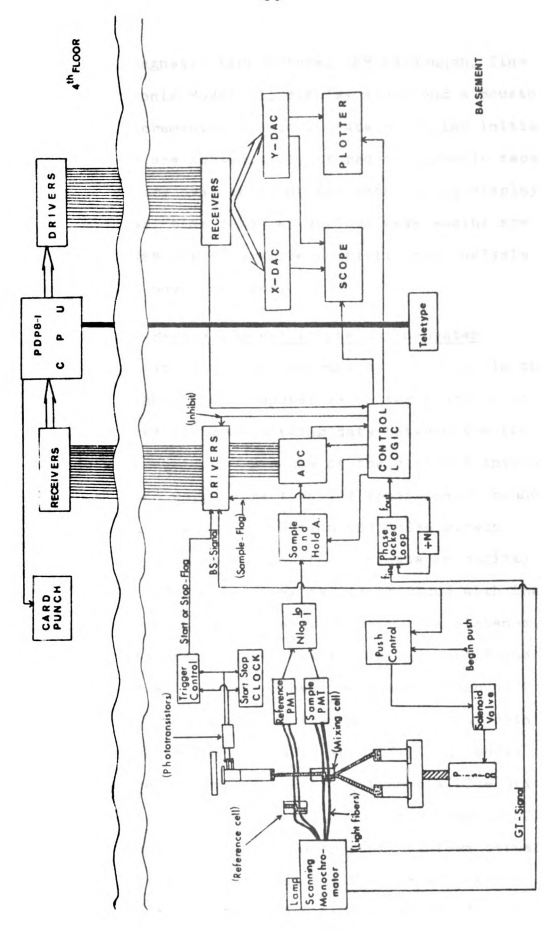
velocity and the timing information permits computation of the zero of time and the corresponding wavelength.

Data acquisition begins with the first sample pulse after the Time Shift Clock is stopped, always at the beginning of a new spectral scan. For fixed wavelength pushes, a Wavetek model 116 Signal Generator is used to provide the 20.4 KHz sampling trigger and the stop flag is used to initialize data acquisition. Once within the sampling mode the system software takes control until sufficient data are collected as determined by the variable bandpass averaging scheme described above.

4.5--System Hardware Description

A block diagram of the overall system is shown in Figure 3. The interface system was constructed from Heathkit modules and printed circuit blanks. Most of the individual circuits such as data latches, octal decoders etc. were constructed on Heathkit printed circuit boards using generally available IC components. The sampling system utilizes an Analogic MP 250 fast acquisition Sample and Hold Amplifier and an MP 2212 12 bit ADC. The display and plotting system uses Analogic MP 1810 high speed 10 bit DAC's.

A Digital Equipment Corporation PDP 8-I computer with 8K of core was used. Computer Input/Output peripherals include Teletypes, high speed paper tape punch/



Block diagram of the computer interfaced scanning stopped-flow system. Figure 3.

reader, dual magnetic tape drives, IBM cardpunch, line printer, Tektronix Model 611 display scope and a Houston Instruments incremental plotter. Data collected initially in core memory are subsequently stored on magnetic tape. After preliminary evaluation of the data on the display scope, selected "time cuts" at various wavelengths are punched onto IBM cards for more sophisticated analysis on the MSU CDC 6500 computer.

4.6--Remote Digital Transmission System

Since the stopped-flow instrument is located in the basement and the PDP 8I Computer is on the fourth floor, a special system for transmitting data between the two locations was required. Because of the distance involved (~150 feet each way), direct analog transmission cannot be used without signal degradation and noise pickup. It was therefore necessary to transmit data in digital form. The Input/Output driver system provided with the computer was incapable of operating over this distance. Conversion kits which permit remote digital data transmission with small computers have recently become available (66). However, these devices utilize serial data transmission which is too low in speed for our needs.

In the present system, Texas Instruments Line Drivers and Line Receivers are utilized in a "party-line" configuration to transmit information in parallel form between the two locations. High speed (up to 10 MHz) data transmission without signal reflections is possible along

a terminated transmission line. In such a system, noise is primarily common mode and is rejected by a set of differential input line receivers and a balanced (two wire) transmission system. The transmission system is capable of driving and receiving noise-free data at frequencies up to 10 MHz and distances of several thousand feet (82).

The transmission system consists of 10 dual TI SN75109 Line Driver and 10 dual SN75107 Line Receiver integrated circuits (approximately \$3.00 per dual circuit) powered by Analog Devices Micro Logic 5 VDC power supplies at each end of the transmission line. This line is a Belden 8769 cable (Newark Electronics) which contains 19 twisted pairs of #22 conductors (approximately \$1.00/foot). All drivers and receivers at each end were mounted on a single 6" X 9" circuit board which is connected to the interface with 3M type flat connection cables. The estimated material cost for the complete data transmission system is \$600 (1970).

This kind of transmission system, in a "party-line" configuration may be extended to include a number of stations which share a common transmission line. In this way several laboratories can use a single transmission line in conjunction with the receiver strobe and/or driver inhibit facilities to place several instruments on-line with a remote computer system.

4.7--Multiplication of Sampling Frequency

To sample data at a constant rate even when the instrument-timing pulses are changed requires multiplication of the frequency of these pulses. One could use a programmable clock or voltage controlled oscillator to achieve virtually any sampling rates desired. However, the system described here permits synchronization of data sampling with the instrument timing pulses.

Since operation at the maximum sampling rate demanded extensive time averaging of the data, we required that all sampling triggers be synchronous to the scanning monochromator. The Phase-Locked Loop and Divide by N (PLL) circuit (Figure 4) was constructed to achieve a frequency multiplication of the fundamental timing trigger (the GT frequency) and to produce the 20.4 KHz sampling frequency. The PLL continually corrects its output frequency to keep the input signals at "a" and "b" in phase and of equal frequency. Thus by changing the divide by N number, the output frequency (20.4 KHz) can be made a multiple of the input frequency (GT). As the monochromator scanning rate is changed from one speed to the next, the multiplication factor N must also be changed in order to maintain the 20.4 KHz sampling rate.

The GT pulses arise from the main gear on the rotation tating mirror shaft. Variations in speed of rotation caused by "play" in the gear train would lead to non-

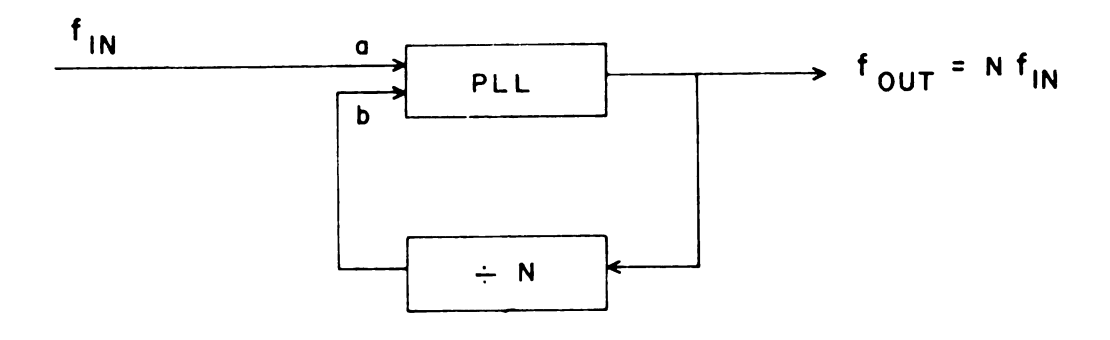


Figure 4. Phase-locked loop and divide by N circuit principle.

reproducibility of the wavelength of a particular sample were it not for the frequency locked system. The PLL system is capable of following the "wander", thereby allowing digital averaging of adjacent samples to be an even more effective technique for enhancing S/N and improving the resolution of the spectrum. The PLL system permits interpolation between GT triggers and, since both the GT and BS triggers originate from the same rotating gear, synchronization of the beginning of scan with individual wavelength markers is automatic. The PLL circuit was constructed on a Heathkit PC board from commercially available components (Signetics NE 565A PLL and Motorala MG 4018P programmable counters).

4.8 -- System Software

This system requires a long and sophisticated set of computer programs. Only 8K of core was available and about half was needed for data storage. To utilize the available core efficiently we divided our software into two main parts: (1) approximately 2.5K of core resident routines which include System Overhead, I/O package, and a Supervisor, (2) Non-core resident routines called Modes or Segments which are loaded into core from magnetic tape one at a time as needed under control of the Supervisor. Control over the system software is performed via Teletype and scope-displayed instructions.

This has proven to be a very efficient way to utilize \$\psi \text{K}\$ of core memory for approximately 18K of software.

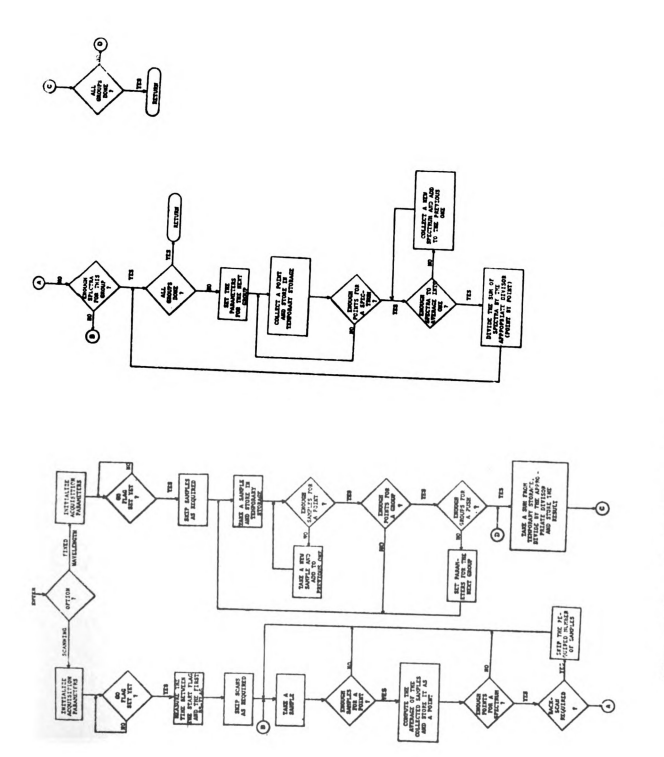
In addition, the amount of software can be easily expanded if necessary.

The flow chart for the data acquisition mode is shown in Figure 5. Only the two main options have been included; namely, scanning and fixed wavelength.

Additional options in this mode provide for absorbance calibration with neutral density filters, wavelength calibration with absorbing glasses, and collection of solvent background and the spectrum at infinite time.

The experimenter merely sets the data collection parameters, or makes changes as required, selects the appropriate option and initiates the stopped-flow experiment (Push). The digital sample collection then takes place according to the following sequence of events:

- (1) start flag occurs push has begun, real time clock is started
- (2) data collection begins on the falling edge of the next BS pulse, real time clock is read and the value stored with the other experimental parameters



Flow-chart for the data acquisition coutines. Figure 5

- (3) The next sample trigger (from PLL) activates the HOLD mode of the SHA
- (4) The same sample trigger is delayed approximately 5 us in order to allow the SHA to "settle", and then triggers the ADC.
- (5) 100 ns before the 12 parallel digital bits are ready, the ADC generates an End of Conversion pulse which after a suitable delay opens the data latch and sends a SAMPLE READY signal to the sample flag.
- (6) The computer recognizes the SAMPLE
 READY FLAG, the inhibit on the data
 line drivers is removed and the sample
 is clocked into the accumulator.
- (7) The computer clears the sample flag
 and proceeds to average and store the
 data. The next sample trigger begins
 the process again. Since the computer
 keeps track of BS pulses, the samples
 are averaged and stored in the correct
 sequence with respect to both time
 and wavelength.

Our scanning system produces a forward and a backward scan on each revolution (one is the mirror image of the other). According to our data acquisition routines, averaging of adjacent spectra does not occur in Group 1. In this way we can collect both the forward and back-scans to obtain better time resolution in the early stages of the reaction. In the remaining groups, back-scans cannot be collected because the time is needed for spectral averaging. If back-scans are collected in the first group they are reversed automatically.

When the fixed wavelength option is selected, the sampling and digitization process begins with the stop flag and goes through steps 2-7. Each data file is stored permanently on magnetic tape. Selected data during flow can be averaged to improve initial absorbance readings which can then be subtracted from the raw data if desired. Solvent backgrounds and/or the absorbance at infinite time can also be subtracted. Subsequently the desired wavelength or time displays can be examined to indicate possible modifications in the experiment. Since the data are routinely transferred to the CDC 6500 computer for kinetics analysis, we have not included data-fitting routines as part of the on-line software package.

Displays of spectral growth and decay with arbitrary scale expansion and selection of particular spectral scans individually or collectively can be obtained on the storage scope. Time developments at any particular wavelength can also be examined on the scope with arbitrary starting and ending times as well as scale expansions. In this way, any desired time period at any point from the beginning of the reaction and at any wavelength can be examined as soon as the push is over. Hardware and software are also available to plot on the incremental plotter whatever data are displayed on the scope. Finally, time displays from the scope can be punched onto computer cards for more detailed data analysis.

4.9--System Performance

In order to evaluate the overall accuracy and precision of the data Input/Output system, known voltages from a Fluke voltage reference source were measured by the computer system and the results were compared by outputing the data to punched cards. The overall accuracy of one part in 4096 showed that the accuracy and precision are limited by the word-size used.

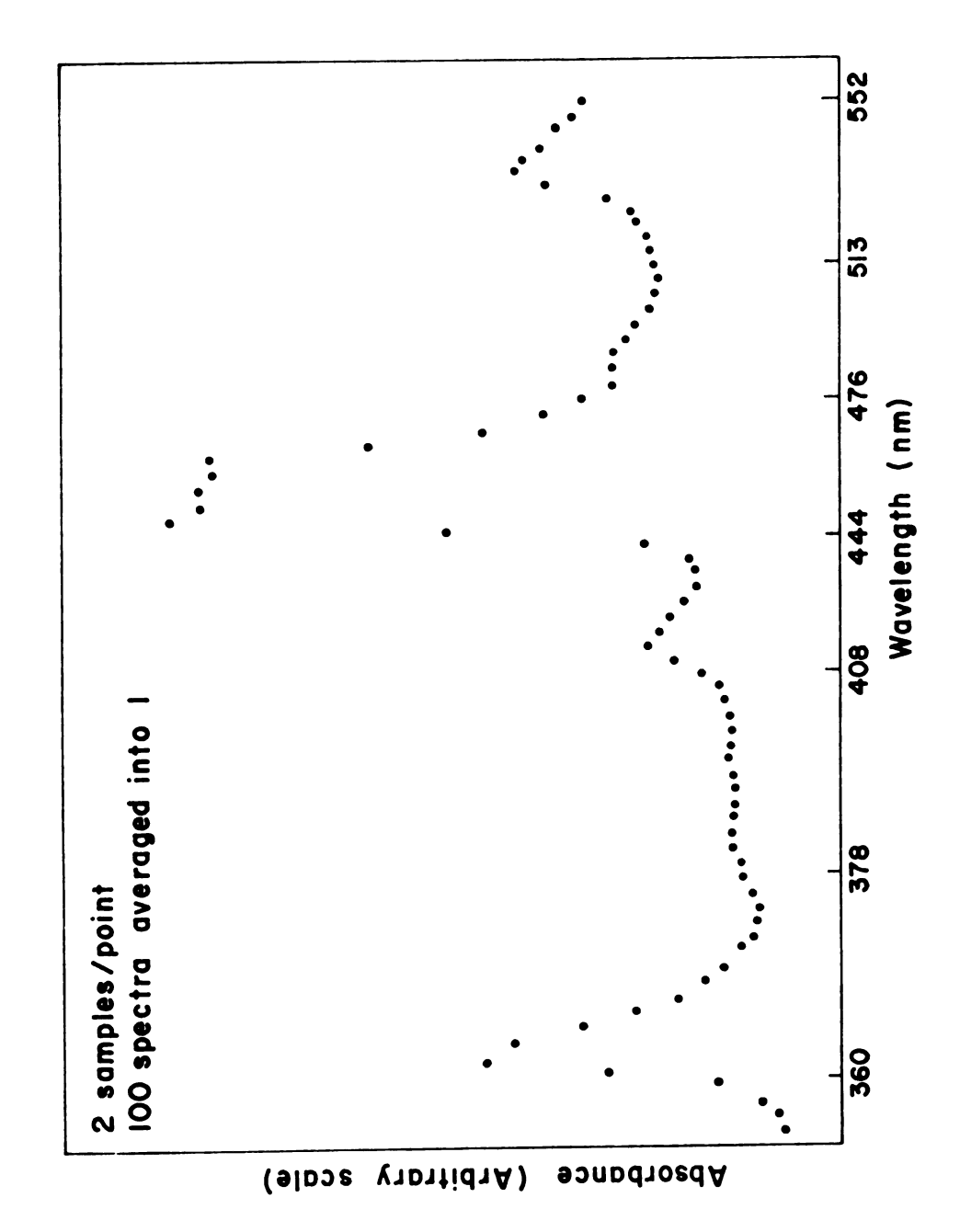
Sampling frequency measurements were also performed with the aid of the computer. For scanning pushes, resolution in time (and wavelength) is dependent essentially on the proper operation of the frequency multiplication

system. With proper tracking and multiplication the PLL system was reproducible to within one sample per scan. Thus the basic digital interface system has proven both accurate and reliable. Elimination of transmission and readout errors resulted in a substatial improvement in S/N over the previous FM tape system.

4.10--Results

Wavelength calibration is carried out for each run with either holmium oxide or didymium glass filters. Typically scan ranges of from 100 to 600 nm are used depending upon the system under study and response limitations of the photomultiplier tube.

Scan speeds from 3 to 150 spectra per second are available with the Perkin-Elmer Model 108 Scanning Monochromator. We have found a speed of 75 spectra per second suitable for most applications. Static (time independent) calibration spectra are collected at the same scan rates as those for the stopped-flow experiments. An example is given in Figure 6. For work requiring higher resolution, slower scan speeds with more points per spectrum can be used in conjunction with narrower slits and more extensive averaging. The system display software permits full scale expansion in two dimensions of any portion of the spectrum as an additional means of detailed wavelength examination.



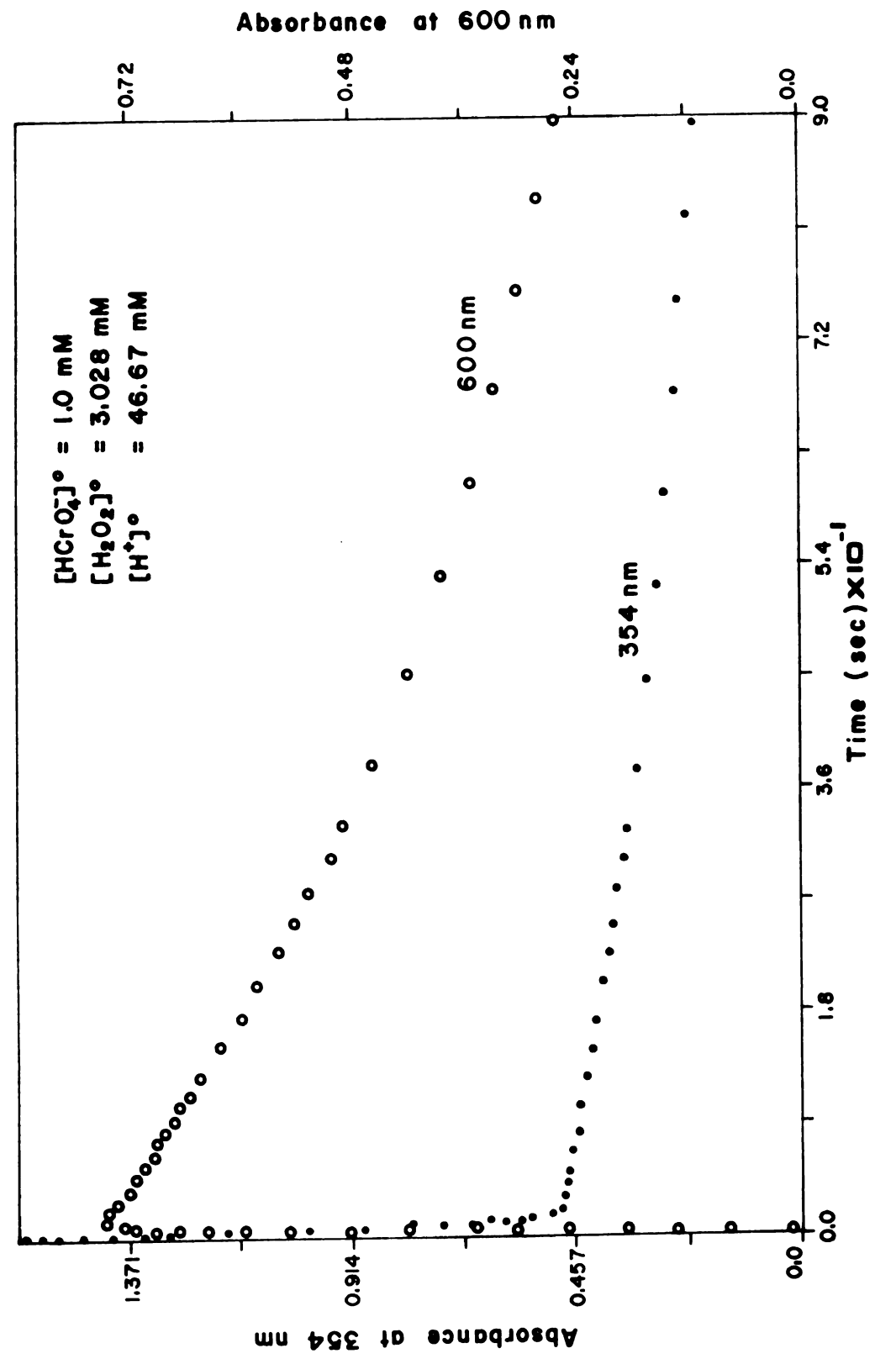
Holmium oxide spectrum, collected while scanning at 75 spectra per second. Figure 6.

The effect of the time dependent spectral averaging on time-cuts at two wavelengths is illustrated in Figure 7. This shows the absorbance changes which accompany the reaction of chromic acid with hydrogen peroxide in acid solution to form peroxychromic acid which subsequently decomposes to give non-absorbing products (83). Figure 7 illustrates the ability to record both fast and slow processes in a single experiment. Figure 8 is a spectrum from the peroxychromic reaction collected at 200 ms without spectral averaging (ie. it is a Group 1 spectrum). The same spectrum collected as spectrum 4 of Group 4 (same elapsed time) shows improved S/N across the whole spectrum since the second spectrum is actually the average of 8 spectra.

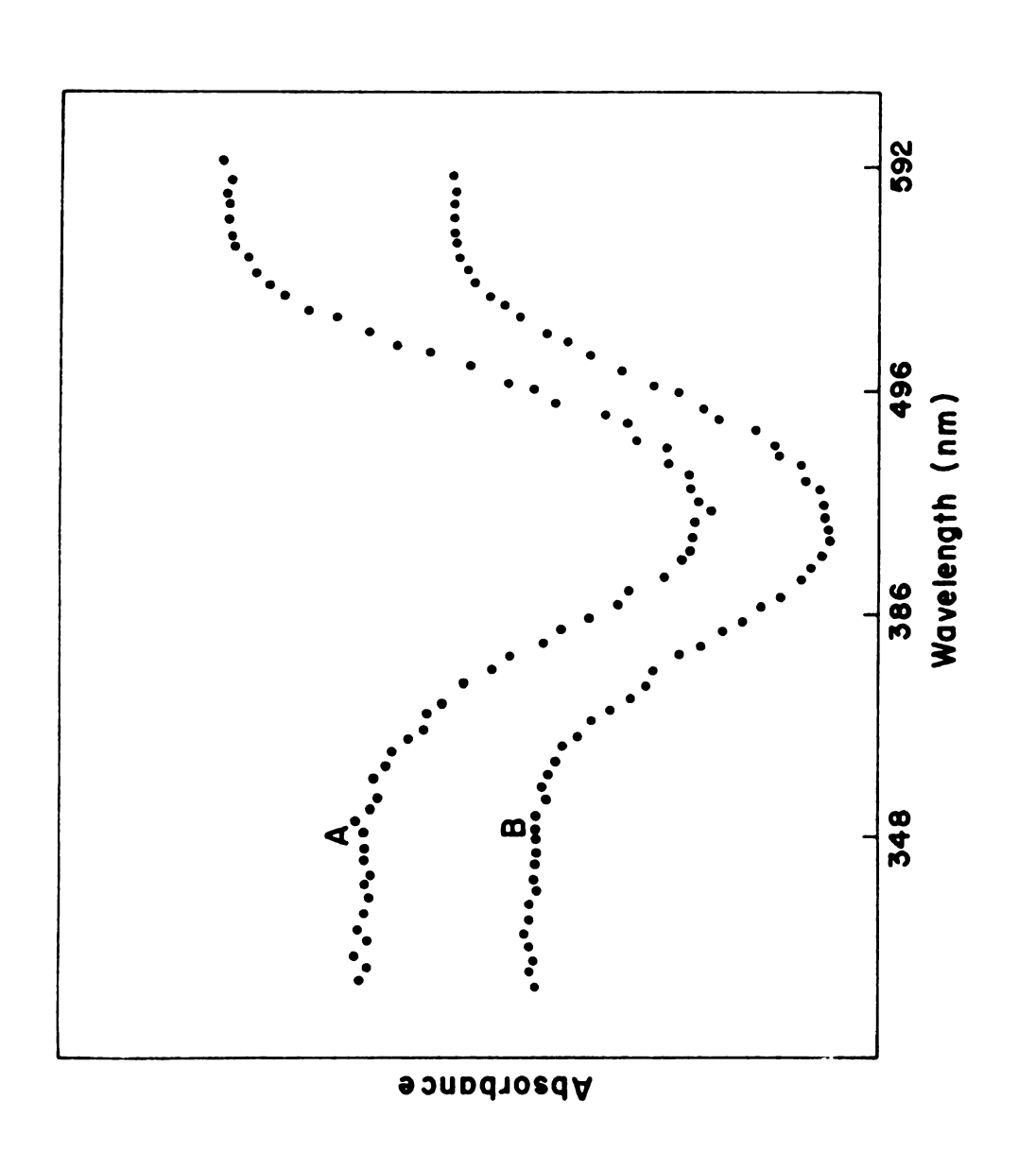
The reader is reminded that a single scanning push provides the kinetics at all wavelengths of interest.

The display software can display any number of "time-cuts" from a scanning push simultaneously for direct comparison.

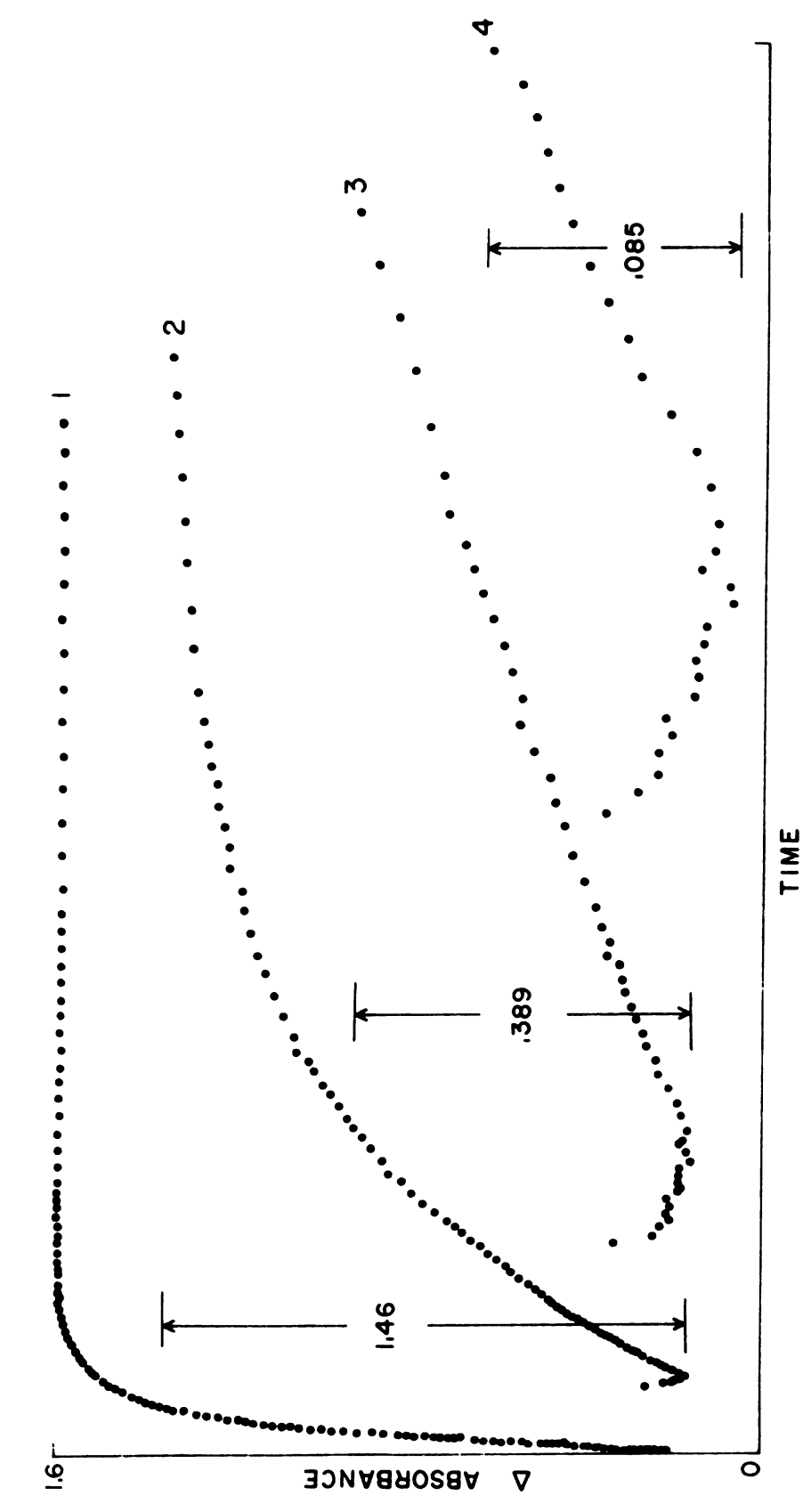
Of course, the scanning system can also be used at fixed wavelength for study of faster reactions. Figure 9 curve 1 illustrates a kinetic record of the complex formed by the reaction of 0.01 M Fe³⁺ with 0.005 M SCN. Curve 2 is an expansion of the first 400 ms of curve 1 (this is a closer look at the same data not a new push); similarly curve 3 is the first 40 ms and curve 4 is the first 11 ms of the reaction shown in curve 1. Note the



Time-cuts for the formation of peroxychromic acid showing the slow decomposition process. Figure 7.



Spectra collected during the reaction for the formation of peroxychromic acid. "A" is from group 1, while "B" is from group 4. Figure 8.

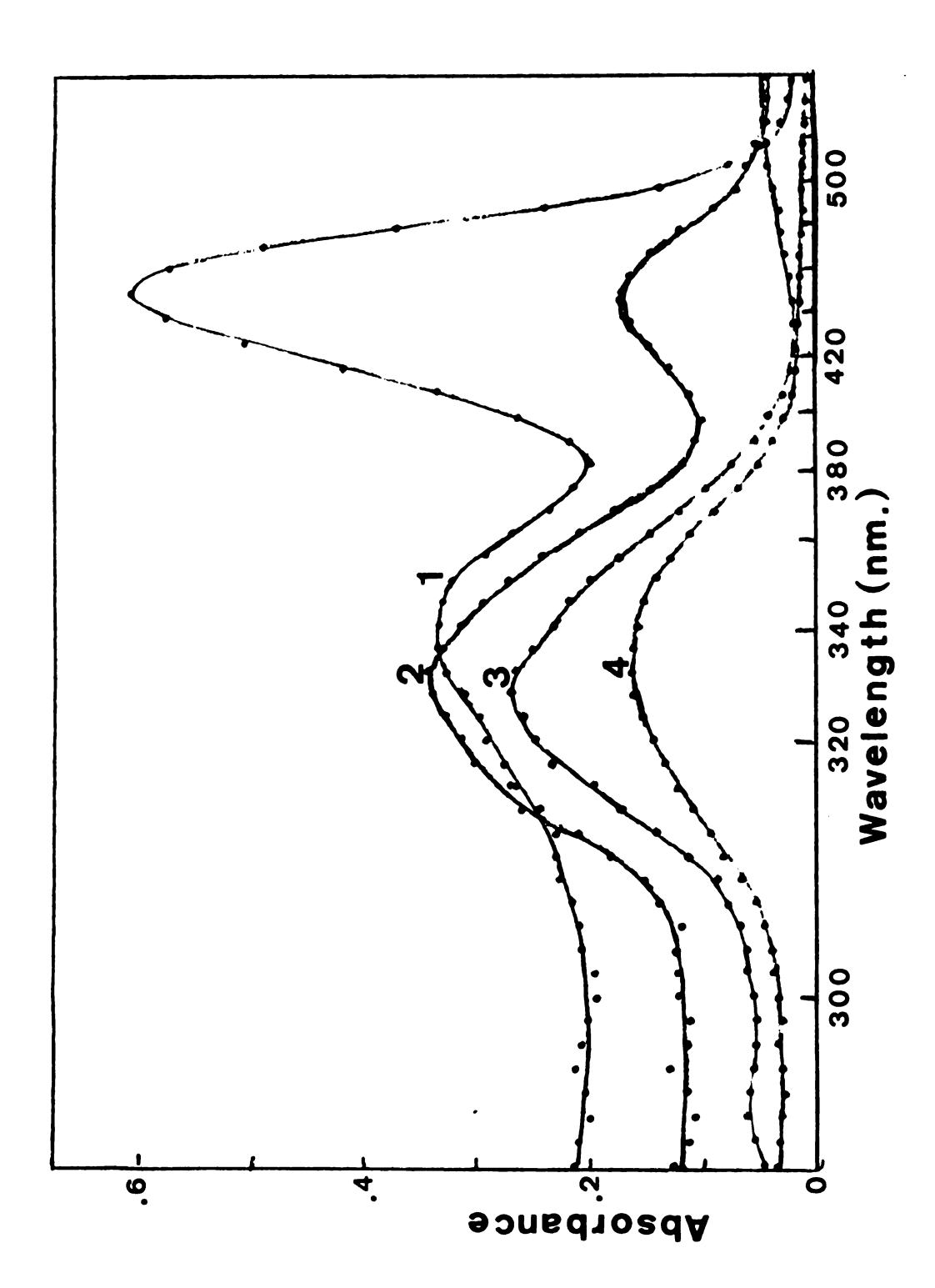


Time-cuts for the formation of the ${\tt FeSCN}^{2+}$ complex showing the capabilities of the display routines. Figure 9.

expansion of both the time and absorbance scales. This scale expansion procedure is useful when examining flow velocity and stopping characteristics of the system, fast and slow processes, large and small absorbance changes etc. Similar flexible display capabilities are utilized for both wavelength and time displays of data obtained in the scanning mode.

The entire system has been used to study the kinetics of a number of complex reactions involving such
diverse fields as transient-state enzyme kinetics and
solvated electron reaction rates. The performance
characteristics have fully lived up to the expectations
developed during the calibration runs. As an example,
the spectra obtained during the equine liver alcohol
dehydrogenase (LADH) catalyzed reduction of the substrate analog N,N - dimethylnitrosoaniline with NADH,
are shown in Figure 10. Three wavelength-dependent time
developments have been extracted and analyzed from data
obtained in the scanning mode.

Details about the construction and performance characteristics of the stopped-flow system are given in the next chapter.



Overall spectral changes in the LADH catalyzed reduction of NDMA by NADH. Figure 10.

V. THE STOPPED-FLOW SYSTEM: DESIGN, CONSTRUCTION AND TESTING

The design of the scanning monochromator-stoppedflow system which had been previously used for studies of reactions of solvated electrons and of aromatic ions in non-aqueous media was used as a basis for the present system (51). However, it was modified to permit the study of changes in the absorption spectrum of enzymic systems and to take advantage of the computer system. project was undertaken to make whatever modifications were necessary for the study of enzyme kinetics with a scanning system. Additional technical improvements were effected to enhance the overall utility and resolution of the apparatus. or as a direct result of the on-line computerization of the flow system. order that the system remain adaptable to many uses it was constructed of inert materials. An improved quartz flow cell featuring a double mixer and a choice of two path lengths was constructed. The entire flow system, including storage reservoirs and syringes was enclosed in a Plexiglas bath for thermostatting and variable temperature operation. Special seals and

syringes were designed and constructed to allow lower temperature operation, reduced volume requirements, improved push-to-push reproducibility, and to provide a multiple-push capability.

Typical of transient enzyme kinetics experiments is the necessity to study small absorbance changes in the UV region of the spectrum. As a partial solution to this problem a more intense light source was enployed in conjunction with an improved light throughput system. However, the greatest enhancement in S/N ratios as well as in overall performance came as a result of the signal averaging capabilities of the on-line computer system.

Thus, the new stopped-flow system incorporates many of the features of its predecessor as well as several additional innovations. The introduction of a variable temperature capability to the anaerobic-inert system imposed severe restrictions on the ultimate configuration and construction materials of the flow and optical systems. The nature and availability of enzyme solutions also imposed certain demands on the solution handling system as well as the system's ability to operate in the UV region of the spectrum. A detailed description of the stopped-flow apparatus is presented below, followed by a presentation and discussion of the performance tests and system characteristics.

5.1--Flow System Design

The flow system was constructed using greaseless vacuum tight seals so that the reacting solutions come into contact only with quartz, Pyrex and Teflon. Since it is a closed system, a specially designed system for solution makeup and handling was required. Teflon seals, joints and valves are used throughout the flow system to insure an inert environment for the reacting solutions and to facilitate system repairs and alterations. A reference cell provides for double-beam operation, and its location beside the reaction cell in the bath insures the same temperature for both cells.

5.2 -- Flow and Reference Cells

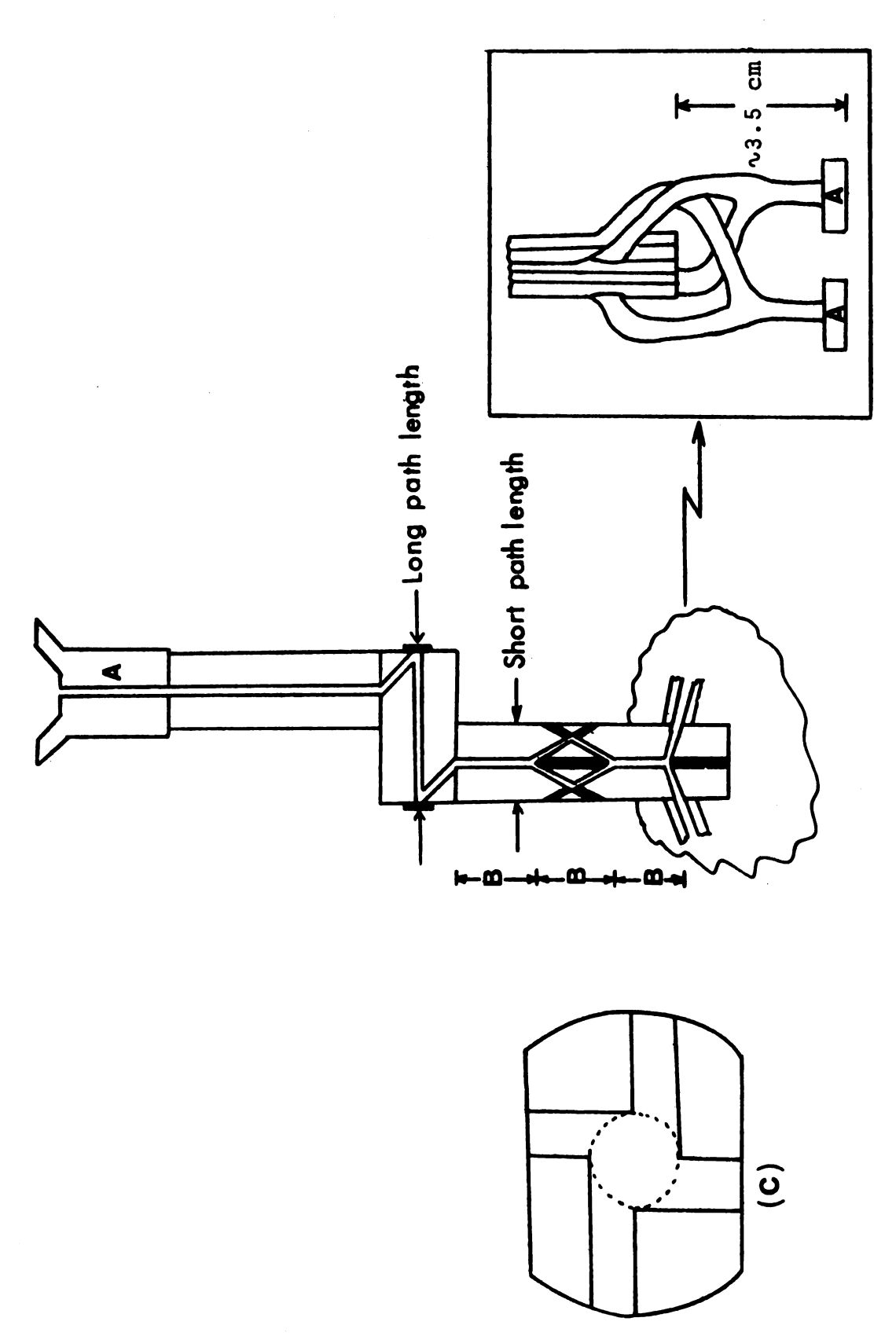
The flow cell was constructed entirely from quartz capillary tubing of known diameter. Quartz is required for UV applications and since the remainder of the flow system is Pyrex, one piece construction of the cell is required. Optical windows for the short path length were provided by first having the capillary tubing ground and polished flat on two opposite sides (Precision Glass Products Co., Oreland, Penn.). Holes were drilled in the quartz by using an "airbrasive" unit (84) which utilizes a fine jet of gas driven alundum powder. A detailed description of the drilling and the glassblowing procedures involved in the actual construction of the cell are given elsewhere (32). A diagram of the flow

cell is shown in Figure 11 (32). Earlier designs consisted of a single four-jets mixer with only a short pathlength. The latest flow cell divides the mixed stream from the first four jets into four additional streams which then rejoin to effect a second four-jets mixing of the reactants. This secondary mixing process resulted in an increase in volume between the mixing and observation point of less than 10µ1. (less than 1 ms increase in dead time).

Because of the small changes in absorbance involved in transient enzyme studies it was necessary to provide for a longer path length. This was accomplished by sealing a length of capillary at right angles to both the entrance and exit tubes (see Figure 11).

Sections of very thin quartz microscope slides were then fused to the ends of the capillary, and subsequently ground and polished to provide for a 1.85 cm effective path length. The one piece system design permits flow through the cell without any volume expansion or contraction. Therefore a common source of cavitation artifacts is eliminated.

Construction of the reference cell was somewhat simpler since no mixing portion was required. Of course care was taken to insure that no dead spaces were present which might interfere with rinsing or introduce bubbles.



Schematic diagram of the mixing and observation cell. A - Fisher-Porter 2 mm quartz joints, B - ~ 0.5 cm, C - cross-section of a mixer. Figure 11.

Both cells were rigidly held in place by clamping them in specially machined aluminum holders, and securing the holders to the flow system frame. The holders also serve as mountings for the fiber optic light pipes and provide for masking of unwanted stray light. Liquid from the surrounding bath is kept out of the light pipes by sealing the exterior of the cell holders with silicone rubber cement.

5.3--Pushing and Stopping System

5.3.1--Syringe and Plunger Design

The construction of leak-free greaseless syringes for variable temperature operation presented special problems. Greased syringes were unacceptable because of the tendency for the grease to "creep" to other parts of the system glassware, and because of the solubilization or deterioration of greases in the presence of many solvents. Commercially available syringes with Teflon plungers overcome the problems of greased syringes.

However, Teflon has a tendency to "cold flow" over a period of time, and will contract at lower temperatures; both of these phonomena lead to leaky syringes. Recently, syringes with adjustable Teflon seals have been made available commercially; however, generally speaking these were not designed for stopped-flow applications.

Over the years, this laboratory has attempted to utilize commercially available syringes in anaerobic and/or variable temperature applications with little success. The most satisfactory solution to the problem has been for the laboratory to design and manufacture its own syringe bodies and plungers.

The syringe bodies are constructed of heavy wall precision bore glass tubing (diameter 0.553 inches, purchased from ACE Glass Co. on special order in 3 foot lengths). The syringe bodies are made by the glass shop as shown in Figure 12. The base of the syringe is flared and ground flat to provide stability, to permit easy insertion of plungers, and to facilitate a liquid seal with the base of the bath. The top of the syringe body is formed by fusing a flat plate across its diameter. This procedure minimizes distortions and dead spaces between the plunger and the glass body. To completely exclude air from the system, the syringes are constructed to permit back-pumping between two 0-rings (Teflon is permeable to oxygen). This is accomplished by attaching a sidearm to the syringe body. These sidearms can also be used as exit ports for the purpose of rinsing the system prior to re-filling, an operation which wastes solution in many stopped-flow systems. Before the sidearm is attached, a small hole (less than 0.5 mm) is drilled through the syringe body using the "Airbrasive" technique. The "Airbrasive" drilling prevents distortion

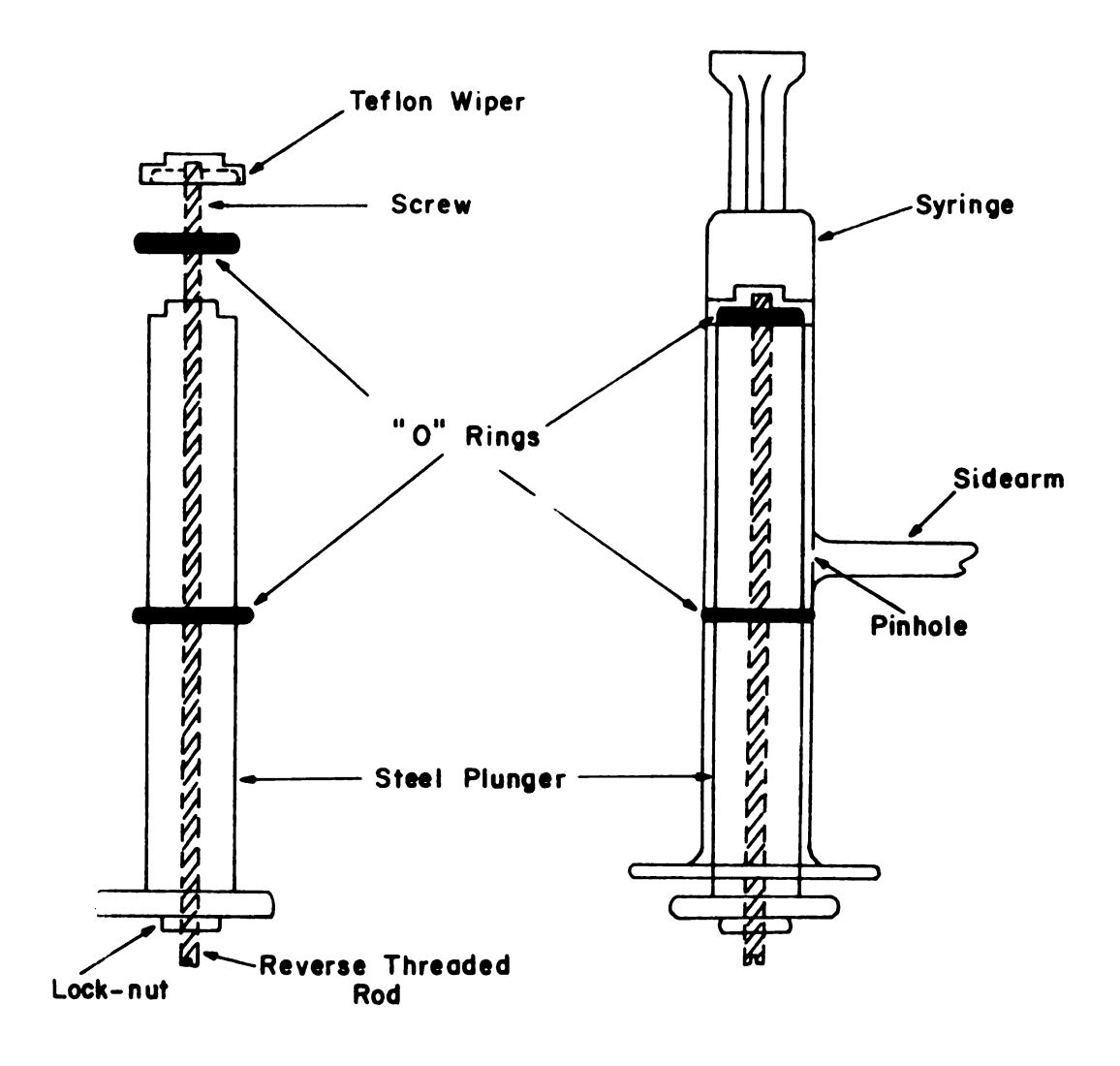


Figure 12. Syringe and adjustable plunger design.

of the inside diameter of the barrel and provides good control over the size and positioning of the hole. Thus the hole is positioned so as to lie below the Teflon wiper when the plunger is in the "fill" position. This allows the space between the 0-rings to be evacuated. The diameter of the hole relative to the width of the Teflon wiper is such that as the plunger is lowered further to the rinse position. a continuous seal is maintained with the inside of the syringe barrel. this position, old solution may be evacuated to a waste vessel and the syringe efficiently rinsed with solvent or solution from a reservoir. Once rinsed, the plungers are returned to the "fill" position and back-pumping may continue. Care should be taken so that materials which attack the 0-rings do not come into contact with them.

The glass sidearms were attached by the glass-shop using a "stick-seal" technique so as not to distort the interior diameter of the syringe body. This process is difficult and is not recommended for amateurs.

The thermal properties of Teflon are such that a seal made at one temperature develops a leak at a lower temperature. To overcome this problem (and the problem of cold-flow), we have designed and tested plungers in which the Teflon seals are forced against the glass wall by Viton O-rings which are held under compression (see Figure 12). A machined Teflon cap is attached to a

threaded brass rod which in turn is reverse threaded into a stainless steel shaft. If leakage develops, the lock-nut is loosened and the rod is turned. This action pulls the Teflon cap down onto the 0-ring causing it to compress and force the wiper against the glass wall, thus effecting a better seal. The adjustable wiper system has been tested outside of the flow system at -30 °C and was able to hold a vacuum of 10-5 mm Hg. The actual low temperature limit under stopped-flow conditions has not been determined because of the presence of other Teflon materials (valves) which would begin to leak severly at around 5 °C. A Teflon valve similar in principle to the adjustable plunger caps is currently under development.

The adjustable plungers are still undergoing testing. Syringe leakage during a run can be halted effectively by tightening the Teflon cap; however, certain precautions are necessary. The relationship between the O.D. of the compression O-ring and the I.D. of the Teflon wiper is critical, and because Teflon does not hold a thread very well, periodic replacement of the cap is required.

5.3.2--Mechanical and Framework

The structural backbone of the flow system itself consists of four threaded brass rods which are fastened vertically at one end to an angle iron frame which in turn is bolted to the floor. Aluminum plates are fastened with large nuts to the brass rods to serve in holding the syringes in place and for added structural support. The top plate acts as the stopping plate and as a mount for the waste system pneumatic piston. The remaining framework consists mostly of lattice rods which serve to support the glassware of the solution handling and delivery system and the vacuum lines. The vertical mounting of the flow system facilitates the movement of solutions into the system and provides an easy means of sweeping out trapped bubbles.

The pushing plungers are mounted in an aluminum block which is in turn connected by a threaded rod to a large pneumatic piston (2" diam. bore, Cathy Co. (Schrader), Lansing, Michigan). Movement of the pushing plungers may be controlled manually with a three position valve which controls the flow of the pressurizing gas. The hand operated valve affords good piston control while the flow system is being filled, rinsed or used to sweep out bubbles. To improve flow velocity reproducibility and to allow for automatic operation, a bypass air system was constructed so that the air pressure to the pneumatic

piston could be controlled by a solenoid valve (Cathy Co. (Schrader) Lansing, Michigan). A simple switching circuit thus permits electrical control of the fill, push and hold modes of the piston. The switching action can also be controlled automatically by using TTL pulses. The BS triggers are ignored until the Begin Push switch is activated. Subsequently, the very next BS trigger will cause the solenoid valve to initiate the pushing action. The overall reproducibility in time of the solenoid valve and pneumatic piston operation is sufficient to provide reproducible flow velocities. Data collection is begun with the next BS trigger after constant flow velocity is achieved. Since the time between BS triggers is constant, and since the period of acceleration is reproducible to within one spectral scan, the scanning monochromator can be roughly "synchronized" with the operation of the stopped-flow system and the collection of data by the computer.

5.3.3--Thermostat System

The flow system, including storage reserviors and syringes is enclosed in a Plexiglas thermostat bath similar to that developed by Dewald and Brooks (85). This is important, not only for the study of the temperature dependence of reaction rates, but also to insure that there are no temperature gradients within the system.

Such temperature gradients can cause optical artifacts even in the absence of absorbance changes (39). A liquid bath has the advantage of a large heat capacity which tends to diminish temperature differences between different parts of the system.

The bath was constructed from 3/8" Plexiglas plates which were bonded together by using methylene chloride. One of the sides and a large section of the back wall are removable to give easy access to the flow system. Wherever holes in the bath were required, silicone rubber sealer (Dow Silicone Rubber Cement or General Electric RTV) was used to prevent leakage of the bath fluid. The transparent Plexiglas allows easy visability of the flow system and acts as a reasonably good thermal insulator.

A variety of bath fluids could be employed. However water or ethylene glycol-water mixtures are generally satisfactory. The present bath circulation system actually consists of three separate baths. Liquid from a large (25 gal) reservoir is circulated through copper coils which are submerged in an intermediate bath located near the stopped-flow bath. Liquid is rapidly exchanged by an impeller pump between the stopped-flow bath and the intermediate bath. Circulation to the jacketed burettes is also possible and is intended for use either to pre-equilibrate the solutions or as a means of slowing down decomposition of labile reactants.

The large capacity of the total bath system affords temperature regulation to better than ±.1°C. However, considerable time is required to establish thermal equilibrium. Thus for variable temperature studies smaller auxiliary baths might be employed.

5.3.4--Solution Mixers

Reagents and solvents are delivered by burettes to two storage reservoirs located on either side of the bath for solution makeup. Mixing is accomplished by a Teflon coated magnetic stirring bar which has been sealed in the storage vessel. The length of the stirring bar and the diameter of its container are such that the bar cannot lie flat. Vortex type mixing is effected by air-driven turbine type immersible magnetic stirrers which have been mounted vertically behind the storage vessels. Control of the stirring process is important to avoid denaturation of the protein by excessive foaming.

5.3.5--Stopping Syringe System

The stopping syringe is similar to the pushing syringes except that the sidearm is used for back-pumping only. The separation between the stopping plate and the base of the stopping plunger determines several important instrumental parameters. First, the total volume required per push is directly related to the length of the stroke for a given cross-sectional area of the top syringe.

Second, sufficient time (distance) must be provided to allow the flow velocity to become constant. Finally, as the scanning speed is decreased, longer periods of constant flow velocity are required in order to obtain at least one complete zero-time spectrum (during flow). Given the above considerations, the system currently requires approximately 0.7 ml of each reagent per push. The period of constant flow is approximately 80 ms. (dependent on the air pressure) and the stopping syringe diameter is 0.553 inches. Because the decomposition rate of solvated electron solutions is increased with a large surface-to-volume ratio, fairly wide diameter syringes were employed. A new micro-system designed specifically for enzyme studies is currently under development.

The pushing syringes contain a total volume of 2.5 ml each when filled. Hence three pushes can be delivered for each filling of the syringes. A small pneumatic piston and valve are used to return the stopping plunger to the ready position while simultaneously expelling wastes. In order to provide more versatile dual-beam operation, the waste line may be connected to the reference cell. Thus the reference cell can be filled with a variety of reference solutions which can be delivered by the flow system. The appropriate solution is simply pushed into the stopping syringe and then expelled to the reference cell through the waste system. Once filled, the

reference cell is isolated from the waste line and the normal flow of actual waste materials is continued.

5.3.5.1--Start and Stop Flags

A versatile and reliable flag system was constructed to indicate not only the stopping of flow but also to monitor the flow velocity and to provide control triggers for the data acquisition system. Motion of the stopping plunger is monitored by two metal flags which are mounted on the plunger barrel. As the plunger moves upward, the flags interrupt two light beams which normally illuminate two light-sensitive phototransistors. This interruption causes pulses to be generated. In this way both Start and Stop pulses are provided which can be used to initialize data acquisition, calculate flow velocities and determine the zero time of reaction.

5.4--Solution Handling and Delivery System

The entire flow system, including the burettes and solution entry ports can be evacuated routinely to less than 10⁻¹⁴ mm Hg. For applications not requiring high vacuum, a roughing pump or water aspirator is utilized either for drying the system or as an aid in moving solutions through the system. There are four solution entry ports located on each side of the flow system.

Each port is connected to the high-vacuum line by a Teflon

valve and to the delivery system through 10 ml burettes. For anaerobic work, solutions are first pressurized with an inert gas in glass bottles which have been fitted with Teflon valves and Fisher-Porter type joints. anerobic studies, solutions are introduced into the system through glass funnels which have been fitted with Fisher-Porter joints. After the bottles have been mounted, and the remaining spaces evacuated, the high-vacuum valves are closed and the valves on each bottle are opened to fill their respective burettes. Each burette is jacketed so that liquid from the flow system bath can be circulated around each solution. The four burette tips for each side have been brought together in a solution receiving area which is designed to permit solution delivery from any burette into a closed system and also to provide for good drainage and rinsing characteristics. From the receiving area. solutions travel to a 40 ml storage reservoir located within the bath. Here solution makeup is completed with mixing accomplished as described earlier. At this point the solutions are allowed to come to thermal equilibrium with the bath. The 10 ml burettes permit good accuracy and precision while the 40 ml storage vessel provides enough volume for multiple push applications.

The five valves which are used to control the direction of flow of solutions are rigidly mounted to the sides of the Plexiglas bath (see Figure 13). Since these valves

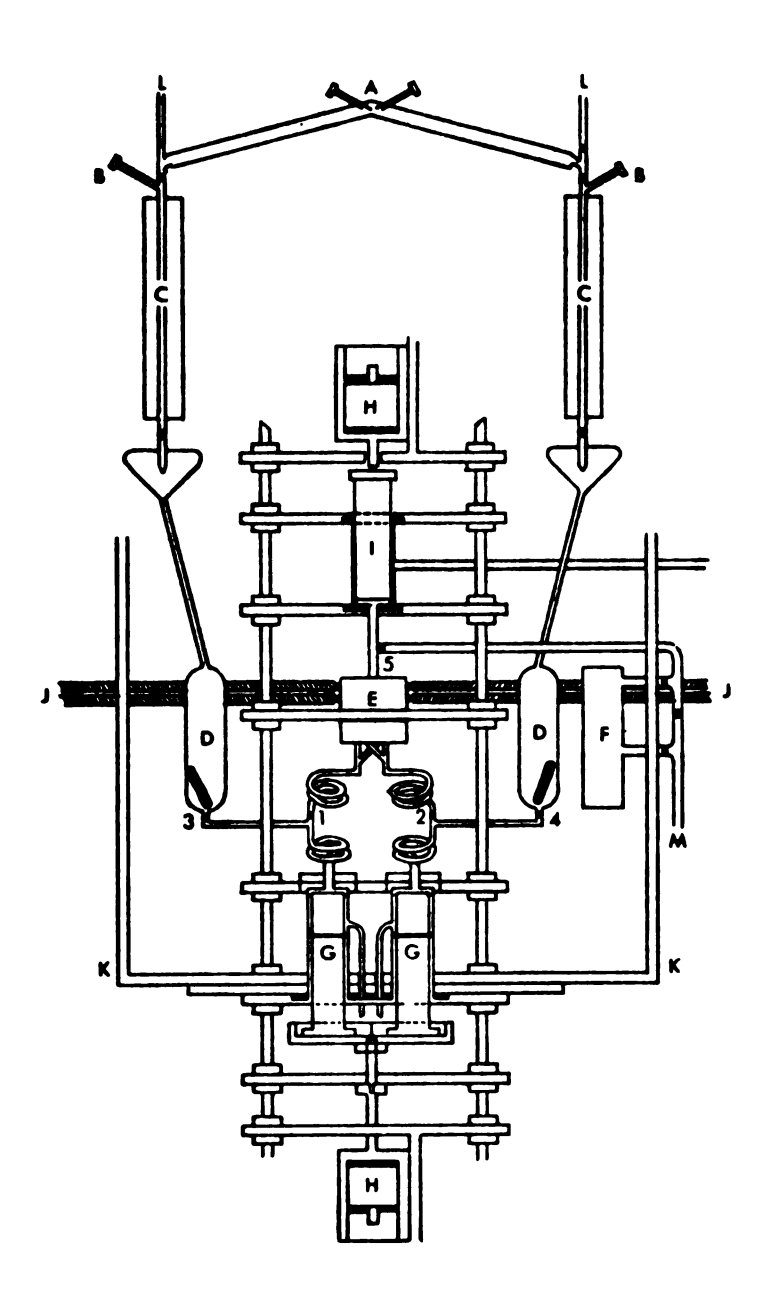


Figure 13. Schematic diagram of the thermostated stopped-flow apparatus. A - Joints for rinsing solutions, B - Joints for reactants, C - thermostated burettes, D - reactant reservoirs, E - mixing and observation cell, F - reference cell, G - pushing syringes, H - pneumatic pistons, I - stopping syringe, J - quartz light fibers, K - thermostat bath, L - to vacuum, M - to vacuum and "waste", 1, 2, 3, 4, 5-flow valves.

are operated frequently during a run, their stability is important so that applied torques are not translated into motion of the glassware which can ultimately cause breakage.

The pushing syringes are filled by closing the inner two valves and opening the two outer valves while the pushing plungers are lowered to the "fill" position.

Reactions are carried out by closing the outer valves and opening the inner valves. The pneumatic piston forces the plungers upward causing the reactants to flow through a short length of spiral tubing included for strain relief and into the mixing chamber. The quartz mixing cell is connected by Fisher-Porter joints to the remainder of the flow system which is constructed from 2 mm ID Pyrex capillary tubing.

The moving solution causes the stopping plunger to strike the stopping plate thus halting the flow of solutions as well as the advance of the bottom plungers. With the inner valves closed and the pneumatic piston in the hold position, the exhaust valve is opened to allow the small pneumatic piston on top to expel the spent solutions while returning the top plunger to the "ready" position. With the exhaust valve closed, and the inner valves reopened, the pneumatic piston is again activated resulting in a second kinetic push. In this way three records can be obtained for each filling of the bottom

syringes.

5.5--Optical System Design

Flexible quartz fiber optic light pipes with water-tight sheathing have been used to bring light through the liquid bath to the cells and from the cells to the detector (86). Attachment of the fibers directly to the flow cell minimize problems caused by cell movement and provides considerable flexibility in positioning the remaining optical components in addition to reducing the problems due to stray light.

Because a double-beam system is used, lamp and photomultiplier supply fluctuations are largely cancelled out. Two additional "noise" sources are shot noise and mechanical noise. The S/N resulting from the former is determined largely by the photocathode current and the frequency bandpass of the total detector system. Mechanical noise results mainly from vibrations of the optical components in the monochromator and decreases when the system is operated at a fixed wavelength. With a scanning system it is necessary to operate with a broader frequency bandpass than is usual at fixed wavelength; that is, there is a wide dynamic range of the output voltage from the photomultiplier tubes during each scan. Variations of both the lamp output and photomultiplier tube sensitivity with wavelength make it not uncommon for the signal to change by a factor of 100 or more during a scan. double-beam technique together with an operational

amplifier logarithmic converter overcome this problem and also provide a more convenient display. The use of double detectors and the ability to provide a variety of reference absorptions, affords the advantages of baseline subtraction and scale expansion techniques.

The gear system of the scanning monochromator is used to provide the basic timing signals for the data acquisition system. Light sensitive transistors are used in the scanning mode to provide 68 wavelength marking pulses for each spectrum, as well as a single pulse each time a new forward scan is begun. The frequency multiplication system is used to provide a constant 20.4 KHz sampling frequency which is independent of scan speed. The BS pulses are used by the automatic start system to synchronize the monochromator to the flow system, and by the computer to synchronize the monochromator to the data acquisition and storage process.

5.5.1--Light Sources and Detectors

Some of the S/N ratio disadvantages of scanning can be overcome by using an intense light source. With this in mind, a 1000 Watt Xenon lamp (Oriel Co.) was installed to provide sufficient light intensity in the UV - VIS region of the spectrum and to overcome lower light levels caused by narrower slits and the use of fiber optic light pipes. Tungsten and deuterium light sources are also available.

The monochromator has a maximum scan rate of 150 spectra per second. It is a four-pass Littrow system with continuously variable slits. The scan width is determined by the angle of nutation of a rotating mirror and is independent of either scan speed or center of scan. Unwanted radiation and/or heat are removed by liquid and glass filters. The lamp is fitted with a 2 inch collimating condenser system for increased light input. A specially constructed holder brings the fiber optic light pipes up to the exit slit of the monochromator for improved light collection. An attempt was made to combine the individual fiber bundles at one end into a slit shape, to serve as a flexible fiber optic beam-splitter which could make optimum use of the light output of the monochromator. By shaping the fibers to match the shape of the exit slit, and by randomly splitting the fiber bundles, more uniform illumination of the cells could be achieved. Unfortunately the cladding on the fibers is quite fragile and the effort was aborted after a large investment of time. Glass or plastic beam splitters with an assortment of area transfer designs are readily available and reasonably inexpensive. UV transmitting quartz fiber beam-splitters are available from Schott Optical Co. on special order but are quite expensive. Future plans in this laboratory include the purchase of such a beam splitter as part of an overall upgrading of the optical system since matching of the two beams is presently

one of the limiting contributors to the noise.

At present two 50 cm lengths of flexible fibers with round 2 mm diameter ends are brought up to the exit slit of the monochromator for each of the path lengths. The other ends of the fiber are secured to the cell windows. Light from the cells is brought to the detectors by similar round ended fibers. Currently two sets of photomultiplier detectors are used; (1) RCA 6903 for UV-VIS and (2) EMI 9684B for VIS-IR applications. The EMI tubes utilize special magnetic lenses and a cooling box which has been described elsewhere (32) for improved dark current characteristics.

The reference and sample output photocurrents are converted to absorbance and amplified by using an operational amplifier circuit. A selection of analog filters is also provided in the circuit. The absorbance signal is biased to allow for full scale utilization of the data acquisition system. The absorbance conversion is linear over the range of 10⁻³ to 10⁻⁹ amps. of photocurrent. The system response as a function of wavelength is calibrated during each run with rare earth oxide glass filters as well as neutral density filters. Computer programs correct the raw data for variations of the instrument response as a function of both absorbance and wavelength.

5.6--Performance Results

The overall performance of the system was evaluated by using a variety of tests including the study of standard reactions.

5.6.1--Optical Calibration Data

The sensitivity of the system depends essentially upon the optical components. Both light intensity and phototube response decrease substantially at shorter wavelengths; and without averaging of adjacent spectra the scanning mode results in significantly poorer S/N. However, the most severe loss in sensitivity arises from fluctuations in the output signal that are caused by "wander" of the Xenon arc. Since reference and sample fibers are intercepting different regions of the arc, these fluctuations are uncompensated and result in vertical deflections in the spectrum. Since the net result of all these effects is a complex function of wavelength and instrument settings, it is not possible to state the overall system sensitivity in general. However, by measuring the deflections in the spectrum of holmuim oxide glass on an analogue scope we estimate the r.m.s. noise to range from 0.002 to 0.01 absorbance units in the 500-300 nm region.

The wavelength resolution of the instrument also depends upon the instrumental settings. A typical calibration spectrum of holmuim oxide glass was shown earlier (see the discussion of the scanning monochromator). The

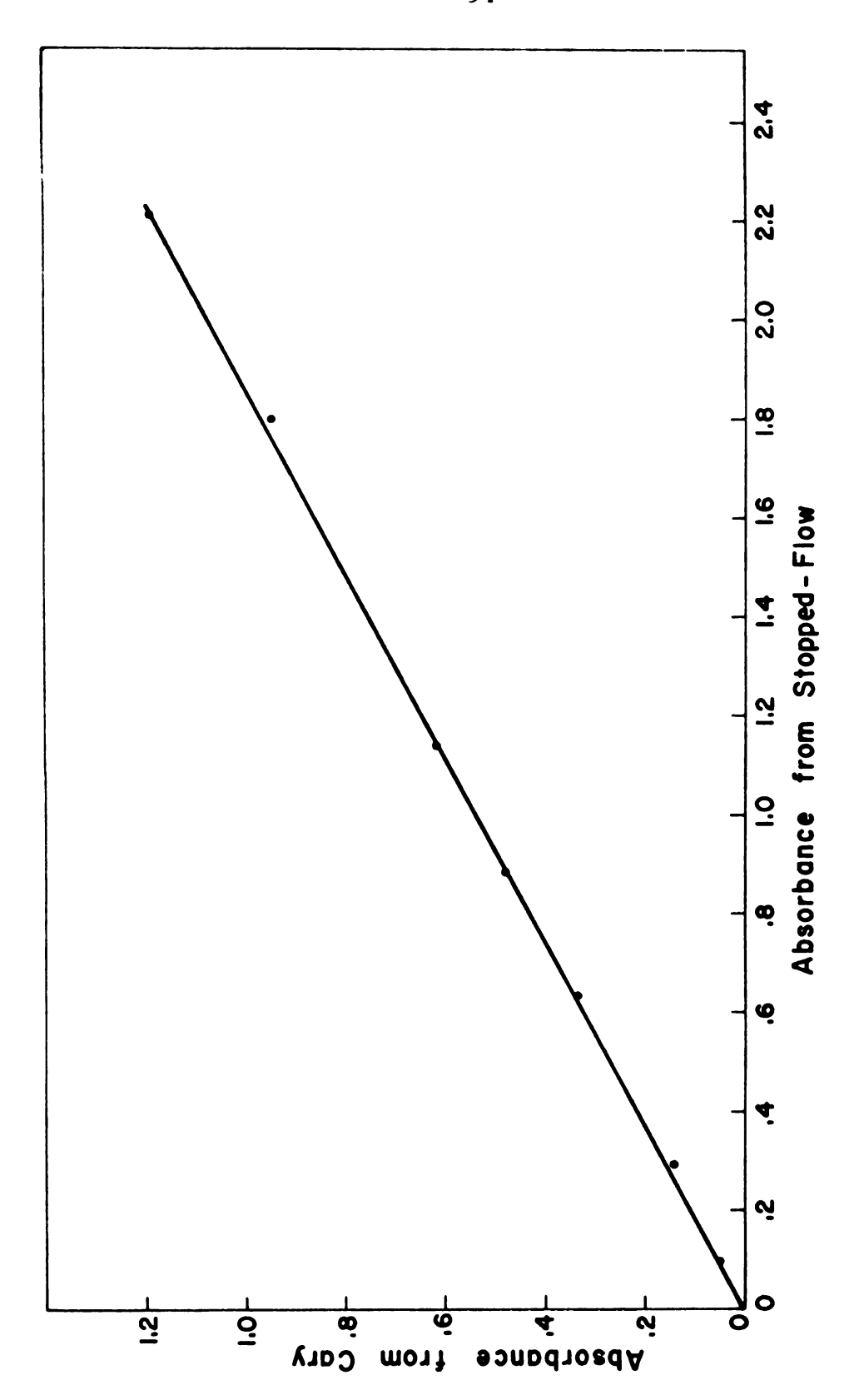
effective path lengths of the cell were determined with Beer's law tests. For the long path length, aqueous solutions of 2,4- dinitrophenolate (360 nm) were used. The solutions were calibrated with a Cary model 15 spectrophotometer using 1.000 ± 0.001 cm Beckman cells. In Figure 14 the results obtained with the stopped-flow system at 360 nm are plotted against the corresponding results from the Cary. Beer's law is obeyed up to an absorbance of approximately 2.0, and the effective path length calculated by using a least squares fit is 1.850 ± .005 cm.

A similar procedure was used for the short path length. In this case, freshly prepared $KMnO_{\downarrow\downarrow}$ solutions were used (524 nm) and gave a path length of 1.99 $^{\pm}$ 0.02 mm (32).

Stray light which bypasses the cell was therefore shown to be negligible at absorbances less than two. In general, scattered light problems were minimized by positioning appropriate cut-off filters between the lamp and the monochromator entrance slit.

5.6.2 -- Flow Calibration

Since it is possible to measure the flow velocity accurately with the phototransistor flag circuit, we are able to determine the time at which the flow velocity reaches a constant value (for a given air pressure on the pneumatic piston). The reproducibility of the absorbance traces during flow depends of course on the reproducibility



The absorbance of solutions of p-nitrophenolate (360nm) which were measured on a Cary 15 plotted against the absorbance measured using the long path length on the stopped-flow apparatus. Figure 14.

of the flow velocity. Data are collected only during the period of constant flow. It is possible to obtain initial absorbance data during a given run which are reproducible to approximately 5 per cent as determined by studies of the reaction of Fe³⁺ with SCN.

5.6.3 -- Flow Cell Performance, Fixed Wavelength

5.6.3.1--Mixing Efficiency

The mixing efficiency of a flow system can be defined as the degree to which the reactants are mixed upon their arrival at the point of observation. In order to test the efficiency of the double mixer cell we studied the reduction of p-nitrophenolate by acid. Under the conditions of the test the reaction was diffusion controlled and the final absorbance was non-zero. Any change in the remaining absorbance after stopping would have indicated incomplete mixing of reactants. Since no such changes were observed on the analogue scope for a series of replicate pushes, it is assumed that mixing is completed within the dead time of the instrument. This test did not provide a quantitative measure of mixing efficiency, however the results indicate that the cell is at least as efficient as any reported to date. In an effort to measure the mixing efficiency quantitatively, additional tests with suitable indicator reactions and more accurate computer analysis are currently underway.

When identical solutions or solvents were mixed no change in signal was observed. This indicates that mixing artifacts due to cavitation or thermal gradients are absent.

The stopping time is approximately 0.5 ms as measured by the "rounding" of the absorbance trace in the reaction of Fe^{3+} with SCN^- .

5.6.3.2--Dead Time

The time required to transfer the solutions from the mixing chamber to the observation point and bring them to a complete stop is called the dead time. The dead time, therefore, depends directly on the flow velocity obtained for a particular experiment as well as the mixing efficiency and the stopping time.

The dead time for the short path length was calculated to be 2.7 ms from the flow velocity and volume displacement for the short path length (32). Similarly the dead time for the long path length was calculated to be 6.7 ms. Using data obtained by studying the formation of peroxychromic acid at 600 nm and extrapolating to the true time zero of the reaction, dead times for the short and long path lengths under these conditions were computed to be 2.5 ms and 5.5 ms respectively (32).

5.6.4--Quantitative Measurements

The formation of blue peroxychromic acid at 30°C was investigated in detail by Papadakis in order to evaluate the performance of the system in an actual kinetics study (32). Measurement of both a pseudo-first order and a third order rate constant for this reaction at several wavelengths, under a variety of concentration conditions, and with both the scanning and fixed wavelength modes gave reproducible values which are in agreement with those reported in the literature.

The calculated rate constant for the base hydrolysis of 2,4-dinitrophenylacetate was unaffected by the choice of sampling parameters which were varied over a wide range. Obviously if an unreasonable averaging bandpass is selected the rate curves will be distorted just as is the case with analog filters.

Good quantitative performance under actual operating conditions has also been demonstrated with several enzyme reactions. The ability of the stopped-flow system to give reproducible rate constants, enhanced S/N, and to detect subtle changes in the spectrum during reaction (including isosbestics) under conditions of relatively poorer S/N is clearly illustrated with the LADH study discussed in the next chapter.

VI TRANSIENT STATE ENZYME RESULTS

6.1--Glyceraldehyde-3-phosphate DEHYDROGENASE (GAPDH)

phate (GAP) to 3-phosphoglycerate (PGA) in the presence of arsenate and NAD⁺. In the absence of NAD⁺ the enzyme exists as an equilibrium mixture of inactive (T_0 , 98.4%) and active (R_0 , 1.6%) forms (26). Stopped-flow mixing of the apo-enzyme with saturating levels of NAD⁺ leads to the rapid formation (less than 10 ms) of a catalytically inactive complex containing four NAD molecules (T_{\downarrow}). The T_{\downarrow} complex subsequently undergoes a slow isomerization to yield an active R_{\downarrow} complex with an absorption band in the same region but with a larger absorbance. The equilibria among the different enzyme forms are strongly temperature dependent and at 40 °C the conversion to R_{\downarrow} is essentially complete.

In solution the substrate (GAP) exists primarily as the acetal. Hence, after a small (3%) initial burst period, the reaction proceeds at a slower rate corresponding to the rate of conversion of the acetal to the catalytically useful aldehyde. This fact was used to advantage in testing the scanning system since detectable levels of the R_{\parallel} complex could be produced even in the presence of

NADH production.

The rationale for studying the GAPDH system was to test the scanning system with a well defined enzyme system (GAPDH has been studied extensively by Kirschner (25, 26) and others (88)), and to illustrate the facility with which subtle differences in enzyme forms can be detected with such an instrument. Since the enzyme was prepared in quantity in our own laboratory, a process which required several weeks of work, it was also hoped that additional information on the GAPDH system could be found.

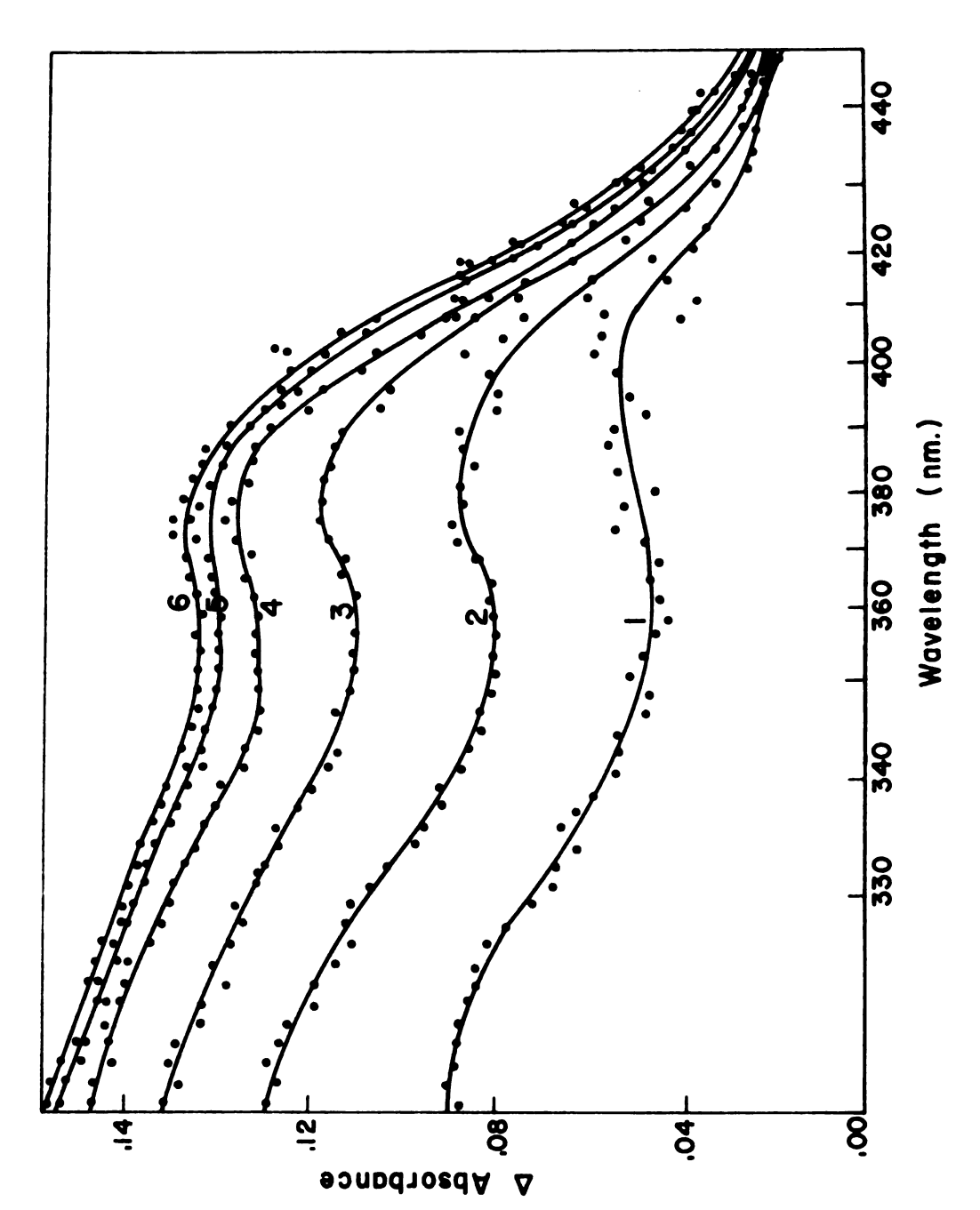
6.1.1 -- Complex formation between NAD and GAPDH

Kirschner determined the spectrum of the T_{\downarrow} and R_{\downarrow} complexes by using a series of fixed wavelength experiments (26). This point-by-point mapping technique resulted in rather ill-defined spectral shapes and left open the question of whether both complexes have the same band shape. By using the rapid scan system it was possible to determine both the T_{\downarrow} and R_{\downarrow} spectra directly. The spectrum at various times during the growth of the R_{\downarrow} complex minus that of the starting NAD⁺ absorbance is shown in Figure 15. There is some hint of a wavelength shift as the isomerization proceeds indicating that a difference in the spectrum of the T_{\downarrow} and R_{\downarrow} complexes may indeed exist. Because of the tail of the NAD⁺

absorption and the small enzyme absorbance at early times in this region however, it is difficult to obtain a true band shape by the available subtraction routines. It should be noted that much of the noise shown in Figure 15 is caused by uncompensated spatial fluctuations of the Xenon arc. These fluctuations could be reduced by a better beam-splitter.

No significant differences in the spectrum of either complex was observed at lower concentrations of NAD.

A time cut from Figure 15 at 366 nm shows the growth of the R_{ji} complex (see Figure 16). Note that the initial absorbance is not zero because of the rapid formation of \mathbf{T}_{l_1} which has a significant absorption at this wavelength. The $R_{j_{\perp}}$ growth was fitted to a simple first order process with rate constant k_{li} . As Figure 17 shows however, there is a systematic deviation of the data from the calculated This is especially true at long times indicating the presence of an additional but slower process. Kirschner has shown that with a GAPDH preparation which showed two bands on electrophoresis, double exponential growth curves for R, resulted. Holland and Westhead (113) have found however, that even the electrophoretically pure band from the column step can be further broken down into isoenzyme components. Based upon the assumption that our GAPDH preparation was actually a mixture of two enzyme forms which have different rates of isomerization, the R growth data were fitted to a double exponential



Selected difference spectra obtained during the $T_4 \rightarrow R_4$ isomerization reaction of the NAD-GAPDH complex at 39.9°C. Figure 15.

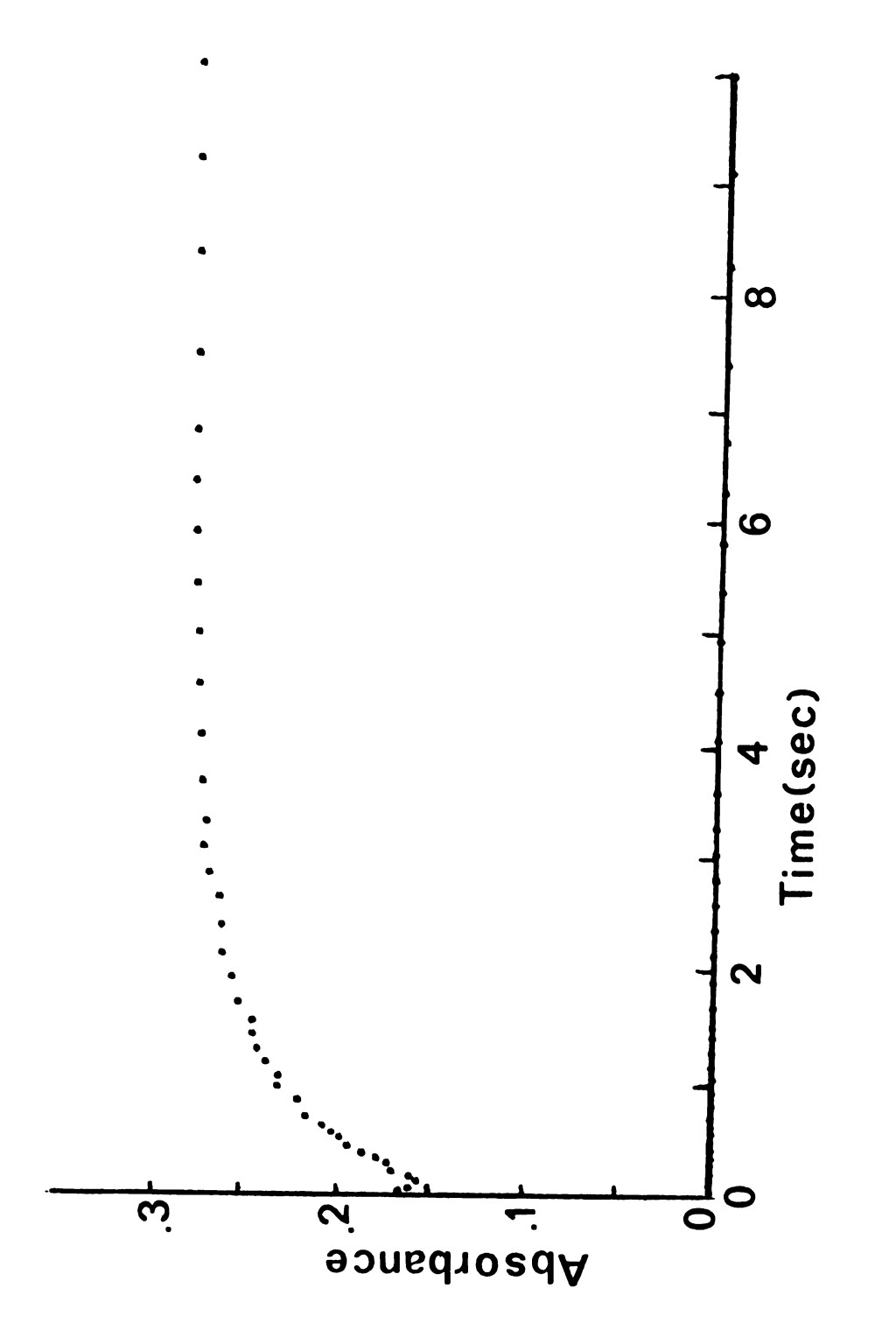
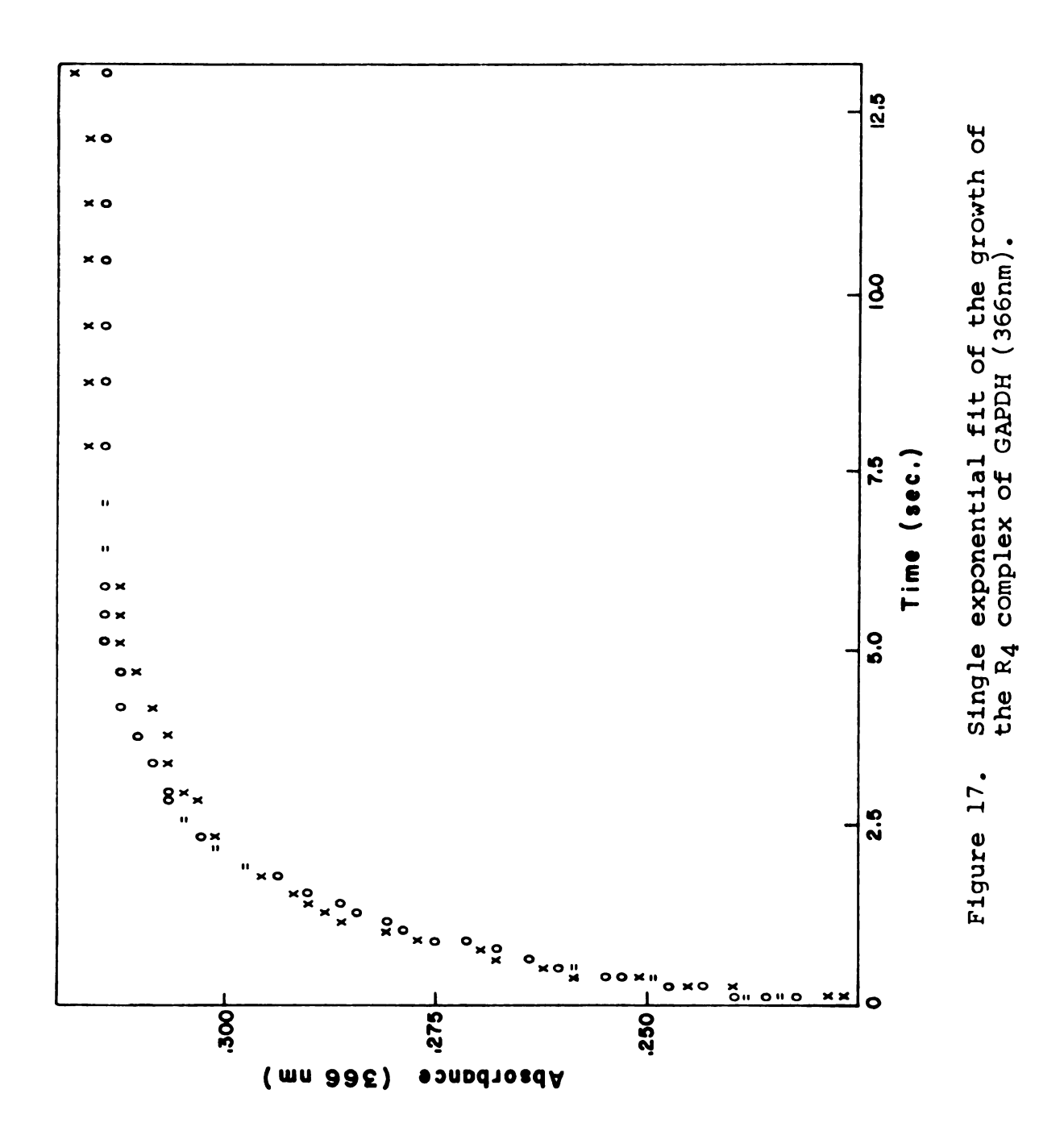


Figure 16. Time-cut at 366nm from Figure 15.



The results are shown in Figure 18 and Table expression. The percentage of each form was allowed to "float" as a parameter along with the rate constants for the isomerization of both the main $(k_{\underline{\mu}})$ and sub $(k_{\underline{\mu}}')$ components. The double exponential expression yielded a better fit based on the non systematic distribution of the experimental points about the calculated curve. The average amount of the minor sub-form was 25% compared to Kirschner's value of 20%. Comparison of the two rate constants (k_{\parallel} and $\mathbf{k}_{L}^{'})$ with Kirschner's results (Table III) shows that our values are somewhat larger. It is difficult to rationalize this discrepancy. Experimental conditions for the run were practically identical with those of Kirschner. specific activity, E280/260 ratio, and the electrophoresis results indicate that the enzyme preparations were at least comparable. The total absorbance change for the growth corresponds precisely with that expected from the concentration of GAPDH used. The fact that the isomerization process is first order in enzyme concentration, and that our values for both k_{μ} and k_{μ}' are several times larger than those determined by Kirschner does not detract from the validity of our results. The relatively large standard deviations that are given for k_{l_1} and k_{l_2} indicate the difficulty in resolving two relatively similar exponential processes from a small absorbance change (.08) on top of a large background absorbance. Kirschner provides only

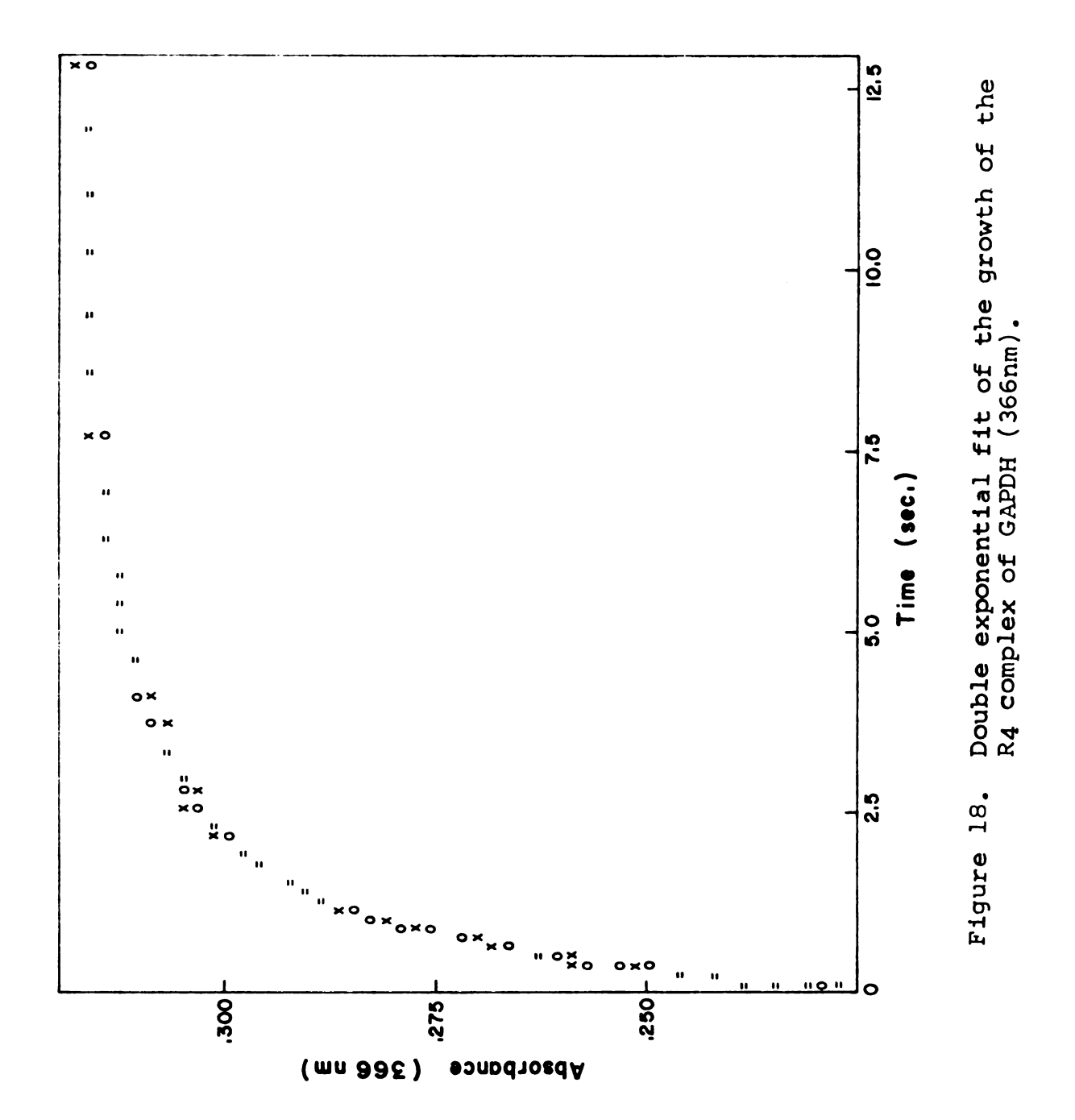


TABLE III

The effect of NAD⁺ concentration wavelength, and functional form on the first order rate constant(s) for the growth of the R4 complex of GAPDH and a comparison with Kirschner's results.

	Single Exponential Growth	Doul	Double Exponential Growth	lal Growth		Kirschner's Results
	366nm	366nm	mu	400m	ım	400m
	5тм иад	SmM NAD	LmM NAD	5mM NAD	lmM NAD	5mM NAD
$k_4(sec^{-1})$	0.845±0.030	1.42±0.09	1.35±0.11	1.41±0.22	1.31±0.13	0.3
$\kappa_4^{}(\mathrm{sec}^{-1})$		0.303±0.094 0.362±0.0490.407±0.114 0.281±0.068	0.362±0.049	0.407±0.114	0.281±0.068	0.15

an estimate of k_{\downarrow} , and in fact used only 80% of the progress curve to determine k_{\downarrow} . There is no indication that a correction for the second exponential process was made. Although our results obtained by using the KINFIT program, represent a much more sophisticated treatment, it is still difficult to rationalize such large differences.

According to Kirschner the isomerization rate for the forward process T→R is independent of the number of NAD molecules bound. He accounts for the predominance of the $T_{\downarrow} \rightarrow R_{\downarrow}$ pathway by assuming that the rate for $R \rightarrow T$ is smallest when four NAD's are bound, and that the reverse rates increase when fewer than four are bound. To test this assumption GAPDH was rapidly mixed with 1 mM NAD. Since the T and R forms have different saturation characteristics, it is possible with this level of NAD to saturate only the R form in a rapid mixing experiment. It was suspected that under such conditions a significant portion of the conformational change might proceed through (say) the $T_3 \rightarrow R_3$ pathway and that this rate might be somewhat different from that for the $T_{\downarrow\downarrow} \rightarrow R_{\downarrow\downarrow}$ reaction. These results are also shown in Table III. No significant difference for the rate of R, formation was observed.

As a further test of the overall resolution of the instrument, data from Figure 15 at 400 nm were also fitted to a double exponential expression. As expected, no effect at either level of NAD was observed, although the

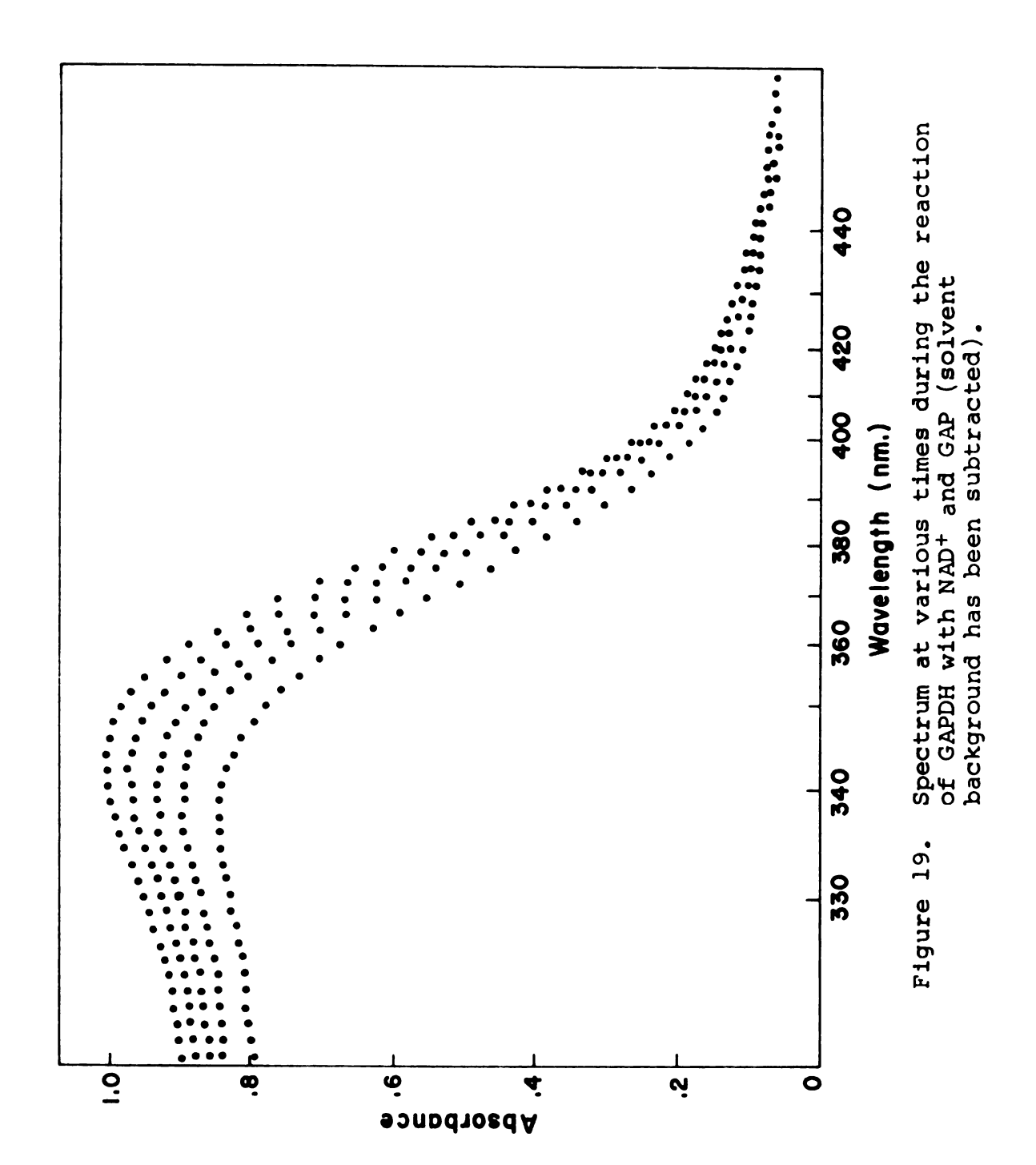
standard deviations at 400 nm are obviously larger because of the smaller absorbance change at this wavelength.

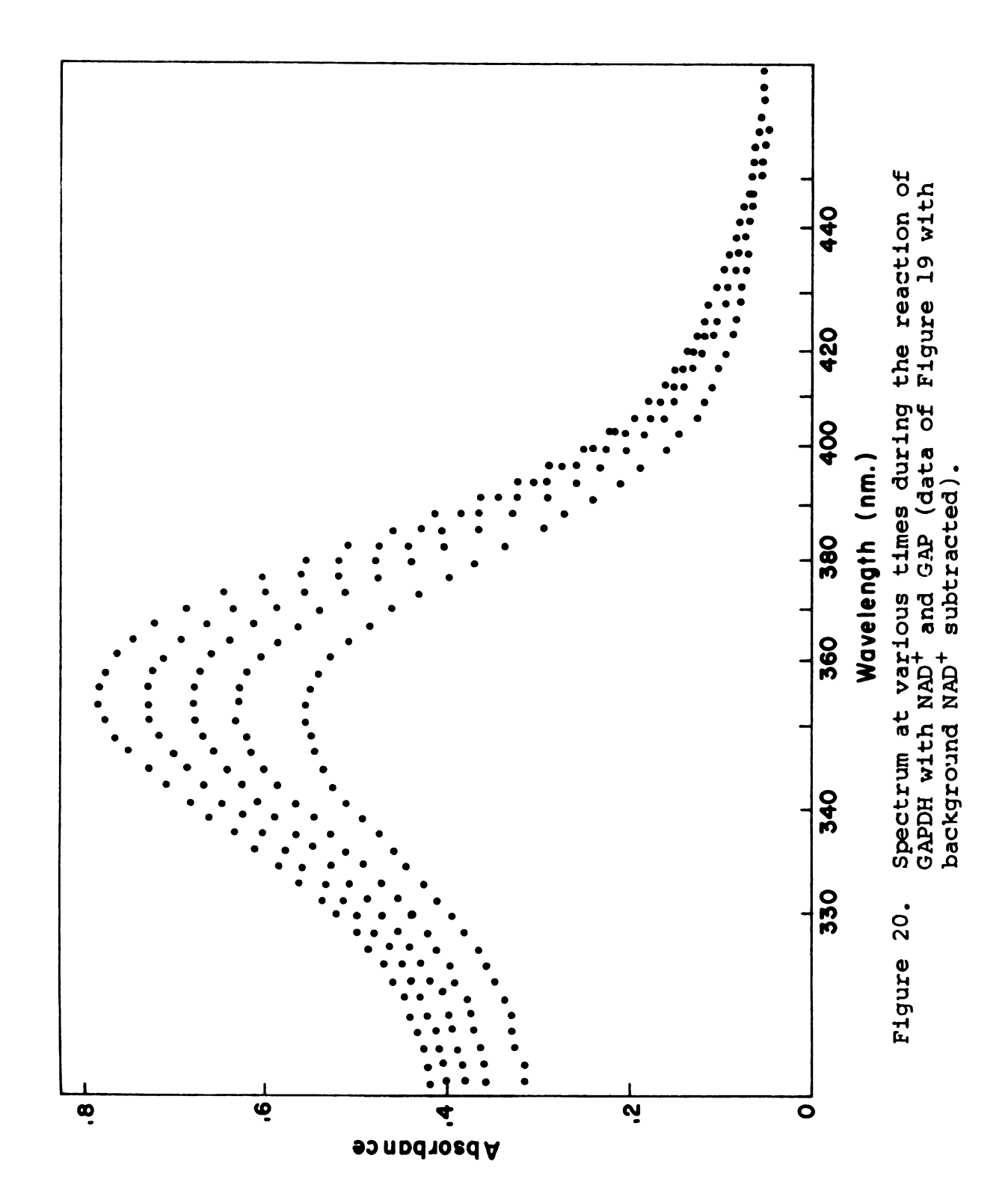
6.1.2--Reaction with Substrate

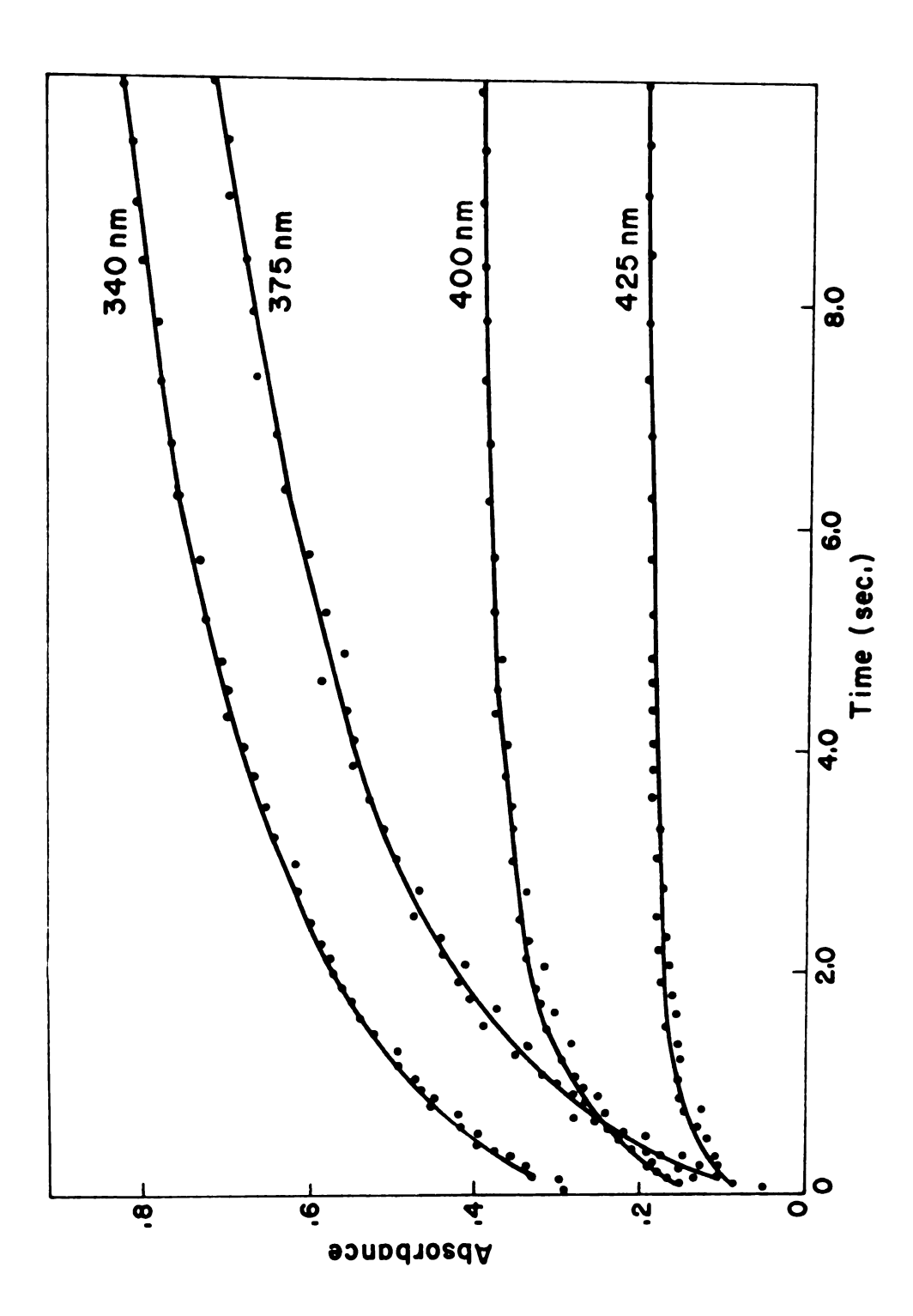
The reaction with substrate (GAP) was carried out under conditions of excess GAPDH and saturating levels of NAD+. Figure 19 shows the development of the spectrum during reaction with only the buffer background subtracted. The R_{μ} complex and NADH have comparable absorptions in this region under these conditions. Note that even when the excess NAD background is subtracted (see Figure 20), it is still difficult to discern a wavelength dependence in the time development. However, when time-cuts are taken at several wavelengths across the band (Figure 21), the presence of at least two time and wavelength dependent phenomena is quite evident. These of course, correspond to the simultaneous growth of NADH and the R, complex, followed by continued production of NADH at a steady state level of R_{j_1} . We feel that these experiments clearly illustrate the utility of the scanning experiment and the need for high resolution and versatile data processing capabilities.

6.2 -- The Threonine Dehydrase System

In an effort to further demonstrate the versatility of the rapid scanning system, we report some results on a collaborative project with Professor Wood of the MSU



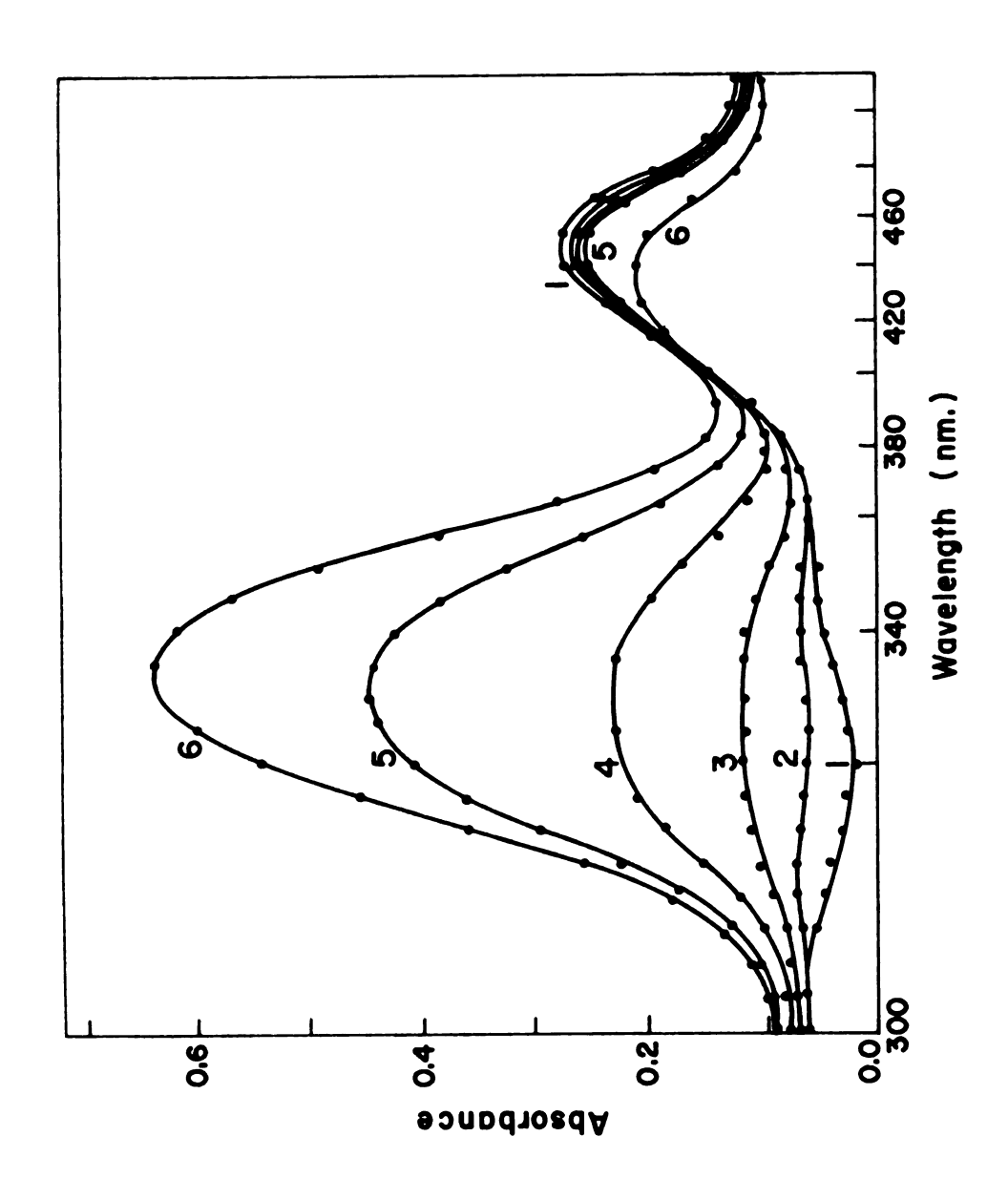




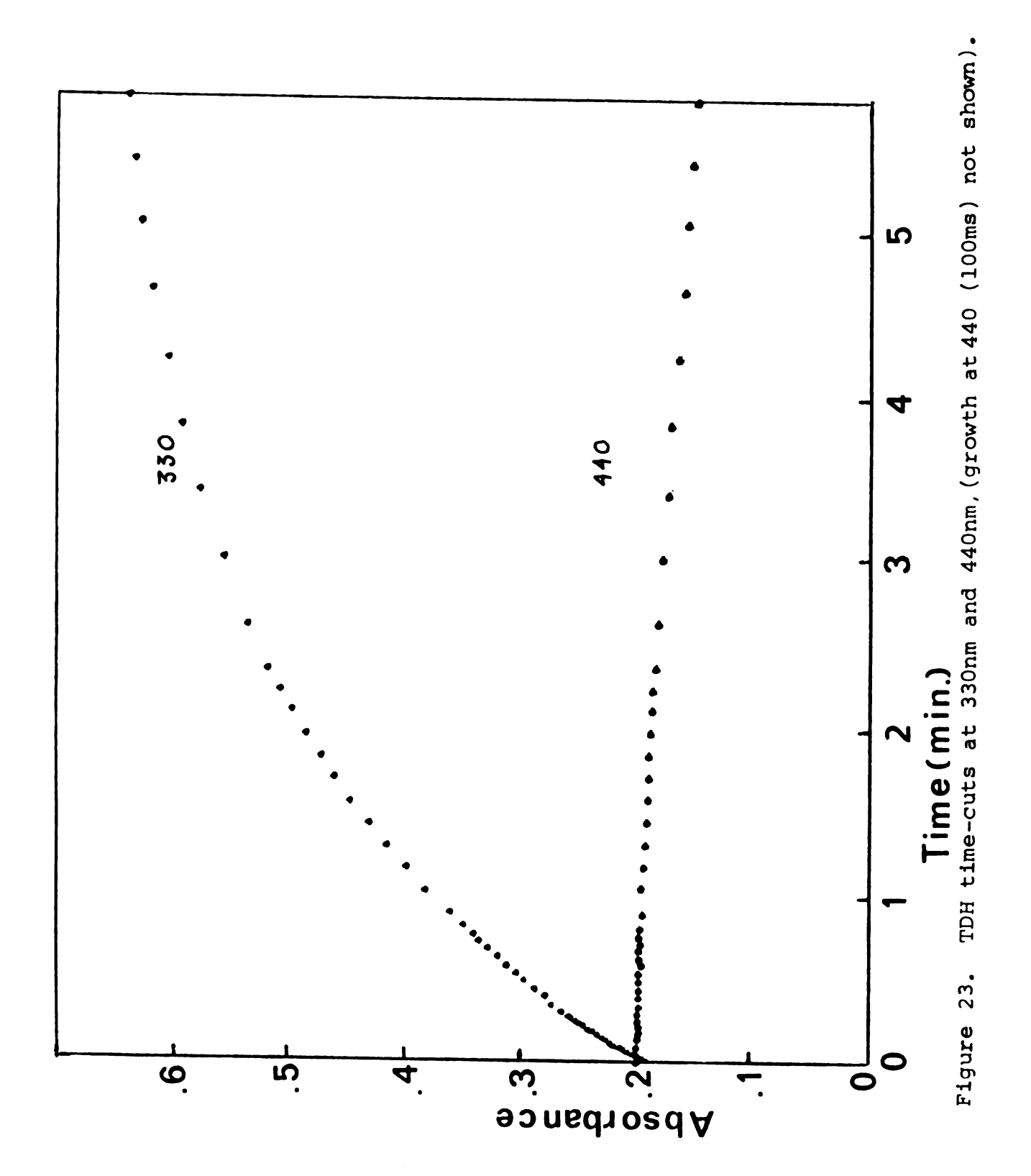
Time-cuts of the data from which Figure 20 was taken. Figure 21.

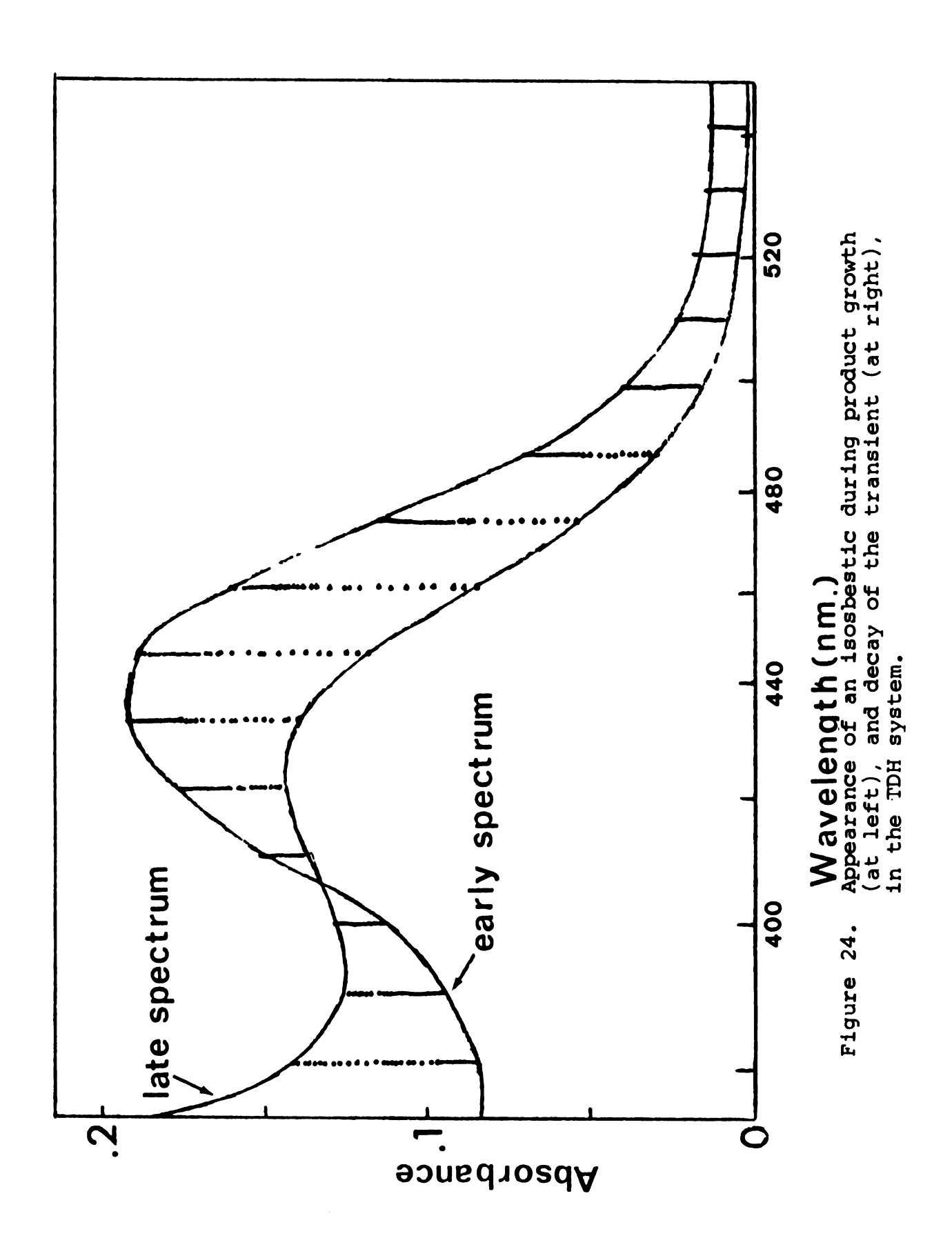
Biochemistry Department on an unusual allosteric enzyme, the L-threonine dehydrase of E. Coli. This proved to be an interesting system since the entire time course of the reaction, from the initial growth and wavelength shift of the absorption of the enzyme-bound complex to the growth of the product absorption, could be followed. The spectral changes are shown in Figure 22 (which does not have the solvent absorption subtracted). The initial single band at 420 nm grew and shifted to 460 nm in about the first 100 ms. During the growth of product the transient absorbance at 460 nm gradually diminished and shifted until at the end of the reaction the band at 420-430 nm was about the same as at the beginning. This is shown by the time-cuts in Figure 23 at 330 nm and 440 nm. The two decay curves are on the same absorbance scale but a constant value has been subtracted from each absorbance for display purposes. Toward the end of the reaction when product formation is nearly complete, the transient absorption of the enzyme-bound complex decays back to that of the enzyme alone. An isosbestic point occurs at about 405 nm. This is shown in Figure 24, which covers the wavelength range from about 370 to 550 nm.

The enzyme itself is known to exhibit a peak at 415 nm due to Schiff base formation between pyridoxal phosphate and a lysine residue (5,75). The shift of the



Selected spectra from Groups 1, 2, 3...for the deamination of L-threonine by TDH (no baseline subtracted). Figure 22.





absorption to give a new band at 450 nm (composite at 430 nm) upon the addition of L-threonine and AMP has been previously observed and presumably reflects the formation of a Schiff base between the enzyme-bound pyridoxal phosphate and aminocrotonate, a dehydrated intermediate derived from L-threonine (89, 90).

The results are somewhat inconclusive concerning any new mechanistic information; however, a few general statements are possible: (1) by using a faster scan rate or under fixed wavelength conditions, the approach to steady-state of the enzyme-complex should be tractable, (2) product growth is first order, (3) other than the 430 nm band, no additional absorptions were detected on the short time scale (less than 10 sec.), (4) in the presence of 25 mM L-threonine, the steady-state concentration of the enzyme-substrate complex was achieved in less than 100 ms.

All of the above information was extracted from a single kinetic record. Although a great deal of information is made available from a single push it is not possible to draw any conclusions about the mechanism of reaction from only one set of experimental conditions. In addition, since the background absorbance due to AMP and dithiothreitol were large, the results below about 310 nm are unreliable.

The amount of information available even from a single push with the scanning system is enormous. For example, in the TDH run. we collected samples at a 20.4 KHz rate as usual and averaged six samples into each point of the spectrum so that during the 13.33 msec required to scan the spectrum in the forward direction, 40 points were stored. The first 12 spectra of 40 points each (group 1) were stored as obtained and the intervening back-scans were discarded. The next 36 spectra were stored as 12 averaged spectra (group 2) with each stored spectrum the average of three successive spectra. This process was continued such that by the time group 7 was reached, each spectrum was the average of 729 adjacent spectra with. of course, a substantially improved signalto-noise ratio. The total elapsed time was 5.83 min., yet the first 12 spectra were collected at the rate of one spectrum every 26.7 msec. Therefore, both fast and slow spectral changes could be observed. With 40 points in each spectrum, adequate wavelength resolution was available so that spectral shifts could be followed. At each wavelength, a "time-cut" could be made if desired containing 84 points with spacing between points ranging from 26.7 msec in group 1 to 19.39 sec in group 7. The ability to punch selected data directly from the PDP 8-I computer for analysis with Program KINFIT on the University CDC 6500 computer makes the analysis of such large amounts of data feasible.

6.3--Alcohol Dehydrogenase (Horse liver)

The third enzyme reaction chosen to test the new instrument was the equine liver alcohol dehydrogenase (LADH) catalyzed reduction of the substrate analog p-nitroso-N, N-dimethylaniline (NDMA) by reduced nicotinamide adenine dinucleotide (NADH). This thoroughly characterized enzyme has been the subject of numerous steady-state kinetics studies (91-95) and binding studies (96-100). Good evidence exists for two coenzyme binding sites per molecule of enzyme (101-103). The enzyme exhibits a rather broad specificity for aldehydes of widely varying structure; however, specificity for coenzyme analogs is somewhat more restrictive (104). The kinetic sequence for the binding of coenzyme and substrate prior to reaction has been demonstrated to be ordered with compulsory binding of coenzyme as the initial step under steady-state conditions (91,94,95). Wratten and Cleland (94.95) have demonstrated the presence of ternary complexes among enzyme-coenzyme-substrate (also under steady-state conditions.) More recently, rapid kinetics techniques have made possible the characterization of some individual steps in the overall transformation (105-111).

Transient intermediates in the LADH catalyzed reduction of several aromatic aldehydes have recently been observed (109,110). It was this last aspect of the LADH system which seemed most attractive as a means of evaluating the potential of the rapid scan technique.

6.3.1--LADH Rate Measurements

Quantitative rate measurements were made by using data from four replicate scanning pushes in conjunction with the KINFIT program. A variety of rate expressions, derived to reflect specific mechanistic alternatives, were tried in order to determine the relationships among the time developments at several wavelengths. Only those expressions which yielded the best fit of the data will be discussed. The approach was somewhat phenomenological. However the quantity and complexity of the data required an economical and systematic procedure for eliminating alternative mechanisms.

6.3.2--Kinetics of NDMA Disappearance (440 nm)

The disappearance of the NDMA band at 440 nm followed Michaelis-Menten Kinetics. By following the entire decay scheme and fitting the data with Program KINFIT, values of K_m (effective) and V_{max} could be obtained from single decay curves. As expected, since saturating levels of NADH were present over much of the reaction, V_{max} is more reliably and reproducibly measured than is K_m . The fit of the data to the Michaelis-Menten expression is shown in Figure 25. Table IV shows a comparison of the results with values which were determined at very low enzyme concentrations, fixed wavelength and with saturating levels of NDMA.

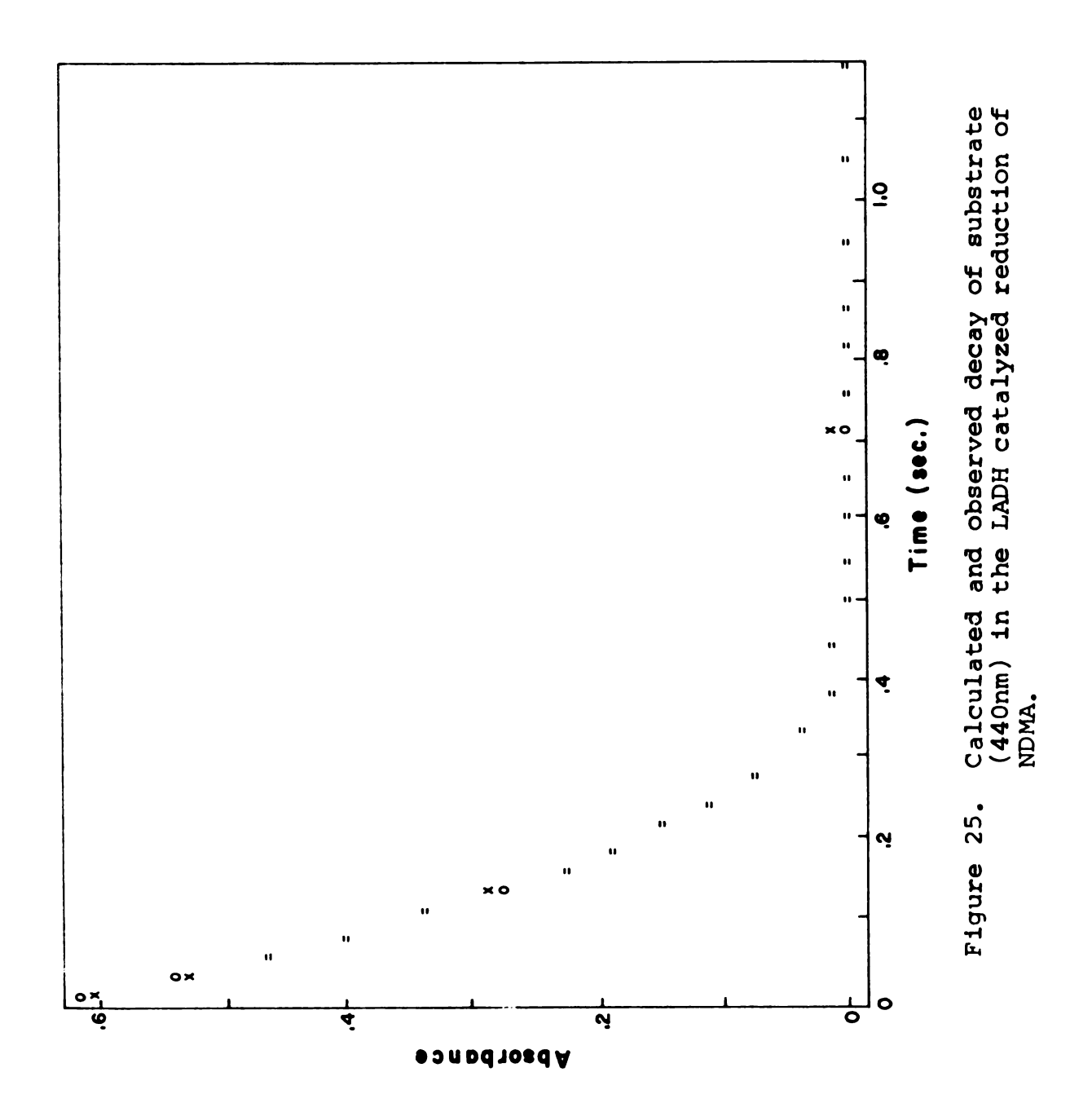


TABLE IV

Comparison between steady-state and full-time course integration kinetic parameters for substrate disappearance in the LADH system.

Kinetic Parameter	Full-Time-Course Integration 23+0.1 C	Steady State (Ref.109) 25 <u>+</u> 1 °C
Km ^{NDMA} (M) Average	4.31±0.46 X10 ⁻⁶ * 7.48±1.6 X10 ⁻⁶ 5.64±0.13 X10 ⁻⁶ 6.19±0.82 X10 ⁻⁶ 5.90±0.74 X10 ⁻⁶	0.7X10 ⁻⁶
** V _{max} Average	24.7±1.3 33.5±4.2 27.7±3.6 30.8±2.4 29.2±2.9	24 <u>+</u> 2

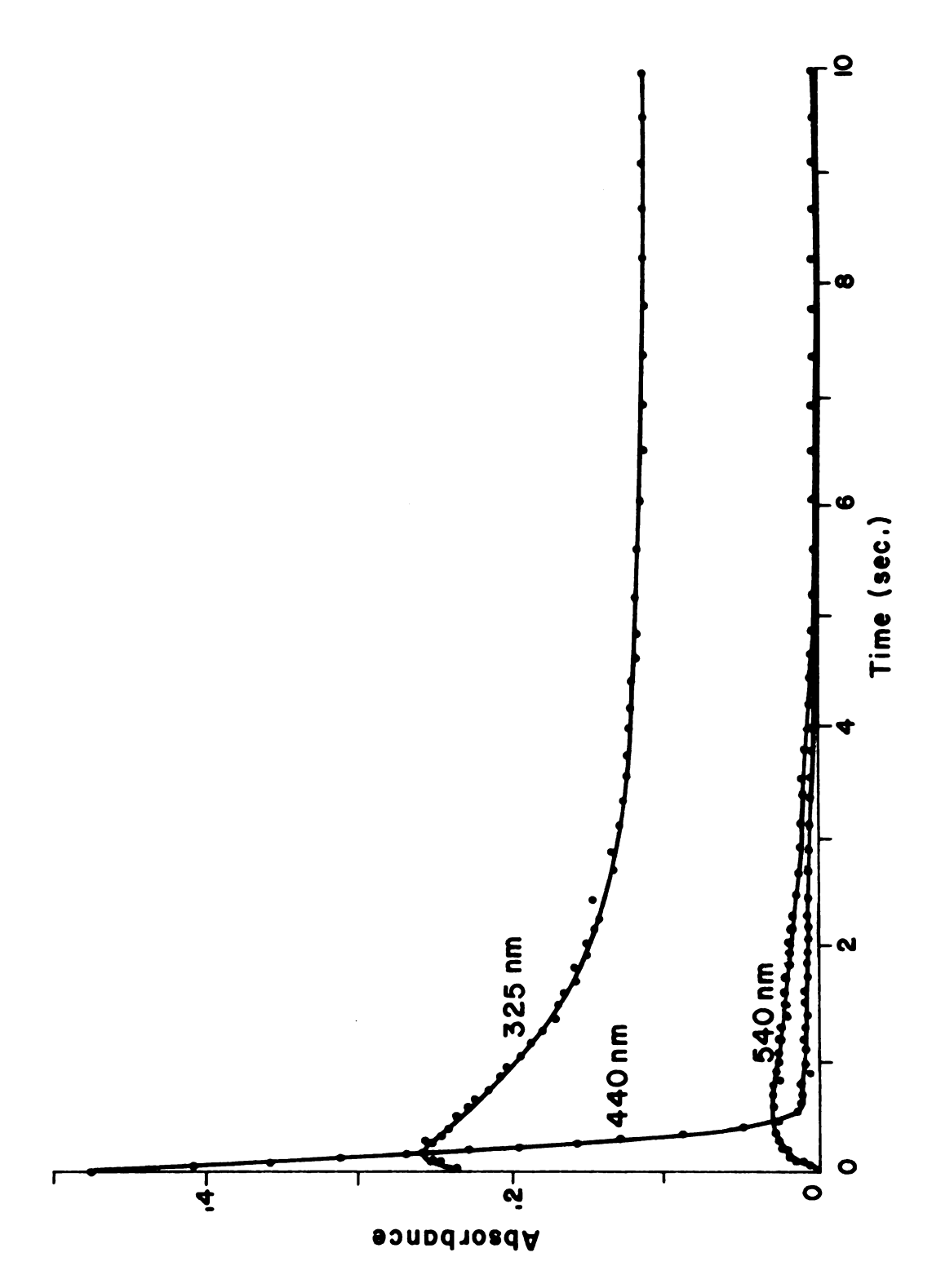
^{*} These values represent an effective \mathbf{K}_{m} for NDMA.

^{**}moles/1 NDMA per sec. per N, where N is the normality of enzyme sites.

6.3.3--Kinetics at 335 nm and 540 nm

During the decay of the NDMA absorption, the absorption band at 340 shifted to 335 nm with a slight increase in the absorbance at the maximum. This is shown by the time-cuts in Figure 26 in which the decay of the 440 nm absorption is compared with the growth and decay of the 335 nm absorption. We conclude that the absorption band at 335 nm is the spectrum of an intermediate species as suggested by Dunn (109). Also shown in Figure 26 is the growth and decay of a new absorption at 540 nm. (Since these experiments we have learned that this band has also been observed by other workers (112)). The position of the maximum absorbance may be beyond the scan range used. However, we will refer to the absorption as the "540 nm band".

Essential to the determination of possible overall mechanisms was the question of whether or not the 335 nm and 540 nm intermediates were actually two absorption bands of the same species. It was not possible to quantitatively compare both wavelengths over their entire time course of reaction because of the underlying interference of the NDMA and NADH decays with the 335 nm absorption; that is, there were too few points during the growth period at 335 nm to quantitatively correct for background decays while simultaneously fitting the data to rate expressions. However, the decay portions of the two curves (330 and 540) could be directly and quantitatively compared. After



Time-cuts at various wavelengths for the LADH system. The residual absorbance at 325nm is due to excess NADH. Figure 26.

approximately one second of reaction, the remaining changes in the absorption spectrum reflect only the changing concentration of the intermediate species. The decay of the 335 nm band was found to be first order as shown by the fit to first-order kinetics in Figure 27. The spectrum in this region after the decay is that of the excess NADH with the peak position and band shape expected for this concentration of free and enzyme-bound NADH. The average first-order rate constant for decay of the 330 nm absorption (four pushes, see Table V) is 0.70 \(\frac{1}{2}\). Oh sec \(^{-1}\) (95% confidence level). The standard deviation of the rate constant for repreated pushes is about equal to that obtained from a single push.

The decay at 540 nm is also first order with a rate constant of 0.447 $^{+}$ 0.01 sec⁻¹ (four pushes, see Table V and Figure 28). Since the <u>same</u> pushes are used to evaluate data at all wavelengths, there can be no doubt that the 540 nm decay is slower than at 335 nm. Therefore, the two absorptions do not represent the same species.

Time-cuts from several wavelengths in the 340 nm region were fit to first order kinetics. The results are in agreement at 330, 335 and 340 nm (see Table V). There is a systematic increase in the first order constant, however, in going from 340 nm to 360 nm. It is worth emphasizing that the values reported horizontally in Table V are from one push, and secondly that these values are the result of fitting the data from the period

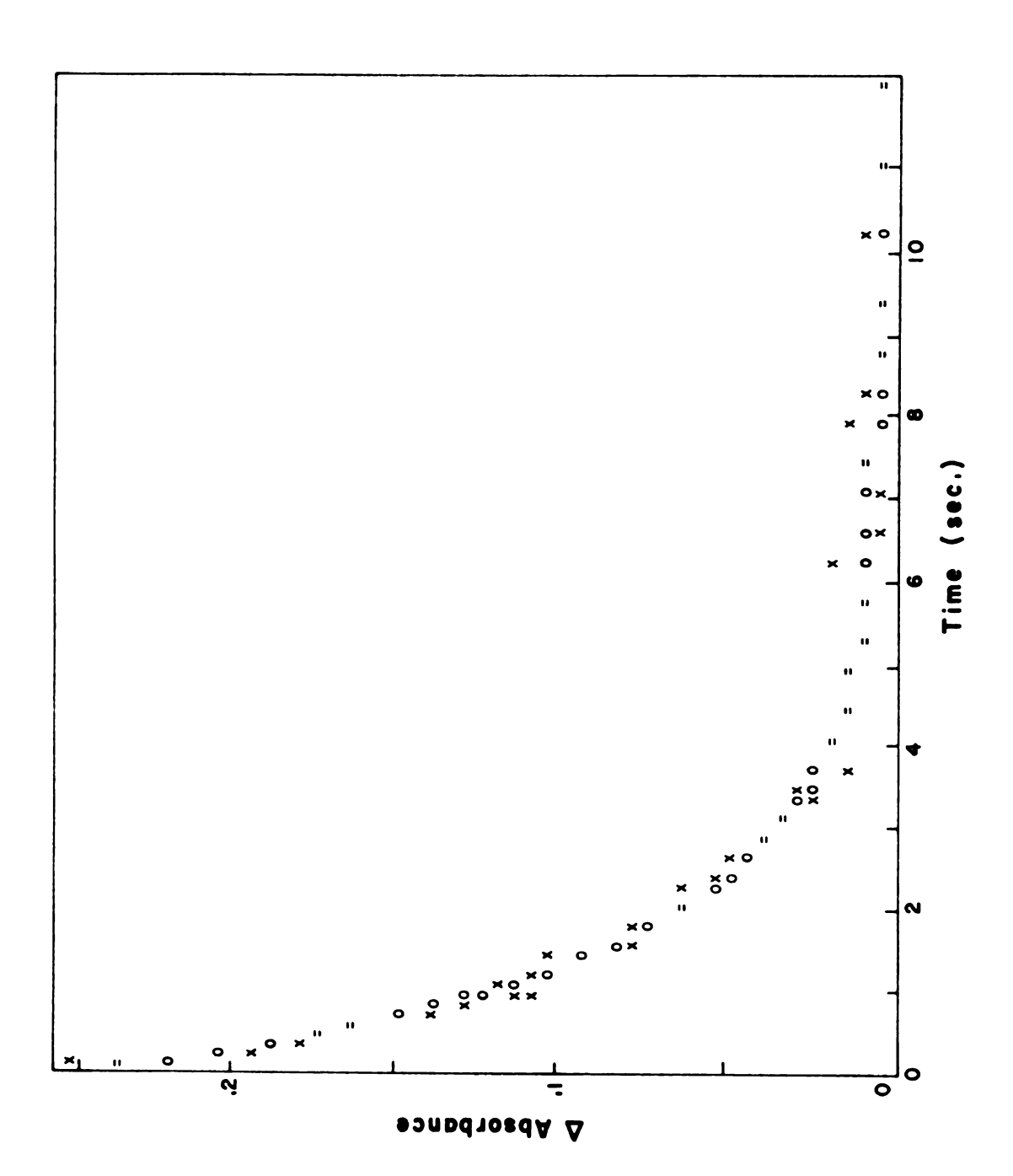


Figure 27. First-order decay of the 325nm transient in the LADH system.

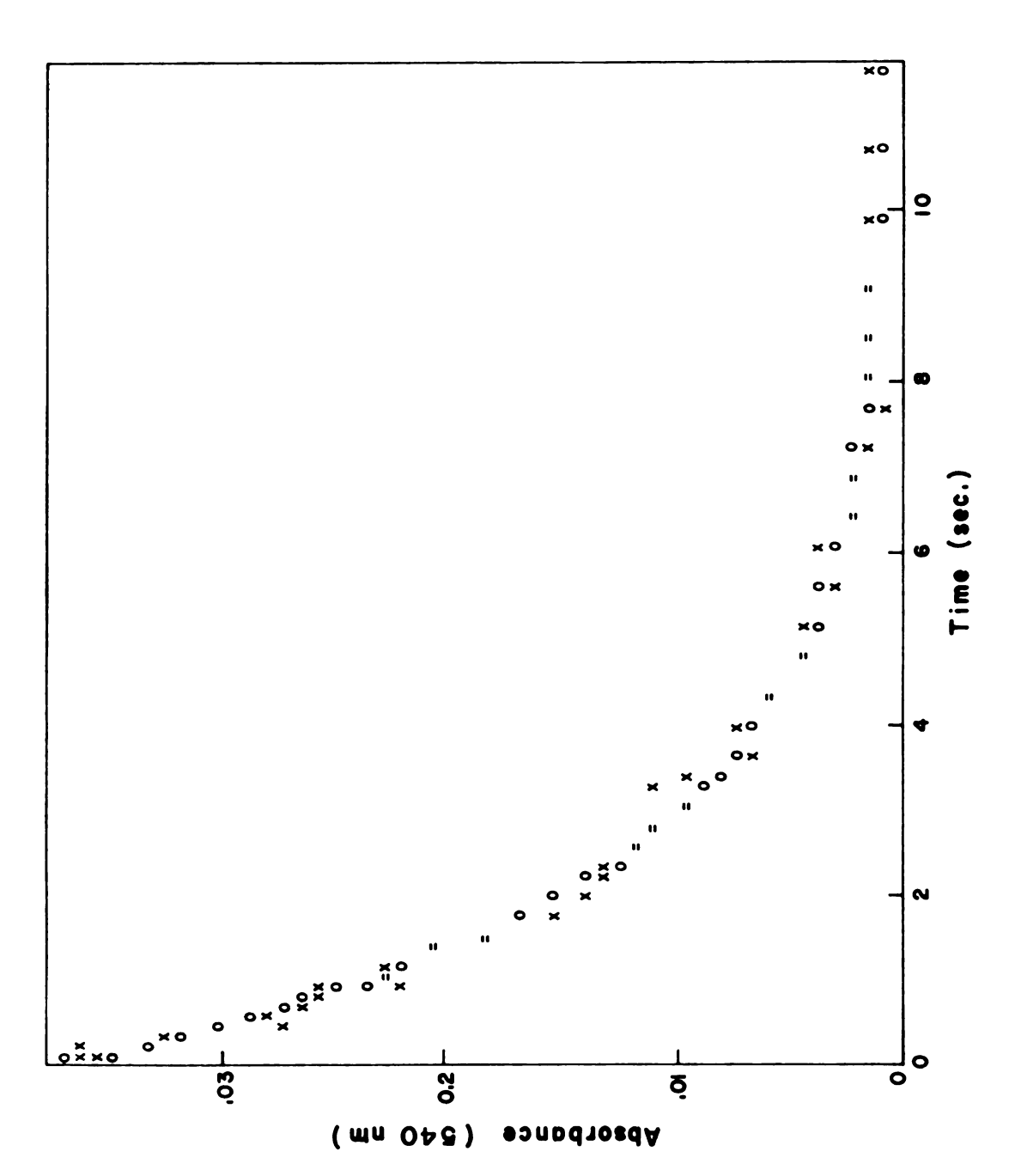


Figure 28. First-order decay of the 540nm transfent in the LADH system.

TABLE V

First order decay constants for the transient intermediates of the LADH system.

Push Code	330nm	335nm	340nm	350nm	360nm	540nm
D.	0.741±0.032	0.732±0.025	0.749±0.025	0.839+0.043	1.12±0.07	1.12±0.07 0.446±0.014
K	0.685±0.024	0.690±0.024	0.707±0.019	0.839±0.026	1.07±0.07	1.07±0.07 0.456±0.013
ī	0.699±0.025	0.696±0.021	0.712±0.021	0.836±0.033	1.06±0.09	1.06±0.09 0.449±0.015
Σ	0.691±0.028	0.682±0.024	0.708±0.023	0.824±0.038	1.05±0.08	1.05±0.08 0.438±0.014

after NDMA has disappeared.

Since the first order constant at 540 nm is the smallest, we infer the presence of an additional time dependent absorption band in the 340-360 nm region. addition, the quantity (A - Am) becomes negative in the 325-380 nm region towards the end of the reaction (not shown), indicating that an additional absorbance is present at infinite time and appears with a half-life of approximately 10 sec. In similar experiments, using the chromophore trans -4- N,N - dimethylaminocinnamaldehyde (DACA, 398 nm) Dunn and Hutchison (110) observed the formation of a long wavelength intermediate (460 nm) analogous to the 540 nm species observed with NDMA. addition, they observed the slow formation of another species which they attribute to be an artifact resulting from the presence of NADH formed via the LADH catalyzed oxidation of residual ethanol in the preparation. Since no extreme precautions were taken in the present work, the very slow increase in absorbance around 360 nm at the end of reaction could be attributed to the same artifact. The rate and magnitude of this slowly forming band are too small to account for the variation of the first order constant with wavelength.

One of the unique advantages of the rapid scanning stopped-flow experiment is the fact that rate data at several wavelengths can be compared by fitting data from

a <u>single</u> push. In this way, variations in conditions from push to push which may affect the rate constant and which often occur with fixed wavelength instruments are eliminated. The agreement (Table V) both within each push and among replicate pushes at 330, 335, 340 and at 540 nm is proof of the excellent reproducibility of the instrument.

6.3.4--Rate Law for 440 and 540 nm

The relationship between substrate decay and the growth of the two intermediates is central to a determination of the overall mechanism of the system. The fact that a single substrate gives rise to two intermediates and apparently only a single product (109) significantly complicates the problem. Since the substrate follows Michaelis-Menten kinetics, and the intermediates decay by first order processes, it was possible to relate the decay at 440 nm to the growth and decay at 540 nm by using Equation (4). A zero order correction was included (not shown) to account for substrate decay during the time (~ 2 ms) which elapsed between the two wavelengths. Since the extinction coefficient of the 540 nm species is not known, the rate constant k_{540}^{G} actually represents the product of a rate constant (k), an extinction

$$\frac{d(X)}{dt} = \frac{k_{540}^{G} \cdot E_{o}}{1 + \frac{K_{NDMA}}{(NDMA)}} - k_{540}^{D}(X)$$
 (4)

coefficient (ε_{540}), and the path length (1.85 cm). The

overall course of the 540 nm intermediate (X) was fitted by a Michaelis-Menten growth term $(k_{5\mu 0}^G)$, and a first order decay (k_{540}^{D}) which of course is independent of both substrate binding (K_{NDMA}) and total enzyme concentration (E_0). The agreement between calculated and experimental points shown in Figure 29 and Table VI are clearly consistent with the postulate that the growth of the 540 nm species is proportional to the rate of substrate decay. However, more recent work by Dunn (Private Communication) has shown that as the concentration of enzyme is increased, the decay time of substrate is decreased and its decay is followed by a first-order growth of a 560 nm band. In the present work only one concentration of substrate was used; hence no conclusions can be drawn about this matter. It is possible that our results represent a coincidental case in which the firstorder growth at 540 nm accidentally matches our particular decay time of substrate. This possibility is supported by the presence of an isosbestic at 510 nm during the growth period. Figure 30 shows an expansion of the region from 400 nm to 540 nm during the decay of the 440 nm band and the growth of the 540 nm absorption. Since the growth of the 540 nm species coincides with the decay of the NDMA band, an isosbestic occurs at 510 nm. It should be noted that the maximum absorbance at 540 nm is only 0.04 absorbance units. In addition, note the agreement between the

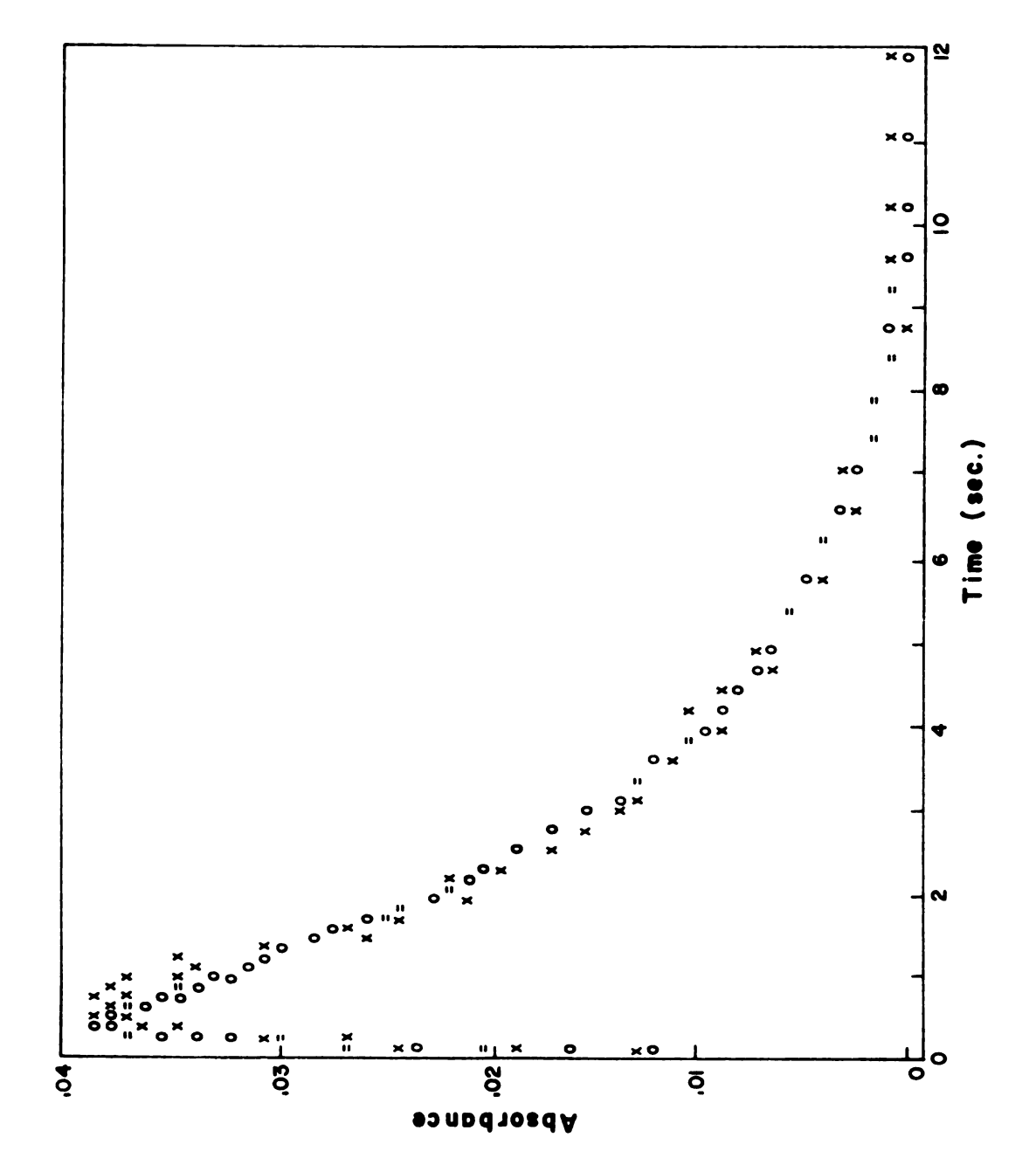


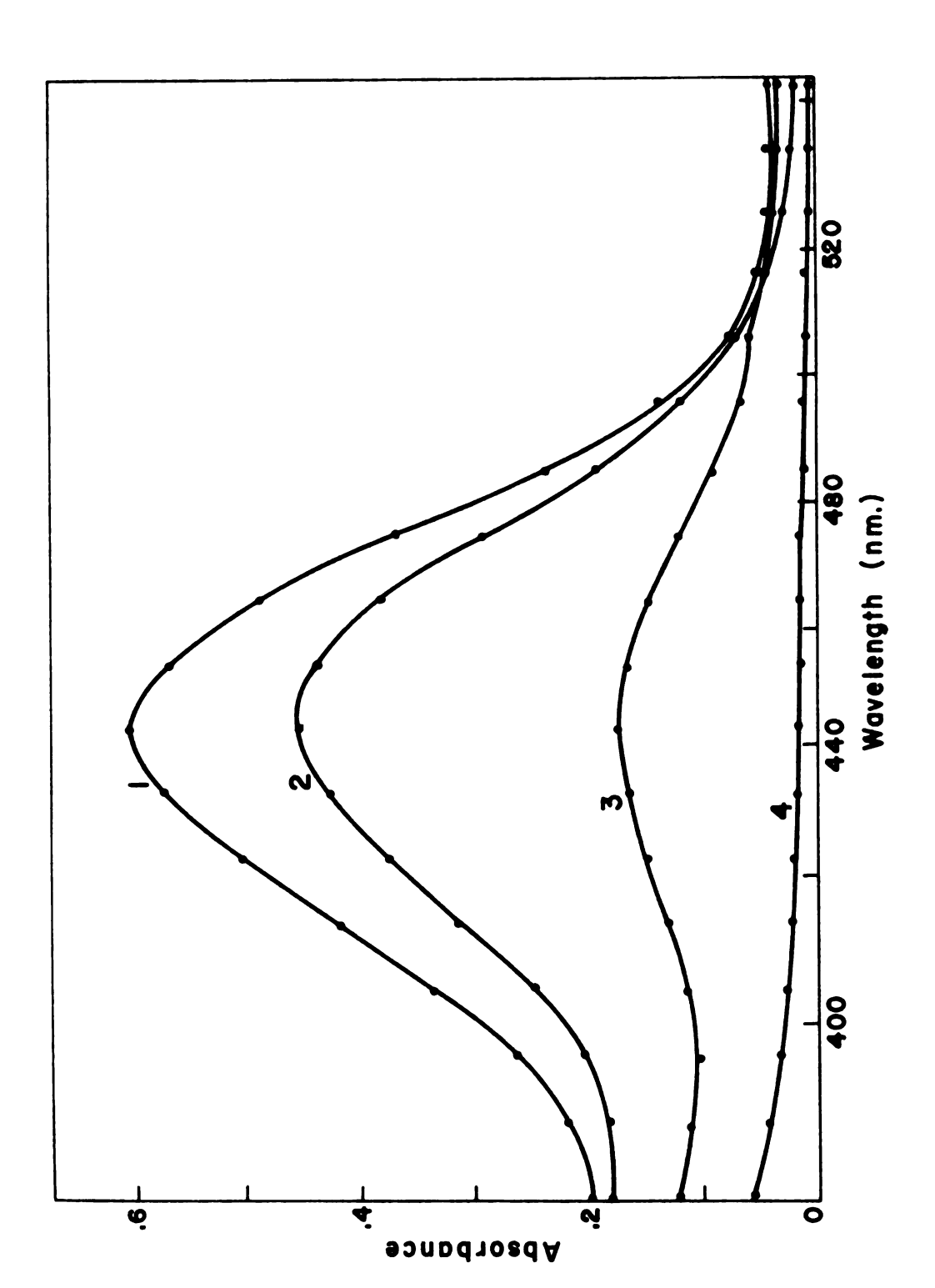
Figure 29. Growth and decay of the 540nm transfent intermediate in the LADH system.

TABLE VI

Rate constants for the Michaelis-Menten growth and first order disappearance of the 540nm intermediate (from Equation 4)

Push Code	k ₅₄₀ =k•€ ₅₄₀ 1•E ₀	$\kappa_{540}^{\mathrm{D}}(\mathrm{sec}^{-1})$	K ₅₄₀ (sec ⁻¹) (From Table V)
J	0.251 <u>+</u> 0.012	0.416 <u>+</u> 0.014	0.446 <u>+</u> 0.014
К	0.280 <u>+</u> 0.012	0.433 <u>+</u> 0.024	0.456 <u>+</u> 0.013
L	0.274 <u>+</u> 0.016	0.387 <u>+</u> 0.015	0 .449<u>+</u>0.01 5
М	0.314 <u>+</u> 0.013	0.560 <u>+</u> 0.103	0.438 <u>+</u> 0.014

Note: $K_{\rm m}^{\rm NDMA}$ =5.9X10⁻⁶M (average from Table IV) was used in fitting data to Equation 4. Total enzyme concentration(E_O)=3.62X10⁻⁶N ϵ_{540} is the extinction coefficient of the 540nm intermediate, and ϵ_{240} =1.85cm.



Substrate (440nm) and transient (540nm) absorptions in the LADH system showing the isosbestic at 510nm during substrate decay. Spectrum 4 is the residual absorption. Figure 30.

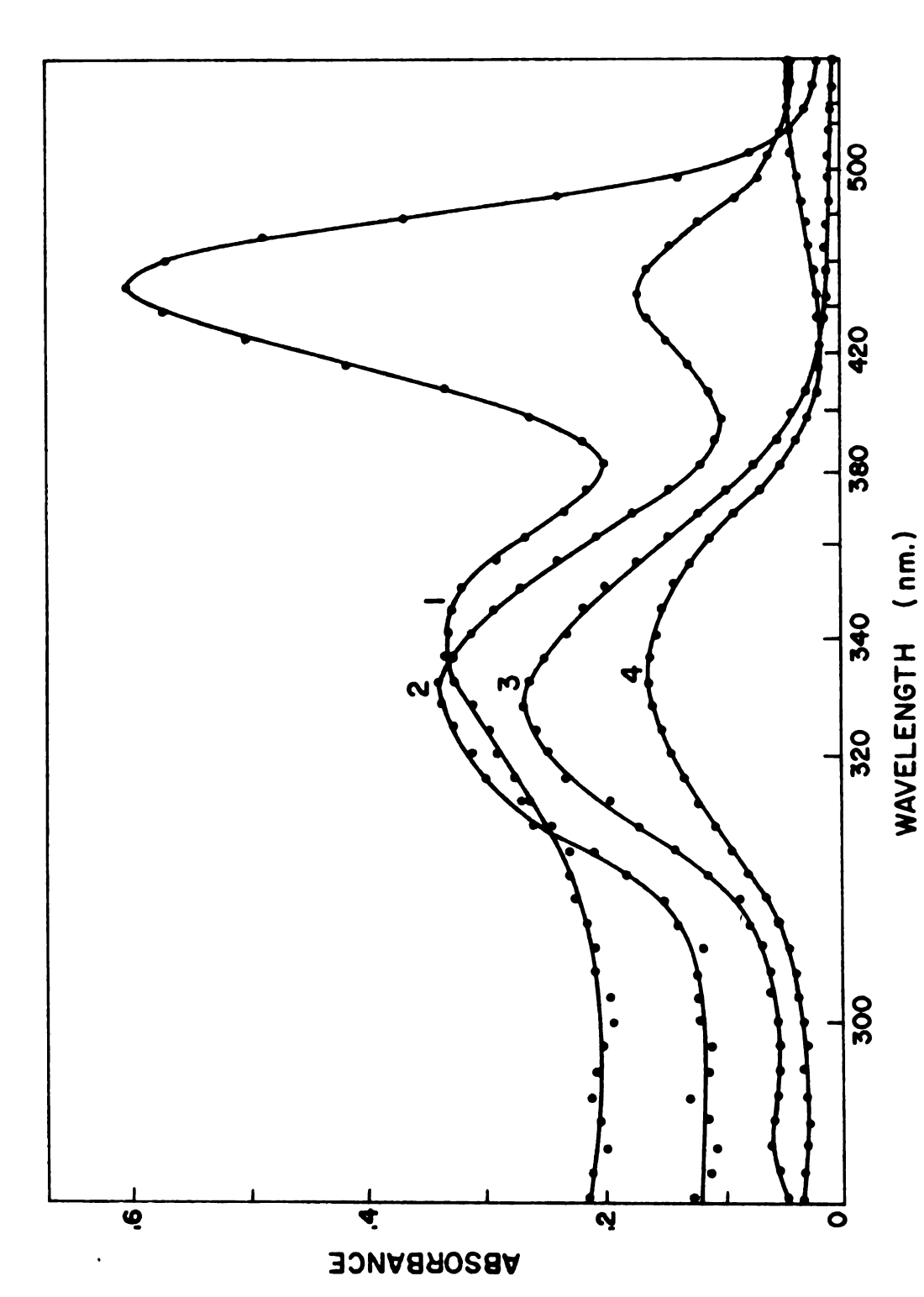
first order decay constant at 540 nm as determined by the decay portion only (Table V), and by fitting two wavelengths over the entire time course (Table VI).

Although somewhat complicated by additional concurrent decay processes, it appears that the band shift and growth at 335 nm (see Figure 26) also coincides with the disappearance of the NDMA band. The subtle changes in spectral shape in this region emphasize the advantages of the scanning system.

The overall changes in the spectrum from 290 nm to 540 nm are shown in Figure 31. Spectrum 1 is that at zero time; spectrum 2 corresponds to the time of maximum 335 nm absorption; spectrum 3 to the decay of the 335 and 540 bands after the substrate band has completely decayed; and spectrum 4 corresponds to the residual NADH absorption after decay of all intermediates.

Although a number of kinetic pushes (reactions) were done with LADH it should be noted that all of the figures shown in this section were taken from a single push. This emphasizes the distinct advantage of the scanning stopped-flow technique over those which utilize fixed wavelength devices.

Although it is not possible to rationalize a unique overall mechanism for the LADH-NDMA system from the results of a single experiment, we feel that the present work significantly limits the number of alternatives.



Overall spectral changes in the LADH catalyzed reduction of NDMA by NADH. Figure 31.

VII. SUGGESTIONS FOR FUTURE WORK

Although the performance of the rapid scan stoppedflow system in transient-state enzyme studies is very
good, several steps can be taken to make it even better
for such research. Specifically, the installation of a
UV grade fused silica prism (recently purchased) will
allow studies in the spectral region below 300 nm.
Because the present sample and reference beams do not
originate from the same portion of the lamp image, it
is impossible to eliminate fluctuations in the output
caused by wander of the Xenon arc. Therefore the existing
optical system should be replaced with a fiber-bundle
beam-splitter (currently being constructed by Schott
Optical Co.). If the fibers within the beam-splitter
can be randomized, the improvement in S/N should be
significant and the set-up time reduced.

The limited availability of most enzymes makes it mandatory to use small volumes of sample. Therefore the present flow system should be re-designed to permit the use of smaller samples. At the same time it would be worthwhile to investigate the use of polypropylene tubing in place of glass tubing for construction of the flow

system in order to increase the flexibility of the system and to minimize its breakage.

The computer interfaced rapid scan stopped-flow system described in this work is an ideal tool for simultaneous study of the kinetics of substrates, products and spectral intermediates. Systems which show development of several spectral intermediates during catalysis, such as those involving B₆ enzymes (TDH), can now be studied more effectively by observing the relative rates and the sequence of development of intermediate species. Thus the computer interfaced rapid scan stopped-flow system should go a long way towards helping the investigator to correlate complex kinetics data and to help sort out the kinetics and the mechanisms of enzyme reactions.

REFERENCES

- 1. M. Dixon and E. C. Webb, Enzymes, Academic Press, New York, 3rd ed., (1967).
- 2. H. Gutfreund, Enzyme Kinetics, Benjamin, New York, (1968).
- 3. K. J. Laidler, The Chemical Kinetics of Enzyme Actions, Clarendon Press, Oxford, (1958).
- 4. C. J. Gray, Enzyme Catalyzed Reactions, Van Nostrand Reinhold, London, (1970).
- 5. Y. Shizuta, A. Nakazawa, M. Tokushige, and O. Hayaishi, <u>J. Biol. Chem.</u>, 244, 1883 (1969).
- 6. W. W. Umbriet, R. H. Burris and J. F. Stauffer, Manometric Techniques, Burgess Publishing Co., Minneapolis, (1945).
- 7. M. Dixon, <u>Manometric Methods</u>, Cambridge University Press, England (1951).
- 8. George G. Guilbault, Enzymatic Methods of Analysis, Pergamon Press, New York, p. 31, (1970).
- 9. H. Pardue, R. Simon, Anal. Biochem. 9, 209 (1964).
- 10. R. K. Simon, G. D. Christian and W. C. Purdy, <u>Clin</u>. Chem. 14, 463, (1968).
- 11. G. G. Guilbault, D. N. Krames and P. L. Cannon, Anal. Chem. 34, 842 (1962).
- 12. T. H. Ridgway and H. B. Mark, <u>Anal. Biochem.</u> 12, 357 (1965).
- 13. G. G. Guilbault and F. R. Shu, <u>Anal. Chem</u>. <u>山</u>, 2161 (1972).
- 14. S. J. Updike and G. P. Hicks, Nature 214, 986 (1967).

- 15. Howard V. Malmstadt, E. A. Cordos and C. J. Delaney, Anal. Chem., 山, 26A (1972).
- 16. C. D. Scott, C. A. Burtis, Anal. Chem. 45, 327A (1973).
- 17. M. Eigen and L. C. de Maeyer, in <u>Techniques of</u>
 Organic Chemistry Vol. 8, <u>Investigations of Rates</u>
 and <u>Mechanisms of Reactions</u>, <u>Interscience</u>, <u>New York</u>,
 pp. 895-1054 (1963).
- 18. M. Eigen in <u>Fast Reactions and Primary Processes in</u> Chemical Kinetics, ed. S. Claesson, Interscience, New York, (1967).
- 19. T. C. French and G. G. Hammes, Methods Enzymol., 16: 3, (1964).
- 20. G. C. Kreshick, E. Hamori, G. Davenport, and H. A. Scheraga J. Amer. Chem. Soc. 88: 246, (1966).
- 21. H. Gutfreund in Annual Rev. Biochem., Esmond E. Snell, ed., Annual Reviews Inc., 40, 315 (1971).
- 22. G. G. Hammes, Advan. Protein Chems., 23: 1 (1968).
- 23. G. G. Hammes and E. J. del Rosario, <u>J. Amer. Chem.</u> Soc. 92: 1750 (1970).
- 24. Q. H. Gibson in Annual Rev. Biochem., 35: 435 (1966).
- 25. K. Kirschner, E. Gallego, I. Schuster, and D. Goodell, J. Mol. Biol., 58, 29, (1971).
- 26. K. Kirschner, J. Mol. Biol., 58, 51 (1971).
- 27. J. E. Erman and G. G. Hammes, Rev. Sci. Instrum., 37 (6), 746 (1966).
- 28. G. G. Hammes and P. R. Schimmel, <u>J. Amer. Chem. Soc.</u>, <u>87</u>, 4665 (see also 4674) (1965).
- 29. S. L. Friess, E. S. Lewis, and A. Weissberger, Eds. Techniques of Organic Chemistry. Vol. 8, <u>Investigation of Rates and Mechanisms of Reactions</u>, Interscience, (1963).
- 30. B. Chance, Q. H. Gibson, R. E. Eisenhardt, K. K. Lonberg-Hohn, Eds., Rapid Mixing and Sampling Techniques in Biochemistry, Academic, New York, (1964).

- 31. K. Kustin, Ed. Methods Enzymol., 16, (1964).
- 32. N. Papadakis, Ph.D. thesis, Michigan State University (1974).
- 33. Q. H. Gibson and L. Milnes, <u>Biochem. J.</u>, 191: 161 (1964).
- 34. H. Gutfreund, An Introduction to the Study of Enzymes, Oxford: Blackwell, (1965).
- 35. R. L. Berger, B. Balks, and H. F. Chapman, <u>Rev. Sci.</u> <u>Instrum.</u>, 39: 493 (1968).
- 36. B. Chance, D. DeVault, V. Legallais, L. Mela, and T. Yonetani, See Ref. 18, 437.
- 37. B. Hess, H. Kleinhans, and H. Schleuter, Z. Physiol. Chem., 351: 515 (1970).
- 38. M. J. Milano, H. L. Pardue, T. E. Cook, R. E. Santini, D. Margerum, and J.M.T. Raychba, Anal. Chem. 46, 374 (1974).
- 39. Q. H. Gibson, Methods Enzymol., 16: 187 (1964).
- 40. H. N. Fernley and S. Bisaz, <u>Biochem. J.</u>, 107: 279 (1968).
- 41. R. L. Berger and L. C. Stoddart, Rev. Sci. Instrum., 36: 78, 85 (1965).
- 42. R. W. Lymn and E. W. Taylor, Biochemistry, 9: 2975 (1970).
- 43. J. A. Sirs, Trans. Faradag Soc., 54, 201 (1958).
- 44. R. H. Prince, Trans. Faradag Soc., 58, 838 (1958).
- 45. B. Chance, Biochem. J., 46, 387 (1950).
- 46. L. C. Clark, <u>Trans. Am. Soc. Artificial Internal</u> Organs, 11, 41 (1956).
- 47. R. L. Berger and L. C. Stoddart, in Rapid Mixing and Sampling Techniques in Biochemistry, see Ref. 30
- 48. L. H. Feldman, R. R. Dewald, and J. L. Dye, "Solvated Electron", Advances in Chemistry Series, No. 50, 163 (1965).
- 49. J. L. Dye, <u>Accounts Chem. Res.</u>, <u>1</u>, 306 (1968).

- 50. E. R. Minnich, L. D. Long, J. M. Ceraso and J. L. Dye, J. Amer. Chem. Soc., 35, 1061 (1973).
- 51. J. L. Dye and L. H. Feldman, Rev. Sci. Instrum., 37, 154 (1966).
- 52. B. Chance, Discussions Faradag Soc., 17, 120 (1955).
- 53. Q. H. Gibson and L. Milnes, <u>Biochem. J.</u>, <u>91</u>, 161 (1964).
- 54. Q. H. Gibson, Methods in Enzymology, Vol. XVI, K. Kustin, Editor, Academic Press, New York, 187-228 (1969).
- 55. K. M. Plowman, Enzyme Kinetics, McGraw Hill Book Co., (1972).
- 56. F. G. Heineken, H. M. Tsuchiya, R. Aris, <u>Mathematical</u> <u>Biosciences</u>, <u>1</u>, 95 (1967).
- 57. S. I. Rubinow, and Joel L. Lebowitz, J. Amer. Chem. Soc., 92, 3889 (1970).
- 58. D. S. Bates and Carl Frieden, <u>J. Amer. Chem. Soc.</u>, 248, 7878 (1973).
- 59. I. G. Darvey, S. J. Prokhovnik and J. F. Williams, J. Theoret. Biol., 13, 90 (1966).
- 60. D. Garfinkel, L. Garfinke, M. Pring, S. B. Green, and B. Chance, Ann. Rev. Biochem., 39, 473, (1970).
- 61. G. Hammes and P. Schimmel in The Enzymes, P. D. Boyer, Ed., Academic Press, New York, Vol. 11, 67 (1970).
- 62. J. L. Dye and V. Nicely, J. Chem. Educ., 48, 443 (1971).
- 63. Laboratory Manual II (Software), see also Ref. 32.
- 64. see Ref. 32, Appendix.
- 65. J. W. Frazer, Chem. Instrum., 2 (3), 271 (1970).
- 66. R. E. Dessy and J. A. Titus, Anal. Chem., 45, 294 A (1973).
- 67. G. L. Booman, Anal. Chem., 1141 (1966).
- 68. G. Lauer and R. A. Osteryoung, Anal. Chem., 40, 30A (1968).

- 69. P. M. Beckwith and S. R. Crouch, <u>Anal. Chem.</u>, <u>山</u>, 221 (1972).
- 70. B. G. Willis, J. A. Bittilsofer, H. C. Pardu, and D. W. Margerum, Anal. Chem., 42, 1340 (1970).
- 71. R. J. Desa, Q. H. Gibson, <u>Comput. Biomed. Rev.</u>, <u>2</u>, 494 (1969).
- 72. M. J. Milano, H. L. Pardue, T. E. Cook, R. E. Santini, D. W. Margerum, J. M. T. Raycheba, Anal. Chem., 46, 374 (1974)
- 73. Tektionix Inc., Beaverton, Oregon.
- 74. Laboratory Manual I (Hardware).
- 75. Y. Shizuta and M. Tokushiga, Methods Enzymol., 17B, 575 (1971).
- 76. K. Kirschner and B. Voigt, Hoppe-Seyler's Z. Physiol. Chem., (Ger.), 349, 632 (1968).
- 77. R. Stancel, Ph.D. thesis, Michigan State University (1971).
- 78. We thank Professor W. A. Wood Dept. of Biochemistry, Michigan State University for the threonine dehydrase sample.
- 79. E. R. Minnich Ph.D. thesis Michigan State University (1970).
- 80. Personal communication to J. L. Dye from L. de Mayer
- 81. B. K. Hahn and C. G. Enke, Anal. Chem., 45, 651A (1973).
- 82. Texas Instruments Application Report, Line Driver and Receiver SN 55107 Series.
- 83. P. Moore, S.F.A. Kettle and R. G. Wilkins, <u>Inorg.</u> Chem., <u>5(3)</u>, 466 (1966).
- 84. Manufactured by the S.S. White Dental Mfg. Co., Industrial Division, 10 East 40th Street, New York 16, New York.
- 85. R. R. Dewald and J. M. Brooks, <u>Rev. Sci. Instrum.</u>, <u>41</u>, (11), 1612 (1970).
- 86. Available from Schott Optical Co., Inc., York Avenue, Duryea, Pa.

- 87. Le Dinh Long, Ph.D. thesis, Michigan State University (1973).
- 88. B. Chance and J. H. Park, <u>J. Biol. Chem.</u>, <u>242</u>, 5093 (1967).
- 89. R. A. Niederman, K. W. Rabinowitz, and W. A. Wood, Biochem. Biophys. Res. Comm., 36, 951 (1969).
- 90. M. Tokushige, and A. Nakazawa, J. Biochem. (Tokyo) 72, 713 (1972).
- 91. H. Theorell and B. Chance, Acta. Chem. Scand., 5, 1127 (1951).
- 92. H. Theorell and J. S. McKinley McKee, Acta. Chem. Scand., 15, 1811 (1961).
- 93. K. Dalziel, J. Biol Chem., 238, 2850 (1963).
- 94. C. C. Wratten and W. W. Cleland, Biochemistry 2, 935 (1963).
- 95. Ibid., 4, 2442 (1963).
- 96. H. Theorell and T. Yonetani, Biochem. Z., 338, 537 (1963).
- 97. S. Taniguchi, H. Theorell and A. Akeson, Acta. Chem. Scand., 21, 1903 (1967).
- 98. D. S. Sigman, J. Biol. Chem., 242, 3815 (1967).
- 99. H. Theorell and K. Tatemoto, Arch. Biochem. Biophys., 142, 69 (1971).
- 100. R. H. Sarma and C. L. Woronuck, Biochemistry, 11, 170 (1972).
- 101. H. Theorell and R. Bonnichsen, Acta. Chem. Scand., 5, 1105 (1961).
- 102. H. Theorell and T. Yonetani, <u>Biochem. Z.</u>, <u>338</u>, 537 (1963).
- 103. G. Geroci and Q. H. Gibson, <u>J. Biol. Chem.</u>, <u>242</u>, 4275 (1967).
- 104. H. Sund and H. Theorell, Enzymes, 1, 26 (1962).
- 105. J. D. Shore, Biochemistry, 8, 1588 (1969).
- 106. S. A. Bernhard, M. F. Dunn, P. L. Luisi, and R. Shack, Biochemistry, 9, 185 (1970).

- 107. P. C. Louisi and R. Favilla, <u>Biochemistry</u>, <u>11</u>, 2303 (1972).
- 108. J. D. Shore and H. Gutfreund, Biochemistry, 9, 4655 (1970).
- 109. M. F. Dunn and S. A. Bernhard, Biochemistry, 10, 4569 (1971).
- 110. M. F. Dunn and J. S. Hutchison (Private communication)
- 111. J. T. McFarland and S. A. Bernhard, Biochemistry, 11, 1486 (1972).
- P. Schack and M. F. Dunn, <u>Abstracts of the 8th Meeting of the Federation European Biochem. Soc.</u>, Amsterdam, 1972, Abstract No. 303.
- 113. M. J. Holland and E. W. Westhead, Biochemistry, 12, 2264 (1973).

